

**POLITECNICO DI MILANO**

Scuola di Ingegneria Industriale e dell'Informazione

Dipartimento di Chimica, Materiali e Ingegneria Chimica "Giulio Natta"

Master of Science in Materials Engineering and Nanotechnology



**SYNTHESIS AND CHARACTERIZATION OF FURAN-  
CONTAINING BIOBASED POLYURETHANES FOR  
FUNCTIONALIZATION VIA DIELS-ALDER REACTION**

Stefano Torresi

ID 918318

Supervisor: Prof. Gianmarco Griffini

Co-supervisor: Prof. Arantxa Eceiza

Academic Year 2019-2020



## Table of Contents

<b>List of figures</b> .....	<b>7</b>
<b>List of tables</b> .....	<b>11</b>
<b>Abstract</b> .....	<b>13</b>
<b>ESTRATTO IN ITALIANO</b> .....	<b>14</b>
<b>FOREWORD</b> .....	<b>18</b>
<b>AIM AND STRUCTURE OF THE THESIS</b> .....	<b>19</b>
<b>1. INTRODUCTION</b> .....	<b>20</b>
<b>1.1 POLYURETHANES</b> .....	<b>20</b>
1.1.1 History of polyurethanes.....	20
1.1.2 Chemistry of the polyurethanes.....	21
1.1.3 Synthesis techniques .....	23
1.1.4 Characteristics and properties of different types of polyurethanes.....	24
<b>1.2 CLICK CHEMISTRY</b> .....	<b>28</b>
1.2.1 Click chemistry overview .....	28
1.2.2 Polymer functionalization and click chemistry .....	29
1.2.3 Thiol-Michael addition .....	30
1.2.4 Copper-Catalyzed Azide–Alkyne Cycloaddition (CuAAC) .....	31
1.2.5 DA reaction .....	32

1.2.6 Mechanism of DA reaction.....	33
<b>1.3 DA AND SELF-HEALING POLYMERS.....</b>	<b>35</b>
<b>1.4 DA REACTION AND THERMOSET POLYMER RECYCLING.....</b>	<b>39</b>
<b>1.5 FURANS.....</b>	<b>42</b>
<b>1.6 MALEIMIDES.....</b>	<b>44</b>
<b>1.7 MALEIMIDE COMPOUNDS .....</b>	<b>46</b>
1.7.1 Flame retardant.....	47
1.7.2 Antibacterial, antifungal and cytostatic activity of maleimide-containing compounds.....	49
1.7.3 Drug delivery nanoparticles .....	50
<b>1.8 SMART TEXTILES.....</b>	<b>51</b>
<b>1.9 ELECTROSPINNING.....</b>	<b>55</b>
<b>1.10 CHARACTERISTICS OF THE POLYMERIC SOLUTION INFLUENCING THE ELECTROSPINNING PROCESS .....</b>	<b>56</b>
1.10.1 Viscosity.....	56
1.10.2 Electric field and distance .....	58
1.10.3 Surface tension.....	58
1.10.4 Temperature.....	59
1.10.5 Molecular weight.....	59

<b>1.11 ELECTROSPINNING OF THERMOPLASTIC POLYURETHANE .....</b>	<b>60</b>
<b>1.12 ELECTROSPINNING OF CLICKABLE FIBERS .....</b>	<b>61</b>
<b>1.13 ELECTROSPINNING OF FUNCTIONALIZED TPU .....</b>	<b>62</b>
<b>1.14 TAILOR SURFACE ENERGY AND WETTABILITY USING FURAN-MALEIMIDE DA REACTION .....</b>	<b>63</b>
<b>2. MATERIALS AND METHODS .....</b>	<b>65</b>
<b>2.1 MATERIALS .....</b>	<b>65</b>
2.1.1 Polymerization precursors.....	65
2.1.2 Functionalizing compounds.....	68
<b>2.1.3 Solvents .....</b>	<b>70</b>
2.1.3.1 Chloroform .....	70
2.1.3.2 Dimethylformamide .....	70
2.1.3.3 Dimethyl sulfoxide (DMSO).....	71
<b>2.2 SYNTHESIS .....</b>	<b>72</b>
2.2.1 SYNTHESIS OF POLYURETHANES .....	72
2.2.2 Synthesis of AMI.....	76
<b>2.3 CHARACTERIZATION TECHNIQUES.....</b>	<b>77</b>
2.3.1 Fourier transformed infrared spectroscopy (FTIR) .....	77
2.3.2 Differential scanning calorimetry (DSC) .....	80

2.3.3	Dynamic molecular analysis (DMA).....	82
2.3.4	Ultraviolet-visible spectroscopy (UV-vis) .....	84
2.3.5	Thermo-gravimetric analysis (TGA).....	85
2.3.6	Optical microscopy (OM).....	86
2.3.7	Scanning electron microscopy (SEM).....	88
2.3.8	Contact Angle .....	89
2.3.9	Electrospinning.....	91
2.3.10	Tensile test .....	92
<b>3</b>	<b>RESULTS AND DISCUSSION .....</b>	<b>93</b>
<b>3.1</b>	<b>DSC.....</b>	<b>93</b>
<b>3.2</b>	<b>DMA.....</b>	<b>96</b>
<b>3.3</b>	<b>TGA .....</b>	<b>98</b>
<b>3.4</b>	<b>FTIR.....</b>	<b>101</b>
3.4.1	FTIR of films .....	101
3.4.2	FTIR of membranes .....	103
<b>3.5</b>	<b>SOLVENT MIXTURE FOR ELECTROSPINNING .....</b>	<b>105</b>
<b>3.6</b>	<b>ELECTROSPINNING RESULTS.....</b>	<b>109</b>
<b>3.7</b>	<b>PROOFS OF DA REACTION ON THE ELECTROSPUN MEMBRANE.....</b>	<b>116</b>
3.7.1	Functionalization using 5-MF .....	116

3.7.2	DA reaction between BHMF-2 membrane and AMI assessed by FTIR .....	121
<b>3.8</b>	<b>UV-vis MONITORING OF DA REACTION .....</b>	<b>123</b>
<b>3.9</b>	<b>SEM RESULTS.....</b>	<b>125</b>
<b>3.10</b>	<b>CONTACT ANGLE.....</b>	<b>131</b>
3.10.1	Film contact angle .....	132
3.10.2	Membranes contact angle .....	133
<b>3.11</b>	<b>MECHANICAL PROPERTIES .....</b>	<b>136</b>
3.11.1	Mechanical properties of films.....	136
3.11.2	Mechanical test of the membrane.....	139
<b>4</b>	<b>CONCLUSION AND FUTURE PROSPECTIVES.....</b>	<b>142</b>
<b>4.1</b>	<b>CONCLUSIONS .....</b>	<b>142</b>
<b>4.2</b>	<b>FUTURE DEVELOPMENT .....</b>	<b>144</b>
	<b>BIBLIOGRAPHY .....</b>	<b>145</b>

## List of figures

Figure 1 Polyurethane types.....	20
Figure 2 Click reactions.....	29
Figure 3 Publications regarding DA reaction (the data are plotted as the number of chemistry publications mentioning the DA reaction over the total number of chemistry publications X 1000.) (11).....	32
Figure 4 DA reaction's scheme .....	33
Figure 5 DMA curve after two heating/cooling cycles of PU2(14).....	37
Figure 6 Healing performance of the three thermo-reversible polyurethane after 20 minutes at 140°C: PU1 (a,b); PU2 (c,d); PU3 (e,f) (14).....	38
Figure 7 Stress-strain curve of polymer: a) with furan in backbone and b) with furan as pendant group (16,17).....	41
Figure 8 Unsaturated heteroaromatic compounds.....	42
Figure 9 First-generation Furan.....	43
Figure 10 Maleimide.....	44
Figure 11 Examples of N-substituted maleimides (23) .....	46
Figure 12 Flame retardant crosslinker containing maleimide moieties (25) .....	47
Figure 13 Synthesis of HMCP (24) .....	48
Figure 14 Self-assembly and functionalization of poly(TMCC-co-LA)-g-PEG-furan (28) .....	50
Figure 15 Shape memory behaviour of functionalized cotton (30).....	52
Figure 16 Different type of PEU produced by Becker et al. (31).....	53
Figure 17 Horizontal electrospinning setup (32).....	55
Figure 18 Fibers resulting from electrospinning process at increasing viscosity of solution (34).....	57
Figure 19 a) Poly(tetramethylene ether)glycol b) Poly(GAP-co-THF).....	62
Figure 20 Poly(butylene sebacate)diol molecular structure .....	65
Figure 21 2,5-Bis(hydroxymethyl)furan molecular structure.....	66
Figure 22 1,3-Propanediol molecular structure .....	66



Figure 23 Hexamethylene diisocyanate molecular structure .....	67
Figure 24 Fluorescein-5-maleimide molecular structure .....	68
Figure 25 AMI molecular structure .....	69
Figure 26 DMF molecular structure .....	71
Figure 27 DMSO molecular structure.....	71
Figure 28 Molding machine.....	74
Figure 29 Resulting films from molding process. From left to right PD, BHMF-2, BHMF-3..	75
Figure 30 Spectrum of AMI.....	76
Figure 31 Molecular vibrations: a) Stretching vibrations, b) Bending vibration(45).....	77
Figure 32 FTIR resulting graph.....	78
Figure 33 Nicolet Nexus spectrophotometer .....	79
Figure 34 DSC instrument scheme(57).....	80
Figure 35 DSC 3+ Mettler Toledo machine.....	81
Figure 36 DMA instrument scheme (59) .....	83
Figure 37 TGA instrument scheme(58).....	85
Figure 38 Representation of OM (46).....	86
Figure 39 Optical Microscopy .....	87
Figure 40 Representation of the three interfaces (47) .....	89
Figure 41 Contact angle's instrument scheme (47).....	90
Figure 42 Fluidnatek LE-10 electrospinning machine .....	91
Figure 43 DSC thermograph of PD, BHMF-2 and BHMF-3 samples .....	93
Figure 44 Storage and loss moduli and $\tan \delta$ vs T of PD .....	96
Figure 45 Storage and loss moduli and $\tan \delta$ T of BHMF-2.....	96
Figure 46 TGA and DTG curves of BHMF-3.....	98
Figure 47 TGA and DTG curves of BHMF-2.....	99
Figure 48 TGA and DTG curves of PD .....	100
Figure 49 FTIR spectra of synthesized polyurethane and HDI .....	101
Figure 50 FTIR spectra of synthesized polyurethane and BHMF .....	102
Figure 51 FTIR spectra of the membranes prepared from PD, BHMF-2 and BHMF-3 .....	103

Figure 52 FTIR spectra of the membranes prepared from PD, BHMf-2, BHMf-3 and DMF .....	104
Figure 53 polymers before electrospinning: a) PD b)BHMf-2 c) BHMf-3, electrospinning equipment and one of the resulting membranes .....	108
Figure 54 Optical microscopy images of different electrospinning operation conditions using the polymer solution of PD 12%wt in DMF:CHCl <sub>3</sub> 2:1 a) 5kV, 7cm, 1ml h <sup>-1</sup> b) 6.7kV, 12cm, 1ml h <sup>-1</sup> c) 7.5kV, 15 cm, 0.2 ml h <sup>-1</sup> and d) 8 kV, 15 cm, 0.5 ml h <sup>-1</sup> .....	109
Figure 55 Optical microscopy images of electrospun mats obtained using polymer solution of BHMf-2 13 wt% at: a) 0.2 ml h <sup>-1</sup> 15 cm b) 0.2 ml h <sup>-1</sup> 20 cm.....	110
Figure 56 Optical microscopy images of electrospun mats obtained using polymer solution of BHMf-2 13 wt% at: a) 0.5 ml h <sup>-1</sup> 15 cm b) 0.5 ml h <sup>-1</sup> 20 cm.....	110
Figure 57 Optical microscopy images of electrospun mats obtained using polymer solution of BHMf-2 13 wt% at: a) 1 ml h <sup>-1</sup> 15 cm b) 1 ml h <sup>-1</sup> 20 cm.....	111
Figure 58 Optical microscopy images of different electrospinning operation conditions using the polymer solution of BHMf-2 14 wt% in DMF:CHCl <sub>3</sub> 2:1 : a) 6 kV, 15 cm, 0,2 ml h <sup>-1</sup> b) 6 kV, 15 cm, 0,4 ml h <sup>-1</sup> c) 6 kV, 15 cm, 0,5 ml h <sup>-1</sup> .....	111
Figure 59 Optical microscopy images of electrospun mats obtained using polymer solution of BHMf-3 16 wt% at: a) 0.2 ml h <sup>-1</sup> 15 cm b) 0.2 ml h <sup>-1</sup> 20 cm.....	112
Figure 60 Optical microscopy images of electrospun mats obtained at using polymer solution of BHMf-3 16 wt% a) 0.5 ml h <sup>-1</sup> 15cm b) 0.5 ml h <sup>-1</sup> 20 cm .....	113
Figure 61 Optical microscopy images of electrospun mats obtained a using polymer solution of BHMf-3 16 wt% t: a) 1 ml h <sup>-1</sup> 15 cm b) 1 ml h <sup>-1</sup> 20 cm.....	113
Figure 62 Optical microscopy images of electrospun mats obtained at using polymer solution of PD 12 wt% : a) 0.2 ml h <sup>-1</sup> 15 cm b) 0.2 ml h <sup>-1</sup> 20 cm .....	114
Figure 63 Optical microscopy images of electrospun mats obtained at using polymer solution of PD 12 wt% : a) 0.5 ml h <sup>-1</sup> 15cm b) 0.5 ml h <sup>-1</sup> 20cm .....	114
Figure 64 Optical microscopy images of electrospun mats obtained at using polymer solution of PD 12 wt% : a) 1 ml h <sup>-1</sup> 15 cm b) 1 ml h <sup>-1</sup> 20cm .....	114
Figure 65 UV-vis Absorption spectrum of 5-MF.....	116

Figure 66 Membrane in solution of 80% DMSO + 20% water: without labelling agent (left) and with labelling agent (right), exposed to two different wavelengths.....	118
Figure 67 Membrane in solution of water: without labelling agent (left) and with labelling agent (right).....	119
Figure 68 FTIR spectra of the same membrane before and after the functionalization ...	120
Figure 69 Spectra of BHMF-2 membrane not functionalized(m-BHMF-2) and functionalized with AMI (m-BHMF-2-AMI) .....	122
Figure 70 UV-vis monitoring of DA reaction between BHMF-2 and AMI.....	123
Figure 71 UV-vis monitoring of retro-DA reaction between BHMF-2 and AMI.....	124
Figure 72 SEM images of BHMF-2 electrospun mats .....	125
Figure 73 SEM images of BHMF-3 electrospun mats .....	125
Figure 74 SEM images of PD electrospun mats.....	126
Figure 75 Diameters distribution of BHMF-2 .....	126
Figure 76 Diameter distribution of BHMF-3.....	127
Figure 77 Diameter distribution of PD.....	127
Figure 78 PD void area (in black) .....	129
Figure 79 BHMF-3 void area (in black) .....	129
Figure 80 Functionalized membrane.....	130
Figure 81 Not functionalized membrane .....	130
Figure 82 Photographs of the contact angle measurements on the films of: .....	132
Figure 83 Photographs of the contact angle measurement of the membranes: a) PD b) BHMF-2 c) BHMF-3 .....	133
Figure 84 Effect of the surface roughness: Young model and Wenzel model (60).....	135
Figure 85 Stress-strain graphs comparison of the synthesized PD, BHMF-2 and BHMF-3 polyurethanes.....	136
Figure 86 Boxplot of Young Modulus, Elongation at break and Ultimate tensile Strength of the three synthesized polyurethanes.....	137
Figure 87 Relation between HS content and resulting Young modulus .....	138
Figure 88 Configuration of the membranes mechanical test (53) .....	139

Figure 89 Stress-Strain graph of the membranes.....	140
---	-----

## List of tables

Table 1 Table representing the three types of polyurethane synthesized. a) GPC in THF b) Not soluble in THF (14).....	36
Table 2 Reactants and quantities for PD .....	73
Table 3 Reactants and quantities for BHMF-2 .....	73
Table 4 Reactants and quantities for BHMF-3 .....	74
Table 5 Thermal transition of the synthesized polyurethanes .....	94
Table 6 Solvent and solvent mixture, weight percentage and resulting fiber of different electrospinning attempts .....	106
Table 7 Weight percentage at which the best fibers are obtained for each polymer .....	107
Table 8 Quantities of BHMF-2 membrane and AMI present in solution .....	121
Table 9 Mean fiber diameter and standard deviation of the three systems .....	128
Table 10 Contact angles values of the film and the membrane .....	134
Table 11 Electrospinning conditions of each membrane tested.....	140



## Abstract

In this work, a novel furan-containing polyurethane has been synthesized and used to produce membrane by electrospinning process which can be easily functionalized by Diels-Alder (DA) reaction.

Poly(butylene sebacate)diol as macroglycol, 2,5-bis(hydroxymethyl)furan or 1,3-propanediol as chain extender and hexamethylene diisocyanate as isocyanate were used. Two different formulations containing BHMF, one with a ratio macroglycol: isocyanate: chain extender of 1:3:2 and another with ratio of 1:4:3, were synthesized. A third polyurethane, containing 1,3-propanediol, with a ratio 1:3:2 was used as reference.

The three different polyurethane has been characterized both after their synthesis and electrospinning process. FTIR, DSC, DMA, TGA and tensile test have been used to characterize the samples.

Functionalization of the surface was tested using two different maleimide-containing compounds: Fluorescein-5-maleimide (5-MF) and maleimide-end acid (AMI).

FTIR, and UV emission were used to verify the effectiveness of DA reaction.

Furthermore, the DA and retro-DA reaction of the electrospinning solution with AMI was monitored by UV-vis spectroscopy, determining time and temperature necessary to both reactions to occur.

Using SEM the diameter distribution and the surface morphology of the electrospun fibers were investigated.

The membrane has been found to be also highly hydrophobic and studies about its biocompatibility is now being performed.

## ESTRATTO IN ITALIANO

La ricerca nel campo dei polimeri si è incentrata negli ultimi anni sulla sintesi di alternative green alle cosiddette commodities, polimeri prodotti in enormi quantità, da materie prime principalmente fossili che risultano difficili da riciclare e che impattano negativamente sul già fragile ecosistema terrestre.

I nuovi composti bio-based cercano di emulare le proprietà dei polimeri prodotti da fonti fossili spesso, però, con scarsi risultati. I prodotti derivanti del riciclaggio di quest'ultimi, hanno proprietà fisiche neanche lontanamente comparabili ai composti ex-novo.

Per quanto riguarda, invece, i polimeri funzionalizzati, il percorso di smaltimento si fa ancora più complesso poichè gli agenti usati per impartire specifiche caratteristiche al prodotto, difficilmente sono biodegradabili e ancor più raramente sono riciclabili, poichè legati in maniera irreversibile alla catena polimerica.

In questo studio si è provato a produrre un poliuretano contenente un'alta percentuale di materie prime rinnovabili (tra l'85 e l'88 % in peso) e che fosse funzionalizzabile tramite una reazione che sia reversibile e che non necessiti di solventi inquinanti, catalizzatori e temperature elevate per essere condotta.

La reazione in questione è la Diels-Alder, una cicloadizione tra un diene coniugato e un dienofilo che ha come prodotto un cicloesene. Tale reazione, conosciuta già dalla fine degli anni '20 e tornata alla rivalse negli ultimi 40 anni, può essere condotta a temperature attorno ai 60 °C, in acqua. Inoltre, la cicloadizione è reversibile: aumentando la temperatura attorno ai 120°C, avviene la reazione inversa dove il cicloesene si converte nel diene e dienofilo iniziali.

Nel campo dei poliuretani, tale reazione è impiegata principalmente per produrre poliuretani termoindurenti autoriparanti e/o riciclabili. Infatti usando come agente reticolante una bis-maleimide (dienofilo) e con la presenza di gruppi furano (diene) nella catena polimerica o come gruppi pendenti, il crosslinking può avvenire tramite DA.

Partendo da queste premesse si è cercato di sintetizzare un poliuretano che contenesse nella catena polimerica gruppi furano che reagissero facilmente tramite DA.

Usando Poly(butylene sebacate)diol come poliolo, esametilene diisocianato come isocianato e 2,5-bis(hidroximetil)furano come estensore di catena, due differenti formulazioni contenenti furano sono state prodotte : la prima contenente un rapporto poliolo: isocianato: estensore di catena 1:3:2 (BHMF-2) e la seconda con un rapporto 1:4:3 (BHMF-3). Inoltre, si è sintetizzata una terza composizione con rapporto 1:3:2 nella quale come estensore di catena si è utilizzato 1,3-propanodiolo. Tale formulazione è stata presa come poliuretano di riferimento.

Tutti i poliuretani sono stati prodotti con il metodo del prepolimero, dove inizialmente sono stati fatti reagire il poliolo e l'isocianato e in un secondo momento è stato aggiunto l'estensore di catena.

Il prodotto risultante da tale reazione è stato sottoposto ad un ciclo termico a pressione costante al fine di ottenere un film solido. Tale film è stato successivamente caratterizzato tramite DSC, DMA, TGA e FTIR, per accertare l'effettiva incorporazione del furano nel poliuretano.

Successivamente, sono state svolte prove di trazione per determinarne le proprietà meccaniche. La formulazione contenente la minor percentuale di furano (BHMF-2), risulta possedere proprietà meccaniche comparabili con il poliuretano di riferimento. Le proprietà meccaniche del poliuretano contenente invece una maggior quantità di furano (BHMF-3), sono sensibilmente minori rispetto alla formulazione usata come riferimento. In tal senso sembra influire negativamente la maggior percentuale di hard segment presente in BHMF-3, la quale previene la formazione di segmenti cristallini ordinati, diminuendo così le proprietà meccaniche del composto.

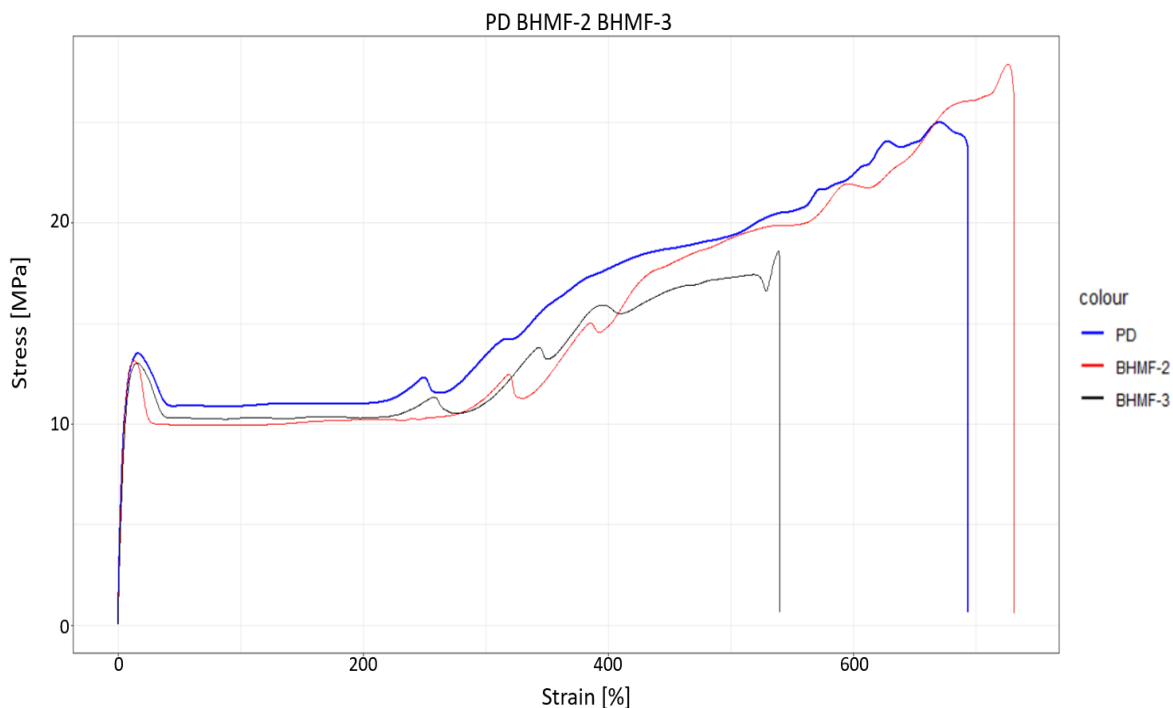


Figura 1 Risultati della prove di trazione, rappresentati nella curva Sforzo-Deformazione



Dopo aver caratterizzato il film anche tramite misurazioni di angolo di contatto, lo studio si è incentrato nella produzione di membrane tramite electrospinning. Il motivo di tale scelta è da ricercare nelle fibre prodotte con questa tecnica. L'electrospinning permette di produrre fibre di dimensioni variabili in un range che va dai micron ai nanometri. La diminuzione del diametro della fibra, infatti, aumenta il rapporto tra area superficiale e volume, permettendo così una migliore funzionalizzazione di quest'ultima.

Uno studio approfondito è stato svolto riguardo i solventi da usare per disciogliere i film e raggiungere viscosità tali da permettere la filatura tramite electrospinning. Finalmente, è stato scelto come dissolvente una soluzione di DMF e  $\text{CHCl}_3$  in rapporto 2:1 . Differenti percentuali in peso sono state usate per ogni sistema, come illustrato nella tabella A.

<b>Materiale</b>	<b>Percentuale in peso (%)</b>
PD	12
BHMF-2	13
BHMF-3	16

*Tabella 1 Percentuali in peso delle differenti soluzioni utilizzate nel processo di electrospinning*

Una volta prodotte, le membrane sono state caratterizzate tramite FTIR, SEM e prove meccaniche. Un'inaspettata proprietà riscontrata nelle membrane è stata l'alta idrofobicità. Tramite misurazioni di angolo di contatto statico sono stati rilevati valori compresi tra i  $120^\circ$  e i  $130^\circ$ , notevolmente più alti di quelli misurati nei film (tra i  $55^\circ$  e gli  $80^\circ$ ).

Infine, è stata studiata la funzionalizzazione di tali membrane, utilizzando due differenti composti contenenti maleimide.

Nel primo caso si è adoperato un composto fluorescente contenente maleimide, utilizzato principalmente come labelling agent nelle proteine, chiamato Fluorescein-5-maleimide (5-MF), e ne è stata comprovata la reazione tramite emissione UV e FTIR.

Come ulteriore conferma, un composto prodotto in laboratorio, il Maleimide-end acid, è stato utilizzato per la funzionalizzazione. La reazione in questo caso, non essendo un composto fluorescente, è stata verificata solamente tramite l'uso di FTIR.

Entrambi i composti mostrano una buona reattività con la membrana alla temperatura di 65 °C.

Per concludere il lavoro si è cercato di funzionalizzare la soluzione prima di sottoporre il sistema ad electrospinning, per poter produrre in futuro membrane già funzionalizzate. Le reazioni di DA e la retro-DA tra il composto AMI e la soluzione di BHMf-2 sono state monitorate con spettroscopia UV-vis. Di seguito sono riportati i risultati della spettroscopia UV-vis, dove si vede chiaramente il consumo di maleimide e il suo successivo rilascio.

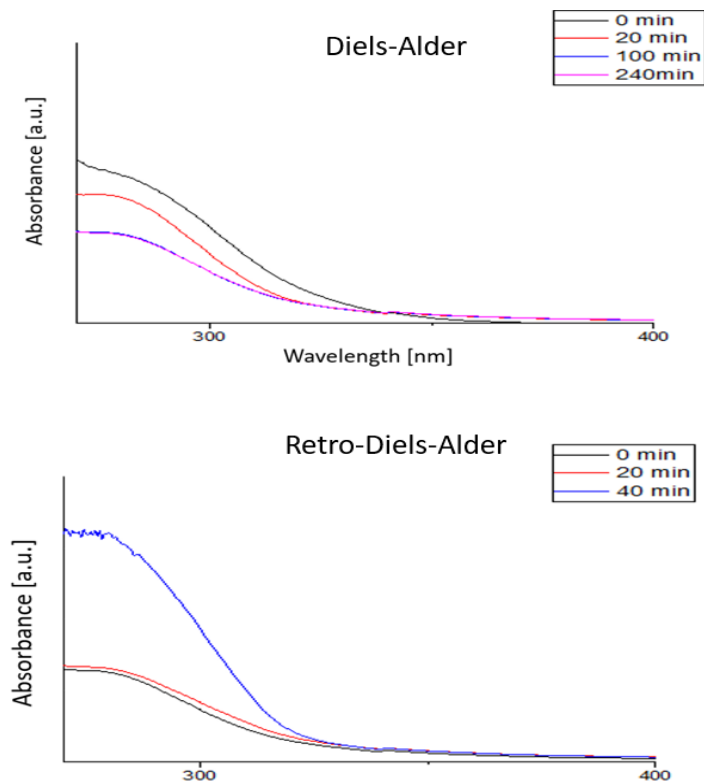


Figura 2 Reazioni di DA e retro-DA monitorate tramite UV-vis

## FOREWORD

DA reaction in the last years has been widely applied in polymer chemistry, mainly in the synthesis of recyclable and self-healing polyurethane. The high reaction yield, the inoffensive and not pollutants byproducts make it a perfect reaction to be applied in eco-friendly material synthesis. In this work, linear polyurethanes with a composition containing between 85 and 88 wt% of biobased material, have been produced with the aim of create a polymer easy to functionalize.

The polymer can be functionalized via DA reactions thanks to the furan groups present in its backbone, which can easily react with maleimide-containing compound.

Between different dienes and dienophiles have been chosen furan and maleimide due to the high reactivity of the amide group which can react with lots of compound, creating a wide range of potential functionalizing agent and also due to the non-fossil origin of BHMF, which is a biomass-derived compound.

It was also proved the possibility and the ease in the membranes production via electrospinning, allowing the creation of very thin and highly functionalizable platforms.

# AIM AND STRUCTURE OF THE THESIS

The aim of this work was to create a polyurethane containing a high quantity of biobased raw material which was also able to be easily functionalized using a green reaction process. Once determined the process to use to functionalize the polymer, the DA reaction, different polyurethane formulations were produced. The good results of the synthesis, both from a chemical and a physical point of view, have encouraged to try to produce membranes via electrospinning process. The membranes were proved to be produced and functionalized quite easily.

The structure of the thesis is reported below:

- Introduction: polyurethane chemistry, types and characteristics the topics of click reactions, with particular attention paid to DA reaction, use of DA in polymers, a general presentation of different maleimides compounds and an overview of electrospinning process are discussed. Finally, a brief review of smart textiles was reported
- Materials and methods: all the used chemicals and the reaction synthesis are described. Furthermore, the employed characterization techniques are explained.
- Results and discussion: The results of characterization tests are presented. The polymer as film and the polymer as membrane are considered together. The monitoring of functionalization reactions is explained and different tests are presented to assess the effectiveness of functionalization.
- Conclusion and future developments: the conclusions of the work are explained and the next steps to be taken are discussed.

# 1. INTRODUCTION

## 1.1 POLYURETHANES

### 1.1.1 History of polyurethanes

The history of polyurethane starts in 1937 thanks to the work of Otto Bayern and his group, who discovered diisocyanate polyaddition performed between aliphatic diisocyanate and glycol. I.G. Farbenindustrie, the industry Otto Bayern was working for, patented the first polyurethane with German Patent 728,981. Industrial production starts in 1952 and after the first attempts using polyester polyol, the use of polyether polyol was preferred, leading to the first commercially available polyurethane produced by DuPont in 1956, using tetrahydrofuran.

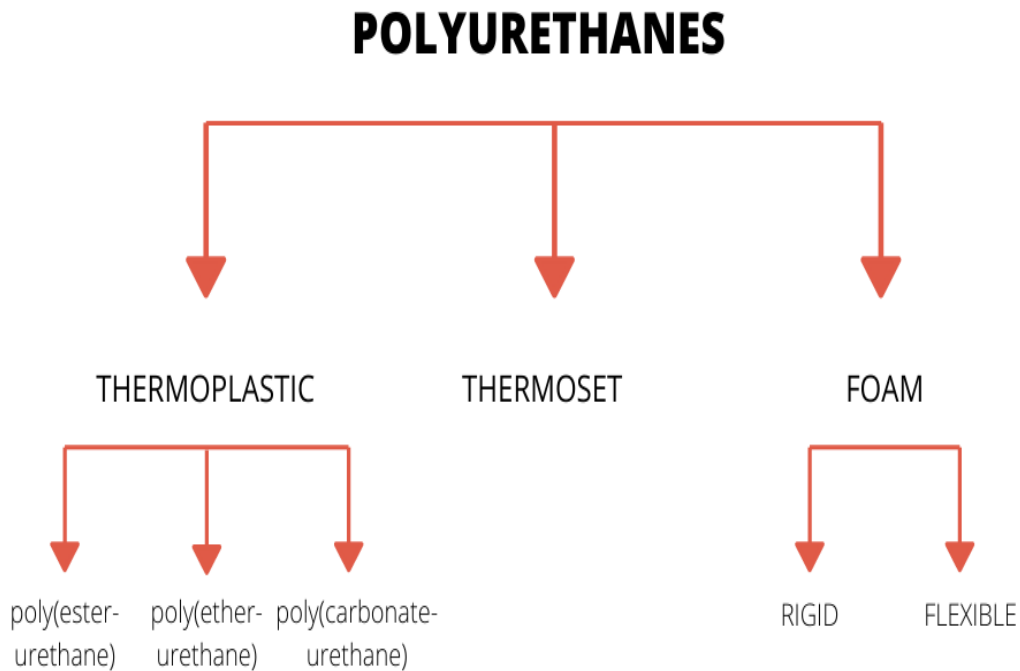


*Figure 1 Polyurethane types*

From the development of the first industrial produced polyurethane, lots of improvements in term of processing and formulation has been provided. Durability, toughness, flexibility and chemical resistance combined with the different physical state in which can be produced (flexible and rigid foam, elastomer, coating, sealant..), as shown in Figure 1, making it suitable to be applied in different field as automotive, biomedical, textile and construction. Nowadays, polyurethane-based materials play a leading role in plastic industry, being the fifth among the most produced plastic in Europe (1).

### 1.1.2 Chemistry of the polyurethanes

Peculiar feature of a polyurethane is the urethane group ( $\text{R-NH-CO-O-R}'$ ), which is formed reacting an isocyanate ( $\text{R-NCO}$ ) with a hydroxyl group ( $\text{R}'\text{-OH}$ ). Isocyanate can react also with amine giving polyurea.

Polyurethane elastomers are usually characterized by the presence of three different components: a high molecular weight polyol (macroglycols), constituting the soft segment, a low molecular weight polyol, used as chain extender and a polyisocyanate, these last two forming the so called hard segment. Depending on their functionality they will act as thermoplastic or thermoset polyurethane elastomers.

Final properties of polyurethane depend on the type of polyol and isocyanate employed in the process.

Two main features have to be considered: crosslinking density and length of polyol. A lower density of crosslinking and long chains polyols (molecular weight usually ranging from 2000 to 10000)(2) make the polymer more stretchable while shorter polyol and higher density of crosslinking give harder polymers.

Furthermore, different precursors are used depending the desired properties: flexible polyurethane needs a low functionality ( $f$ ) initiator ( $f$  between 2 and 3) while a rigid polyurethane needs a high functionality initiator ( $f$  between 4 and 8).

Isocyanates are fundamental characters in the formation of urethane group. Industrially, the most used are methylene diphenyl diisocyanate (MDI) and toluene diisocyanate (TDI) thanks to low cost and high reactivity. Both are aromatic compounds and this imply some disadvantages like poor resistance to UV light and potentially harmful release of aromatic amine, that make them not suitable for biomedical application. Other linear or cyclic

aliphatic isocyanate, like 1,6-hexamethylenediisocyanate (HDI) or isophoronediiisocyanate (IPDI) find a lower application in industrial processes.

Like most of the reactions in chemistry, also the synthesis of polyurethane could be mediated by catalysts. There are two main families: metal complexes and amine compounds.(2)

Amine compounds like 1,4-diazabicyclooctane (DABCO) and triethylenediamine (TEDA) are composed by tertiary amines which have the ability to drive either urethane or isocyanate trimerizations reactions.

Instead, metal complexes compound based on zinc, bismuth, tin, mercury and lead are more indicated for application where reactions involving polyol and isocyanate are required.

What allows the synthesis of high or infinite (talking about 3D networks) molecular weight are chain extenders and crosslinkers. At first glance, the main difference between the two are the functionality with  $f=2$  for chain extenders and  $f=3$  or more for crosslinkers.

As we said, chain extender and diisocyanate compose the hard segment, thus different chain extender are used for different applications. Hard segments are stiff and immovable and are responsible for high temperature behaviour. Furthermore, they determine the elastomeric effect: in thermoplastic polyurethane covalent coupling of hard and soft segment hinder the plastic flow, providing resiliency to the polymer and giving it the ability to align along stress direction when stress is applied and realign when the sollicitation is removed. In this process an important role is also played by the hydrogen bond created between the polymer chains which, at low temperature, act as physical crosslinking providing mechanical stability and, at high temperature, can be easily broken, though allowing flow and deformation necessary for processing.

It seems clear that chain extender affects high tensile strength, shear resistance, chemical resistance and flexural properties of polyurethane.

Another factor playing an important role in determining the mechanical and thermal properties, mainly in polyurethane block polymers, is the degree of hydrogen bonding. Indeed, NH of urethane group acts as donor and either the carbonyl group of urethane or the macroglycol act as acceptor. Depending on the group acting as acceptor, two possible structure can be identified: the urethane-urethane interaction is characteristic of a microphase separated domain structure, while the urethane-macroglycol occurs when the hard phases are dispersed in the soft segment region resulting in phase mixing.

### 1.1.3 Synthesis techniques

The synthesis of polyurethanes can be performed using different techniques. What differentiates those techniques are the medium of propagation (bulk, solution, water) in which the reaction occurs and the order by which the reactants are added (one step or prepolymer polymerization method, also known as two step method).

In bulk polymerization there is no need of solvent, just monomers and catalysts are used. This imply cost savings, an appreciated characteristic in the industrial field, but a lower control of the reaction both in term of heat transfer and fluid flow. Furthermore, high temperature is needed and adding all the component together and not separating the formed polyurethane gives diisocyanate a longer time to take part to unwanted secondary reactions.

In solvent polymerization, instead, the diisocyanate is dropped in the solution and the formed polyurethane is separated, avoiding secondary reactions. Even if this method implies a longer and more expensive process, it is preferred when the priority is a linear, high molecular weight product.

In one shot polymerization all the reactants are added simultaneously and different rates of different reaction are adjusted using catalysts. The great exothermicity of the reaction make it suitable from an industrial point of view but the microstructure (and so the final properties) are more difficult to control.

The use of an intermediate polymer, as in the prepolymer technique, allows a better control over the reaction without the use of catalysts because it avoid the competitiveness of different simultaneous reactions. Indeed, a stable intermediate is produced, usually making react the long chain macroglycol and the diisocyanate, creating a prepolymer with final isocyanate group. Then a chain extender is added to the end group of prepolymer in order to increase the molecular weight.



## 1.1.4 Characteristics and properties of different types of polyurethanes

### **Thermosetting polyurethanes**

Thermosetting polyurethanes could be classified by density of crosslinking and length of soft segment: short soft segment and high density of crosslinking result in hard polymer; long soft segment and low crosslinking density give elastomers and an intermediate crosslinking density and soft segments length allow the creation of foam. It is important to specify that the crosslinking considered here is chemical crosslinking, more resistant than the physical crosslinking present in thermoplastic polyurethane.

Thermosetting polyurethane undergoes a curing process, in order to crosslink the structure and reaching the desired mechanical, thermal and chemical properties.

The curing process could be driven by radiation (UV curing) or by heat (thermal curing), with the presence of curing agents or catalysts, these last one added directly to the liquid mixture.

High resistance to impact, high resistance to wearing, the low swelling, the high chemical resistance and light weight make thermosetting polyurethane an optimal choice for coatings and adhesives as for insulating materials.

As all thermosetting polymers, it is hard to recycle once it is cured.

### **Foams**

Polyurethane foams can be divided in two classes: rigid and flexible foams. However, the production principles are the same. Foams consist of solid polymer matrix and a gas phase. The gas phase can be produced by physical, mechanical or chemical means.

The most common resulting structure of foam is the closed-cell one. Structure influences the thermal and mechanical properties, so it is important a good control of the reaction. In this sense, the use of blowing agents is fundamental. There are two types of blowing agents, physical and chemical. The physical blowing agents, as cyclopentane, act expanding the polyurethane, vaporizing thanks to the heat developed during the endothermic reaction. Chemical blowing agents, instead, cause the expansion of the polymer matrix by reacting with the isocyanate, resulting in an exothermic reaction. An example of chemical blowing

agent is water, which reacts with isocyanate, creating unstable carbamic acid which decomposes giving carbon dioxide, creating bubbles. Important parameters to consider during the production of such foams are the rate of gelation and the rate of bubble creation. These processes have to balance one another. A too rapid evolution of gas provokes the collapse of the structure, after the initial expansion, because gelation process is not fast enough in creating a network to trap the bubbles.

The gas inside the void interacts with the matrix influencing the mechanical behaviour of the polymer.

Density of void determines the insulation ability of the foam. The gas is not a good heat conductor, so the heat has to find a path around the pores in order to be transferred: more pores means more tortuous pathway and better insulation.

Depending on the cell type structure, two different classes of foam are produced, flexible or rigid. In open-cell structure, where the pores are directly or indirectly connected with the surface, the gas is not held in the cells and so, once compressed, the foam is able to reform, sucking up air, even if regain exactly the initial shape is impossible. This property makes the polyurethane flexible. In closed-cell structure, the pores are not connected with the surface, thus avoiding the flexible behaviour and giving a rigid polyurethane. Both the structures impart good impact and sound absorption.

### **Thermoplastic polyurethanes**

Thermoplastic polyurethanes (TPU) consist of a linear polymer structure constituted of hard segments alternated by soft segments. The hard segments linked together by hydrogen bonds result in a physical crosslinking. Hard and soft segments are thermodynamically incompatible, thus thermoplastic polyurethane can be defined as segmented block copolymer.

Thanks to the conformation described before and depending on the type of polyol used, the resulting thermoplastic polyurethane can present a wide range of proprieties from those typical of a soft elastomer to the ones possessed by a hard plastic.

Varying ratio and type of hard and soft segment and changing temperature of reaction, type of solvent and catalysts allow to customize mechanical and thermal properties.

Thermoplastic polyurethanes can also be classified by the type of polyol used to synthetize them: polyether-, polyester- and polycarbonate-based polyol are mainly used in industrial production.

### **Poly(ester-urethane)**

Commonly used polyester polyol are based on aliphatic or aromatic dicarboxylic acid and low molecular weight diols (3). Aromatic compounds, more stable than aliphatic ones, impart to TPU good mechanical properties, resistance to solvents and thermal stability. The amount of hard segments, usually comprised between 30 and 60 wt%, is fundamental to determinate mechanical properties of the TPU. Hard segments comprise chain extender and diisocyanate, responsible of the physical crosslinking which regulates the tensile strength and hardness of the material. Increasing the number of physical crosslinking results in a less elongation at break due to the soft segment's mobility reduction, not able to realign along the stress direction.

The thermal behaviour of polyurethanes is regulated by the nature of different components, so mainly three different transition can be observed during a DSC analysis, ordered by increasing temperature: the glass transition of soft segments, the glass transition of the amorphous part of hard segments and the melting peak of hard segments. A higher concentration of hard segments, meaning higher stability, shift the glass transition of the soft segments towards lower temperatures and the other two transitions of hard segments to higher ones. When the polyol structure contains high number of methylene groups or when the polyol has a high molecular weight, a melting peak related with the soft segment, around or just above room temperature, is usually observed.

Semicrystalline soft and hard segment domains usually show both transitions, glass transition and melting. The observation of one or both depends on the crystallinity degree. Thermal degradation starts around 290°C when the breakdown of urethane groups occurs and then around 370°C initiates the breaking of soft segment with a random scission of ester linkage.

One of the main problem of the poly(ester-urethane) is the scarce resistance to water and humidity, given by the ease of suffer hydrolysis.

### **Poly(ether-urethane)**

This kind of polyurethane possesses a higher hydrolysis resistance in comparison to poly(ester-urethane).

Usually, the quantity of hard segment is around 40-50 wt%, a narrower range with respect poly(ester-urethane).

Mechanical and thermal properties are similar to the aforementioned type of polyurethane,

but a lower glass transition temperature confers it a higher elongation at break while regarding the thermal response, it shows a worse behaviour with respect to poly(ether-urethane) when submitted to high temperature for a long time.

Thanks to the good hydrolysis resistance, it was used for long time to produce biomedical devices. However, the soft segment has been demonstrated to suffer oxidation after a long exposure in vivo.

### **Poly(carbonate-urethane)**

The majority of poly(carbonate-urethane) are stiff at room temperature, due to the crystallization of the soft segment. The presence of hard segment is the highest between the three, in a range of 30-70 wt% and this makes it the hardest and most rigid type of TPU. A so high percentage of hard segment implies a scarce chain mobility, resulting in lower elongation at break. There is a low degree of phase separation due to the presence of a much higher quantity of hydrogen bonding than in other polyurethanes because of the carbonyl groups present in soft segments, able to hydrogen bonding with urethane group of hard segments. This hydrogen bonding environment favours the combination of the two phases(3). Further confirmation of this well mixing behaviour is given by the big shift in glass transition temperature between the virgin polyol and the first glass transition temperature in the polyurethane: only a well bonded hard segment can justify such an increase.

The use of polycarbonate soft segment, with higher oxidative stability with respect of ester and ether soft segment, makes it the most suitable type of polyurethane for medical devices.

## 1.2 CLICK CHEMISTRY

### 1.2.1 Click chemistry overview

The term click chemistry was coined in 2001 by Kolb, Finn and Sharpless in the review "Click Chemistry: Diverse Chemical Function from a Few Good Reactions" (4). The authors were focused on the problem of the enormous number of possible drug candidates, between  $10^{62}$  and  $10^{63}$ , and their guidance rule was "*all searches must be restricted to molecules that are easy to make*". A click chemistry reaction has to fulfil the concept previously expressed and so it must be modular, thus allowing the joining of different small modular units, providing a very high reaction yield and producing only inoffensive by-products. The process' characteristics should include only simple reaction occurring between readily available starting materials and reagent, the solvent should preferably not be used but where it is strictly necessary, it must be easily removeable. (5)

Initially studied for drugs discovery, nowadays click chemistry is mainly applied in three macro-fields: bioconjugation, material science and drug discovery.

Regarding material science, more precisely polymer engineering, in the last years lots of effort has been made in the application of click chemistry both in the polymerization reaction and in the post-polymerization modification.

Post-polymerization modification can occur basically in two different ways: chemisorption, where between the adsorbate and the solid surface there is a sharing of electrons, resulting in a covalent or ionic bond; and physisorption, where the forces at work are weaker, not implying an electron sharing but electrostatic interaction, hydrogen bond and van der Waals interaction between the adsorbate and the solid surface.

The chemisorption is desirable due to the greater stability of the attached compound.

The use of click chemistry in post-polymerization modification well addresses the need of functionalize polymers by chemisorption, using a coupling strategy that produce high yield and non-hazardous by-product, in accordance with the principles of green chemistry.

The different reactions belonging to this field of chemistry can be grouped in 4 different macro-groups, as in Figure 2.

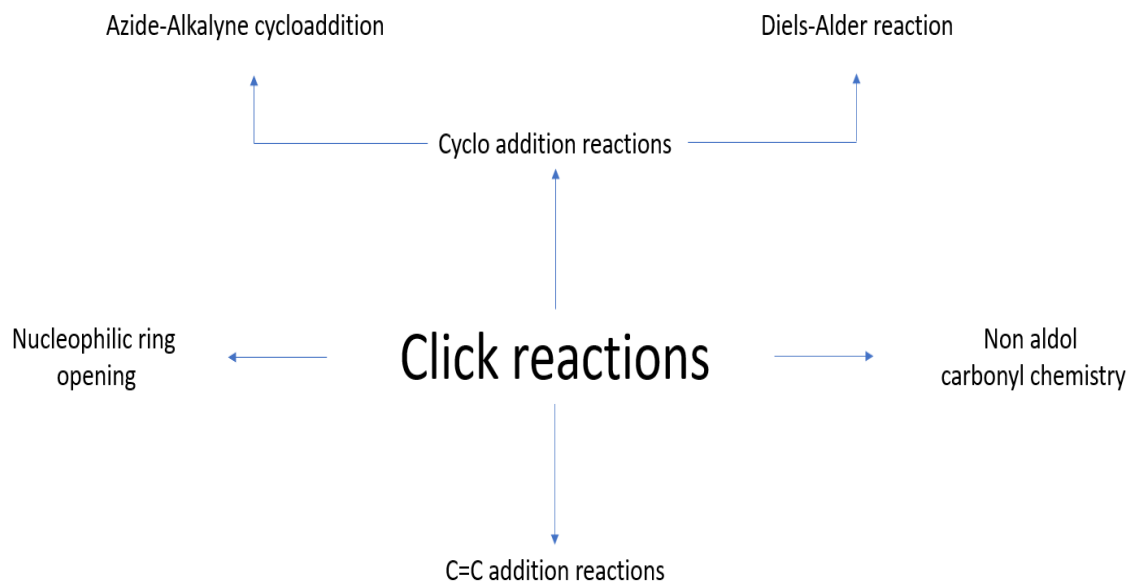


Figure 2 Click reactions

### 1.2.2 Polymer functionalization and click chemistry

The post-polymerization chemistry born to the necessity of creating complex macromolecules possessing specific properties which cannot be provided during the polymerization reactions. It permits to split the work in two different tasks: first of all, creates a polymer, easily reproducible, as saying possessing always the same degree of polymerization, tacticity and molecular weight, and in a second process, functionalizes it. This work methodology is far easier than try to make all in one step, with possibilities of undesired side reaction and with a lower control over the whole reaction.

This technique was considered for a long time as the second option, to be used only in case the direct polymerization was considered unviable. The advent of click chemistry and reversible-deactivation radical polymerization (RDRP) allowed to rehabilitate the role of

functionalization.

The progresses in chemistry were successfully applied here to create macromolecules with complex architectures and infinite different properties. Furthermore, an unprecedented precision was reached, attaching functional groups on well-defined position of polymer chain.

Guidelines in discovery of new functionalization reactions are the same of click chemistry: rapidity, absence of harmful by-product, ease of scalability, high stereoselectivity and production of stable products.

The viable ways to perform functionalization are numerous and here will be shortly explained the more used.

### 1.2.3 Thiol-Michael addition

Thiols (compound of chemical formula R-SH) are well studied and its high commercial availability make them a perfect choice for functionalization. The set of reaction involving thiols are called Thiol-X reactions. Sulphur was one of the first component used in polymer transformation processes, being used in vulcanization process of rubbers, firstly by Goodyears in 1844. But it was only at the end of the 90's when it started to begin used in post-polymerization functionalization. It is involved in the thiol-ene polymerization, a reaction employed for the end-group or side chain functionalization.

Between the different Thiol-X reactions stands the Thiol-Michael addition, a click reaction. It is defined as the conjugate addition of thiols or thiolate anions, to electron-deficient C=C bonds.(6)

During the last 20 years, it was exploited for bimolecular synthesis, surface modification, dendrimer synthesis and conjugation reactions. The reasons of his success must be sought in the easy activation of the weak sulphur-hydrogen bond and in the high electronegativity of the sulphur, which allows the initiation of reaction using different precursors under mild and solvent-less conditions.

Side-chain functionalization can be performed using a monomer containing a thiol protected group, even if Thiol-Michael addition is mainly used for end-group functionalization due to the difficult polymerization of monomers containing thiol or Michael acceptors.

Maleimides find a wide use in Thiol-Michael additions. As in the DA reaction, the more electro-deficient is the C=C bond, the more prone the molecule to undergo a Michael addition, for this reason maleimides result one of the most reactive compounds. (7)

Such reaction was used by Li et al. to attach to maleimide-containing tannic acid a thiolated carboxymethyl chitosan, with antifouling and antibacterial properties, creating a protective coating for stainless steel. (8)

Thiol maleimide reaction has been also used to produce crosslinking and fluorescent labelling agents.

#### 1.2.4 Copper-Catalyzed Azide–Alkyne Cycloaddition (CuAAC)

Most chemists agree that this specific click reaction is the spearhead of click chemistry. In azide-alkyne Huisgen cycloaddition an azide and an alkyne react together to give a 1,2,3-triazole, giving as product a mixture of 1,4-adduct and 1,5-adduct. CuAAC improve the mechanism in term of regioselectivity: only 1,4-adduct are produced. Obtained triazole is chemically inert to reactive conditions such oxidation and hydrolysis, thus resulting in a highly stable product.

As catalyst can be used copper in different forms like copper (I) salts or copper (II) salts subsequently reduced to copper (I). Cu(I) catalysts make the reaction quantitative even at low concentrations, orthogonal with other chemistries and extremely robust. (9) Concentration of Cu(I) has to be maintained at high level during the whole reaction. Copper is not the unique metal that can be used as catalyst but also iridium (IrAAC) and ruthenium (RuAAC) are reported to be effective in the formation of the substituted 1,2,3-triazoles.

Its growing application in polymer chemistry can be attributed mainly to the possibility of directly polymerize functionalized monomer and block copolymer. A good application, combined with DA cycloaddition can be found in the work of Durmaz et al. (10), where two triblock ABC type copolymers (PMMA, PS and PCL/PEG) are synthesized. Another way to exploit this technique is preparing azide-containing polymers that can subsequently undergo a CuAAC with an alkyne-containing functional group.

Finally, in the construction of complex molecular architectures, like dendrimer, functionalization of end groups by azine or alkyne groups allows ligation of polymers in well-defined positions.



## 1.2.5 DA reaction

Even if the CuAAC reaction is the most used cycloaddition in polymer chemistry (6), a powerful tool for post polymerization functionalization is the DA reaction. The importance of the discovery of such reaction, dated back to 1928, made Diels and Alder to be awarded by the Nobel Prize in 1950.

The increasing interest regarding DA reaction can be confirmed looking to the number of chemistry publication regarding this argument. In Figure 3 can be seen the ratio of chemistry publication mentioning DA reaction in the last 40 years.

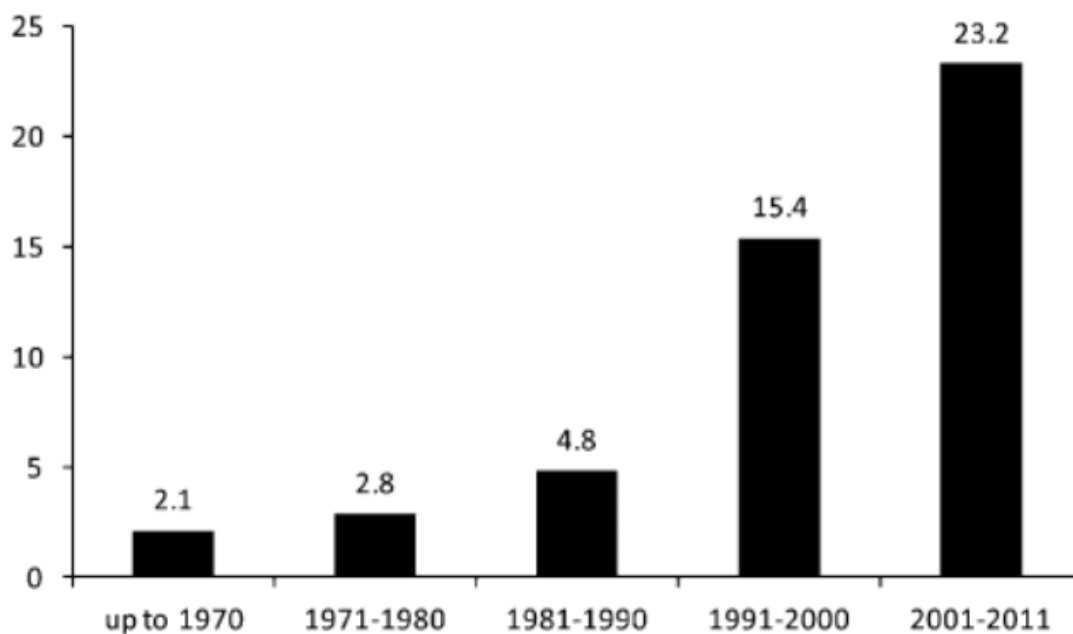


*Figure 3 Publications regarding DA reaction  
(the data are plotted as the number of chemistry publications mentioning the DA reaction over the total number of chemistry publications X 1000.) (11)*

## 1.2.6 Mechanism of DA reaction

DA reaction is a [4+2] cycloaddition involving one diene and one dienophile. Generally speaking a diene is a compound containing two  $\pi$ -bonds, most often between carbon atoms, while a dienophile, from the etymology “diene”-“o”-“phile”, is an alkene or alkyne which reacts with a diene. The cycloaddition is written as [4+2] indicating the number of  $\pi$ -electrons involved in the reaction, 4 from the diene and 2 from the dienophile; the driving force of the reaction is the formation of a  $\sigma$ -bond, thermodynamically more favourable than the  $\pi$ -bonds. Furthermore, the transition state has aromatic character, making it more stable. The process results in a high degree of stereo- and regioselectivity. The typical representation of a DA reaction can be seen in Figure 4.



*Figure 4 DA reaction's scheme*

What happens during the reaction is the overlapping of the highest occupied molecular orbital (HOMO) of the diene and the lowest unoccupied molecular orbital (LUMO) of the dienophile. The presence of electron-withdrawing substituent groups in the dienophile lowers its LUMO energy level and, at the same time, the presence of an electron-rich substituent in the diene increases the energy level of HOMO, both conditions favour the reaction to occur.

There are two important requirements to be satisfied in order to have a DA reaction: (i) the diene must be conjugated, a non-conjugated diene will never react; (ii) the diene must be able to exist in the *s-cis* conformation, it could exist in *s-trans* conformation but with a small rotational barrier.

An appreciated property of DA is that of being self-contained: all the starting atoms present in the reagents will be found in the resulting adduct.

Apart from the great variety and complexity of compound that can be created and the relatively easy way to obtain them, one of the most important properties of the DA reaction is its reversibility: providing it enough energy is possible to regenerate the initial diene and dienophile. Even if, there are some cases where the retro-DA can be considered neglectable, thus the reaction is irreversible.

The energy to push forward the reaction is usually supplied as UV-rays or, more commonly, by heat. That of temperature is an important factor to consider in the design of a DA reaction. An important role in this sense is played by entropic factors of the molecules involved in the reaction, more specifically chain length and molecular mass of side chain substituents and of the moieties directly involved in DA which provide different contribution on vibrational, rotational and transitional entropy thus influencing temperature and degree of debonding.(2)

What makes DA reaction so attractive for functionalization are the mild reaction conditions, the fact that can be performed also without catalyst and his rapidity, a part of all others click reaction's characteristics.

DA post-polymerization functionalization results to be very effective in carbon-based materials. So, it is not surprising to find it applied in one of the nowadays most studied material, multi-walled carbon nanotubes (MWCNTs). It should be pinpointed the double behaviour of the MWCNT which can at occurrence acts as dienophile or diene, lends itself to be functionalized by a wider range of molecules. From this point of view an interesting work is that published by Chia-Ming and Ying-Ling (12) where Furfuryl Alcohol (acting as diene) and N-(4-hydroxyphenyl)maleimide are alternatively attached to the MWCNT, without any pre-modification or reaction promoter/catalyst. Here, MWCNT's surface functionalization aims to improve its solubility in organic solvents.

In the functionalization of polymer, DA can occur on end-groups allowing the creation of great variety of polymer architectures like graft, heterograft and cyclic copolymer and star-shaped polymers. The most interesting applications, however, are the ones involving side-chain functionalization. Indeed, last-generation self-healing and thermo-reversible crosslinked polymer exploit the potential of DA reactions.

## 1.3 DA AND SELF-HEALING POLYMERS

Historically man-made engineering materials were created with two purposes: accomplish the specific requirements they are projected for and last long. All materials, over time, are subjected to a process of damage or deterioration. In nature, damage processes, can be healed because animals, plants, humans are living organisms which, on necessity, are able to repair injuries occurred. Starting from this principle and trying to imitate nature, scientists start to work on self-healing material, a material that is not only long-lasting but also able, upon external stimuli, to repair damages.

In last years, the interest around this kind of materials has grown enormously. Just think about the amount of money paid by industries in substitutions and repairing of installation, plants and machines; with self-healing materials a huge amount of money can be saved both in material replacement and manpower.

For a self-healing material is important not only the ability of repairing itself but also the set of properties once it is healed, which must be as similar as possible to undamaged ones. In fact, an object that only seems to be repaired but result in lower properties could be even more dangerous and implying an overall cost higher than a damaged one. This concept is well represented by concrete: a cracked column that seems to be repaired aesthetically but showing lower mechanical property could imply the collapse of the whole structure.

In the early stage, in 70's, self-healing polymer investigation was focused on polymers used in high demanding application like space exploration (Apollo and Shuttle) or ballistic missiles. (13) The need of self-healing polymers was then expanded to a wider range of applications and this can be easily explained thinking about the durability of polymeric materials. The action of stresses, chemical agent, microorganisms, photoinduced and thermal degradation heavily affect polymers and finally a replacement of the pieces results more advantageous than the reparation. Mechanisms like self-healing well fit the requirements of plastic waste reduction policies that the market is looking for.

It is possible to subdivide the different self-healing mechanisms in two different macro group: extrinsic and intrinsic. Extrinsic mechanisms, as the name suggest, relies on agents that are added to polymer, one of the first example was synthesized at the beginnings of 2000, monomer containing capsules and catalyst are dispersed on matrix and on damage are disrupted, releasing the contained monomer that react with catalyst to heal the crack. Obviously, this mechanism can happen once, so different mechanisms were studied, using, for example, interconnected vessel instead of capsules, allowing the repairing of further damages. However, the extrinsic mechanisms' concept works for a limited number of times,

until the monomer or catalyst end. This was the reason that push onward the research towards different solutions, leading to development of the intrinsic self-healing mechanism. This technique exploits the temporary increasing of mobility of the chain to stimulate a reflow of the material in the damaged zone. Such a behaviour is possible thanks to particular molecular structures, which favour the reformation of chemical and physical bonding, under external stimuli. No external agent is inserted in the polymer and theoretically there is no limitations in the number of repairing events, making it preferable to extrinsic mechanisms.

The most attracting intrinsic techniques are the ones based on reversible reactions happening in the polymer backbone because the healing effect can be controlled by ionic or supramolecular interactions or by external stimuli such as light and temperature.

The temperature-dependent reversibility, the not necessary use of catalyst and the high yield of DA were obviously exploited in this sense, becoming one of the most studied technique for intrinsic self-healing.

Fundamental property of a self-healing polyurethane is the high mobility chain, which aim to rapidly close the crack. In this sense, low molecular diols are used.

Polyurethanes, unlike most of polymers, thanks to the urethane bond can maintain structural integrity at the high temperatures at which lots of retro-DA reactions take place.

In the work of B. Willocq et al.(14) furan and maleimide-based diol monomers were synthesized in four steps and incorporated in polyurethanes with the presence of 1,6-hexamethylene diisocyanate (HMDI) and polypropylene glycol soft segments (PPG), in dimethylformamide (DFM) at 70 °C for 6 hours, obtaining a gel. Maintaining constant the molar ratio (1:1) between maleimide diols and furfuryl diols and that between urethane group and hydroxyl group, they prepared three different polymers changing the molar ratio between DA moieties and PPG and using different molecular weight PPG.

Polymer	$n_{\text{DA-diol}} : n_{\text{PPG}}$	$M_w$ PPG ( $\text{g mol}^{-1}$ )	$M_n$ ( $\text{g mol}^{-1}$ ) <sup>a</sup>
PU1	75 : 25	2000	9500
PU2	90 : 10	2000	8700
PU3	90 : 10	1000	ND <sup>b</sup>

Table 1 Table representing the three types of polyurethane synthesized. a) GPC in THF b) Not soluble in THF (14)

To determine the thermal reversibility, the solution was heated at 130 °C for 2 hours resulting in de-reticulation and dissolution in DFM, assessing the effective DA adduct dissociation. Furthermore, storage modulus ( $G'$ ) was measured during a Dynamic Mechanical Analysis (DMA). Just the results for PU2 are reported because the other two polymers show similar behaviour.

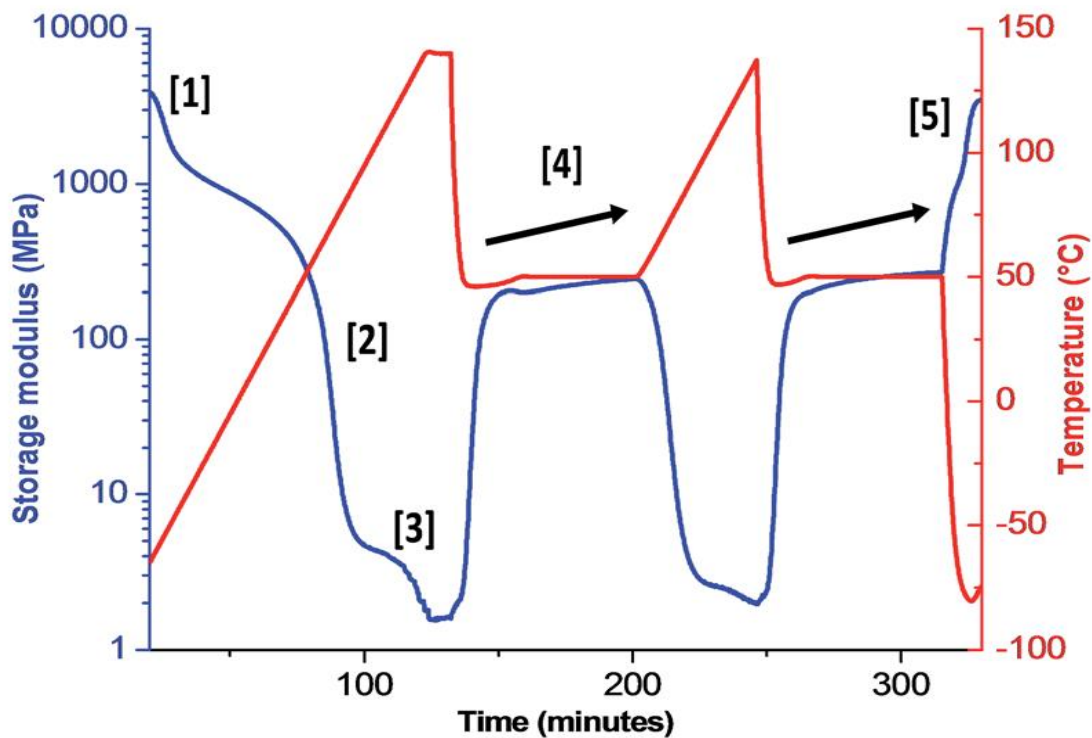


Figure 5 DMA curve after two heating/cooling cycles of PU2(14)

As can be seen, leaving apart the first two transition at  $-50\text{ }^{\circ}\text{C}$  and  $60\text{ }^{\circ}\text{C}$ , the third one at  $130\text{ }^{\circ}\text{C}$  is attributed to the de-crosslinking by retro-DA process. Two cycles were performed and both show analogous behaviour, assessing the good thermal reversibility of the sample, confirmed also by the similar values of  $G'$ . The DMA analysis of the three different polyurethanes corroborates that shorter chains exhibit better  $G'$  recovery with respect to longer ones. Furthermore, how easily can be intuited, a higher concentration of DA moieties results in a more crosslinked network.

The scratch recovery test shows a different situation for which regard the self-healing capability: the polymer with lowest molecular weight PPG has the worst healing behaviour, opposite from which was stated before. The explanation is found in the high crosslink density, which hinder chain mobility. Same bad healing behaviour is exhibited by the polymer with lowest density of DA moieties, here the reason is precisely the low amount of DA moieties, responsible for the healing behaviour. The polymer with intermediate characteristic (high density of DA moieties and medium crosslink density) shows the best performances, with a breaking strain and tensile stress recovery of 40 and 68% after 30 min at  $130\text{ }^{\circ}\text{C}$  and 24 h at  $50\text{ }^{\circ}\text{C}$

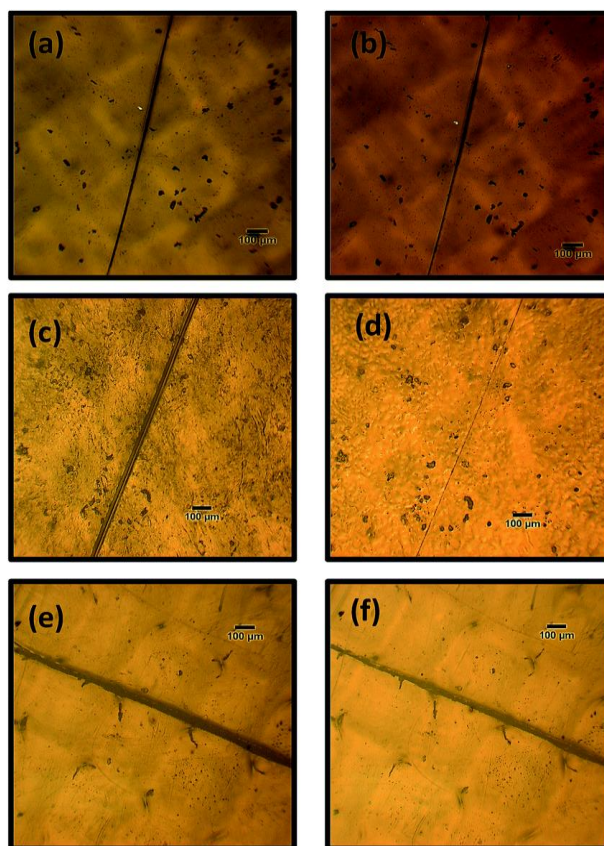


Figure 6 Healing performance of the three thermo-reversible polyurethane after 20 minutes at  $140\text{ }^{\circ}\text{C}$ : PU1 (a,b); PU2 (c,d); PU3 (e,f) (14)

## 1.4 DA REACTION AND THERMOSET POLYMER RECYCLING

In 2016 the recycling of plastic material worldwide, was about 10% (1). Regarding the recycling, the classification of the polymer in thermoplastic and thermoset, for long time, has been synonym of recyclable and non-recyclable. Thermoplastic polymer from a technological point of view are recycled quite easily, while the recycling of thermoset polymer is considered a very challenging goal. The roots of this different behaviour can be found in the chemical structure of the two classes. Thermoplastic polymers are characterized by the presence of physical entanglements. These physical entanglements are easy to break and can be re-melted once their lifetime has ended. Obviously, the overall properties will not be the same and the melted product is usually mixed with virgin material or is used to realize component with less demanding performance requests, thus allowing the recycle of the thermoplastic polymer in a relatively easy way.

Thermoset polymers, in contrast, are characterized by bridging or crosslinking chemical bonds. The presence of such bonds allows thermosets to reach a more stable and durable material with respect to the thermoplastic polymer. Nevertheless, properties that are advantageous during the lifetime of this kind of polymer, become unwanted and annoying problems in the end-of-life treatment.

There are basically three different ways to recycle plastics: mechanical, chemical and thermal processes. Thermal processes are ineffective from a recycling point of view, because heating up thermoset polymers has the unique effect to degrade them. Chemical processes are also ineffective, cause this material, as intrinsic characteristic, has a good resistance against chemical agents. Mechanical processes are, so far, the most promising processes applied. It consists in cutting and grinding the polymer in flakes of size in the order of millimetres and then reuses it as low-performing filler, in a down-cycle process. Nevertheless, the use of thermoset polymer as matrix in composites makes it difficult to separate from the fillers and fibrous reinforcements. For these reasons, most of the time thermoset polymers are burned in order to recover energy or disposed in landfill. (15)

Researchers have focused their efforts basically in three different ways, all with the same objective, finding a polymer structure that is able to debonding using a low energy demanding mechanism. Mechanisms investigated were polymer degradation in low molecular weight substances, oligomers/monomers recovery and network de-crosslinking.



The idea of de-crosslinking thermoset polymer is based on the DA reaction thanks to its temperature-dependent reversibility. In this sense, an interesting work is the one of Q.-Y. Wu and L. Gu. (16), where the synthesis of a biobased, self-healable and recyclable polyurethane is presented. The polymer is synthesized by prepolymer polymerization, using as prepolymer polylactide copolymer diol and diisocyanate and as chain extender 2,5-furandimethanol (BHFMD). The reversible crosslinking is reached using bismaleimide which react with the furan groups present in the backbone of polyurethane. Resulting polymer possesses high molecular weight ( $2.7 \times 10^4$ ), high values of elongation at break and Young modulus if compared with the high molecular weight PLA.

The effective thermal recyclability and remoldability were assessed using two different methodologies. In the first one, a sample of polymer was immersed in N,N-dimethylformamide (DMF). At room temperature the polymer is only swollen, the network constituted by the DA is still connecting the polymer chains. Instead, when the temperature reaches 130 °C, the retro-DA occurs, destroying the network and dissolving the polymer in DMF. The recycled polyurethane swell in the same way of the virgin one and the elongation at break are almost identical, although the tensile strength decrease.

In the second method, cracked polyurethane pieces are remoulded under a pressure of 10 MPa at 160 °C for 10 minutes, reforming a solid polymer film. The mechanical properties also here are lower and this can be attributed to a minor crosslinking density, resulting from the loss of bismaleimide at high temperature.

Another example will be presented, where furan moieties are not directly incorporated in polymer backbone but are present as a pendant group (17) . Here a Poly(ethylene glycol) diglycidyl ether (PEGGE) is functionalized using furfurylamine and then crosslinked using bismaleimide. After 24h in DMF at 65 °C, the polymer became a gel without flow. 5 minutes at 120 °C are sufficient to disrupt the polymer structure and return to its initial state. The process can be repeated many times, demonstrating the thermal reversibility of the material. In this case, the mechanical properties of the recycled polymer are quite similar to the virgin material, demonstrating the high recycling ability of the material.

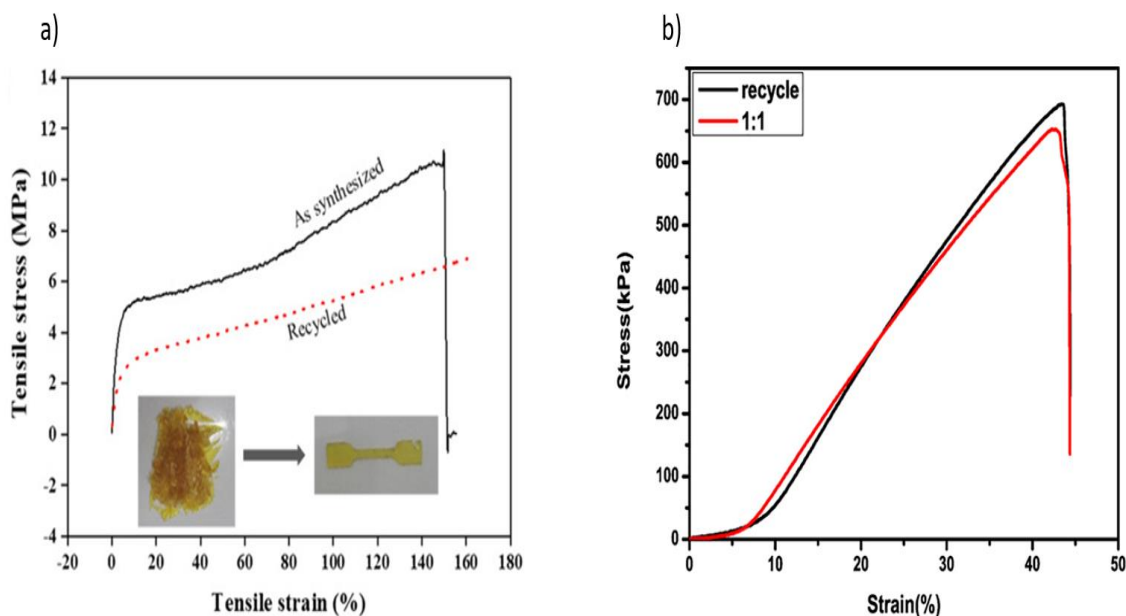


Figure 7 Stress-strain curve of polymer: a) with furan in backbone and b) with furan as pendant group (16,17)

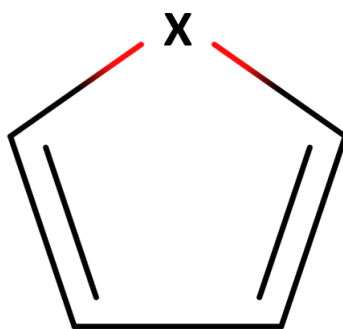
Comparing these two different studies, seem that the polymer with furan pendant group, once recycled, is able to recover the virgin material mechanical properties, while the one with furan in backbone, once recycled, reaches far lower mechanical properties than the virgin material ones, despite the fact that the methodology of recycling is the same. It can be due to the higher mobility of furan pendant groups, which favour the crosslinking process and so the crosslinking density, that is the main responsible for the mechanical properties of polyurethane synthesized in this way.

## 1.5 FURANS

The name furan comes from the Latin word “Furfur” which means bran or zest of the grain. This might be due to the source of this molecules, which can be obtained by lignocellulosic biomass.

Furan, with chemical formula  $C_4H_4O$  is also called in IUPAC denomination 1,4-epoxybuta-1,3-diene or 1-oxacyclopenta-2,4-diene. It was firstly discovered by Heinrich Limpricht, a chemist who studied pyrrole and furans, the 29<sup>th</sup> of January of 1870. (18)

It is a colourless liquid soluble in most organic solvents with a boiling point of 32 °C. It is carcinogenic in human diet and can be encountered during thermally driven processes in foods like baking, pasteurizing, roasting and sterilizing.(19)



X=O, furan

X=NH, pyrrole

X=S, thiophene

*Figure 8 Unsaturated heteroaromatic compounds*

Furan is a heterocyclic compound, more precisely a five membered unsaturated aromatic ring where a carbon is substituted by an oxygen. It belongs, together with pyrrole and thiophene to the series of unsaturated heteroaromatic compounds. All the chemical compounds containing such structure are referred as furans. Furan possesses four different resonance structures but, since the substitutions occur mainly on the carbon C5 and on carbon C2, the structure represented above is the predominant resonance structure. Furan

shows the highest diene and the lowest aromatic character with respect to pyrrole and thiophene, properties that explain its wide use as diene in the DA reaction.

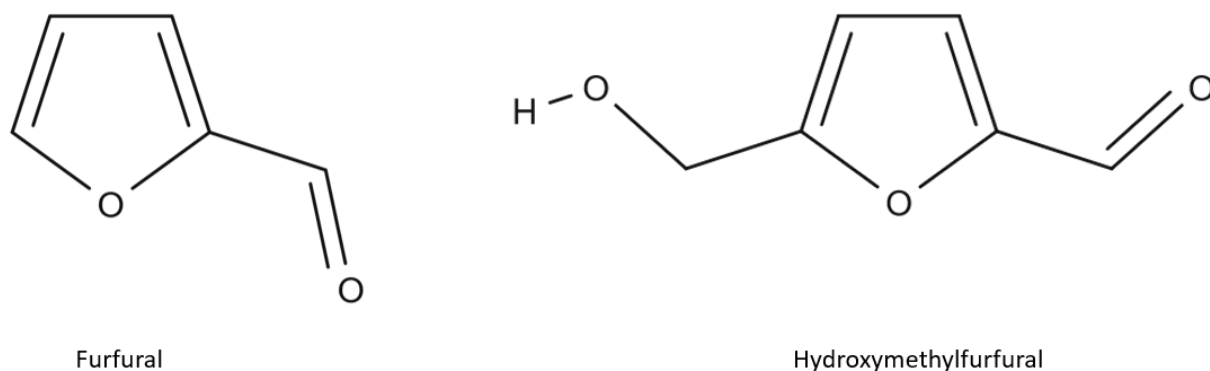


*Figure 9 First-generation Furan*

Talking about the synthesis, we find two first-generation furans, 2-furancarboxaldehyde (called Furfural) and 5-hydroxymethyl-2-furancarboxaldehyde (hydroxymethylfurfural or HMF) from which all the other furans are obtained. As the etymology of the name suggest, furfural can be produced from different vegetal biomasses containing pentoses, like corn cobs, sugar-cane bagasse and wood chips, by an easy and cheap process. The global market size of furfural was estimated around USD 1.2 billion in 2019 and is expected to reach 2.1 billion on 2027. (1)

Hydroxymethylfurfural is produced using the same processes of furfural but from different biomass sources containing hexoses like sucrose, glucose, fructose.

These two first-generation furans are mainly used in the production of furfuryl alcohol which is then converted in 2,5-bis(hydroxymethyl)furan by formylation (20).

In the process of substituting petroleum-based product, a great step forward was done in epoxy resin field, where the petrol-based networks from diglycidyl ether of bisphenol A (DGEBA) holds a market share of 90%. Furan-based bioepoxy resins from 2,5-bis((oxiran-2-ylmethoxy)methyl)furan (BOF) have been reported(21,22) outperforming DGEBA from a mechanical point of view, with higher tensile and flexural strength, a higher crosslinking density and better performances against fire. However, BOF based epoxy resins are characterized by lower decomposition temperatures.

## 1.6 MALEIMIDES

Maleimide, reduction of the name maleic acid imide, is a compound, with chemical formula  $\text{H}_2\text{C}_2(\text{CO})_2\text{NH}$ , formed by the reaction of maleic anhydride and ammonia. It makes parts of the bigger family of maleimides, that are produced by the same reaction but using amines instead of ammonia.

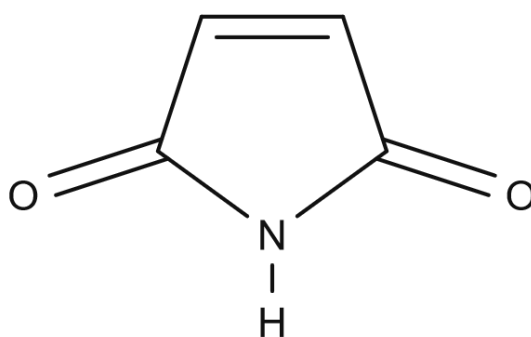


*Figure 10 Maleimide*

This class of heterocyclic compound finds a wide range of applications thanks to its double bond that can easily participate in Michael addition, where most of the time reacts with thiols, and DA reaction, where it reacts mainly with furans. The high reactivity of  $\text{C}=\text{C}$  bond in maleimides seems to be due to two main factors: (i) the bond angle distortion and the ring strain and (ii) the carbonyl groups being in the cis-conformation.<sup>(7)</sup> Furthermore, it possesses the amine group, one of the most versatile linkage in chemistry. The position of double bond and amide group allows maleimide to be functionalized, avoiding the steric hindrance that a big and complex substituent could imply, thus leaving double bond prone to further reactions. High reactivity of the double bond makes its production not simple and usually implies the use of protected-maleimide. The principle is to “protect” the molecule from unwanted reaction by bonding it with an easily cleavable molecule, in order to activate it exactly when it is needed.

The great variety of possible compounds obtained from maleic acid, using amines with different substituent groups creating, for example, fluorescence emissive group, make

maleimides perfect for production of organic functional material or its use as detector of thiols in biological systems. In this study, the success of DA reaction was assessed using exactly a fluorescent maleimide compound.

Another important application in the field of polymer chemistry is its use as crosslinking agent in the form of bismaleimide.

## 1.7 MALEIMIDE COMPOUNDS

Maleimide is an easy functionalizable molecule, thanks to the high reactivity of the NH group and N-substituted maleimides are synthesized by numerous strategies. The most commonly used method is the reaction of maleic anhydride with primary amine derivatives leading to maleamic acid intermediates, which are subsequently dehydrated into the corresponding cyclic maleimides. (23)

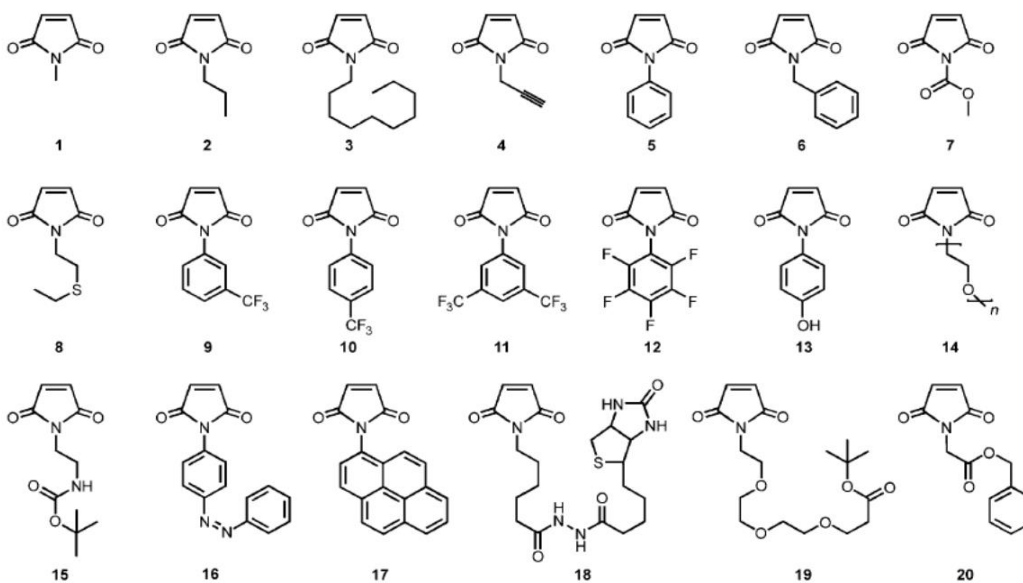


Figure 11 Examples of N-substituted maleimides (23)

This results in a wide range of commercially available compound, easy to modify at necessity and providing an enormous source of functionalizing maleimides.

Antimicrobial, flame retardancy, anti-inflammatory and labelling agents are just some of functionalizing properties, which can be provided by maleimide-containing molecules.

### 1.7.1 Flame retardant

Flame retardants are fundamental compounds in polymers. In the last years, lots of efforts have been spent to find an alternative to the toxic halogen-containing flame retardants. Phosphorus-containing flame retardants have stood out among the others and it has been observed that the incorporation of functional groups such as S-triazine, triazine-trione, phosphaphenanthrene, phosphazene, silsesquioxane and maleimide enhance the flame retardance properties. (24)

In the study of Fang et al. (25) a flame retardant, showing three maleimide terminations, was synthesized making react *N*-(2-hydroxyethyl)maleimide (HEMI) and hexachlorocyclotriphosphazene (HACTP) as shown in Figure 12.

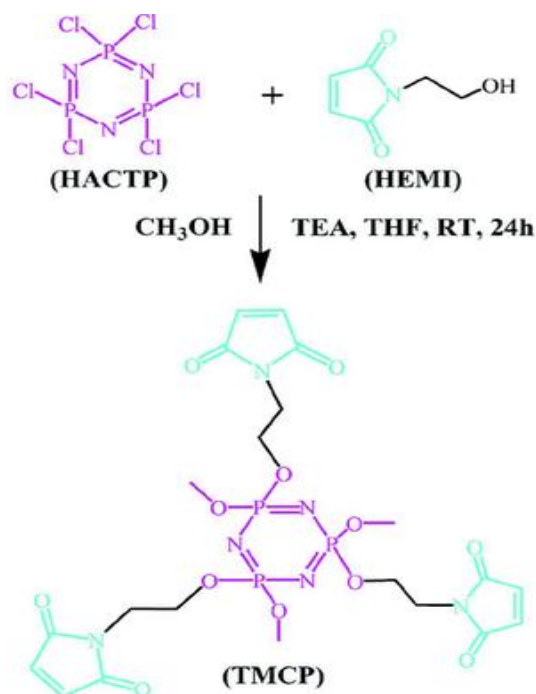


Figure 12 Flame retardant crosslinker containing maleimide moieties (25)

This flame-retardant acts on the char formation, decreasing the  $T_{d5}$  (temperature at which the sample loses 5% weight and increasing the loss weight rate). The phosphorus compound acts as a porous phase which favors the formation of char, shielding the surface from air. No



phosphorous-containing volatile product has been detected during the process.

In the work of Yang et al.(24) hexa(4-maleimido-phenoxy)-cyclotriphosphazene (HMCP) has been synthesized by nucleophilic substitution reaction starting from HACTP and N-(4-hydroxyphenyl) maleimide, resulting in a molecule containing six maleimide terminations. It has been tested as flame retardant in epoxy resins, reaching a classification of V-0 without dripping in the UL 94 standard and a limiting oxygen index (LOI) of 35% when a HMCP weight content of 17% was added.

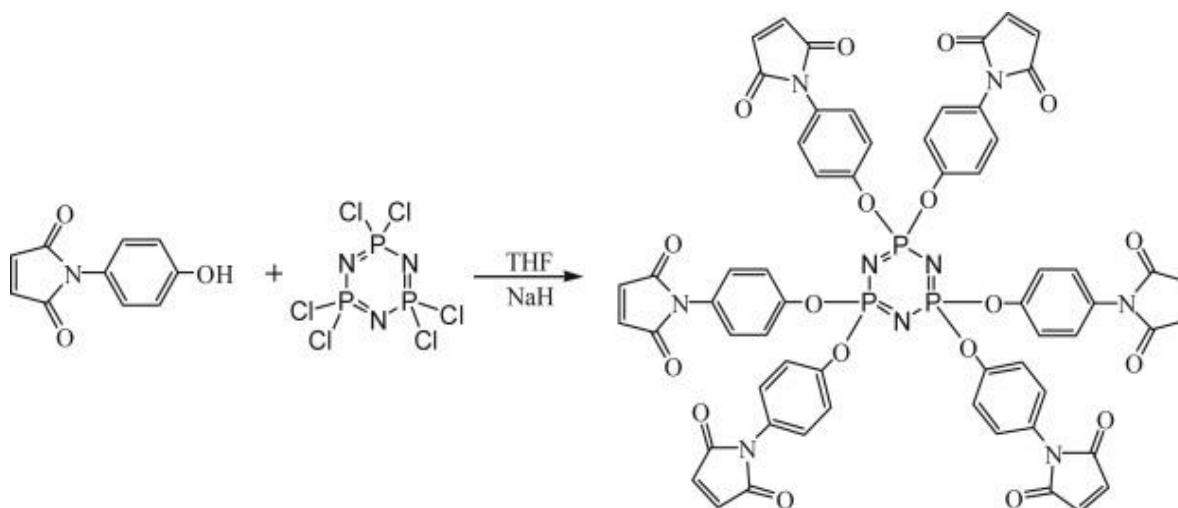


Figure 13 Synthesis of HMCP (24)

### 1.7.2 Antibacterial, antifungal and cytostatic activity of maleimide-containing compounds

The problem of microbial resistance to antimicrobials has always been a problem in medicine and research on this field is a continuous discovery of new suitable compounds. Since 1990s N-substituted maleimide are known to display an important antifungal and antimicrobial activity.

In the study of Singh et al. (26) three different chloro-substituted *N*-phenyl maleimide were synthesized and their antimicrobial activity were evaluated.

The presence of chlorine imparts antimicrobial properties to all three maleimides compounds even if the 4- substituted ones show the best antimicrobial activity, against all kind of bacteria.

Lots of studies have been performed, testing a great number of N-substituted maleimides like the one of Salewska et al. (27) where twelve different compounds were tested. All show antibacterial and antifungal activity even if at different levels.

These properties, possessed by a great number of maleimide compounds, could be exploited in the production of antimicrobial and antifungal polymer surfaces, strongly required in hospitals.

### 1.7.3 Drug delivery nanoparticles

Drug delivery systems have been widely investigated in the last years, involving researchers from different fields: organic chemists working on metalorganic frameworks, biologists creating delivery membrane and also polymer chemists investigating polymer nanoparticles.

An interesting work in this sense has been published by Meng et al. (28) . They succeeded in synthesizing a self-assembled nanoparticle from an amphiphilic copolymer. This copolymer as can be seen from the Figure 14, has furan pendant groups on the outer corona which can easily undergo a DA reaction. In this case, maleimide functionalized anti-bodies were clicked to furans. The so-created particles can be delivered to target cells which express the corresponding antigen receptors, resulting in a versatile method to create drug delivery systems with well-defined target cells.

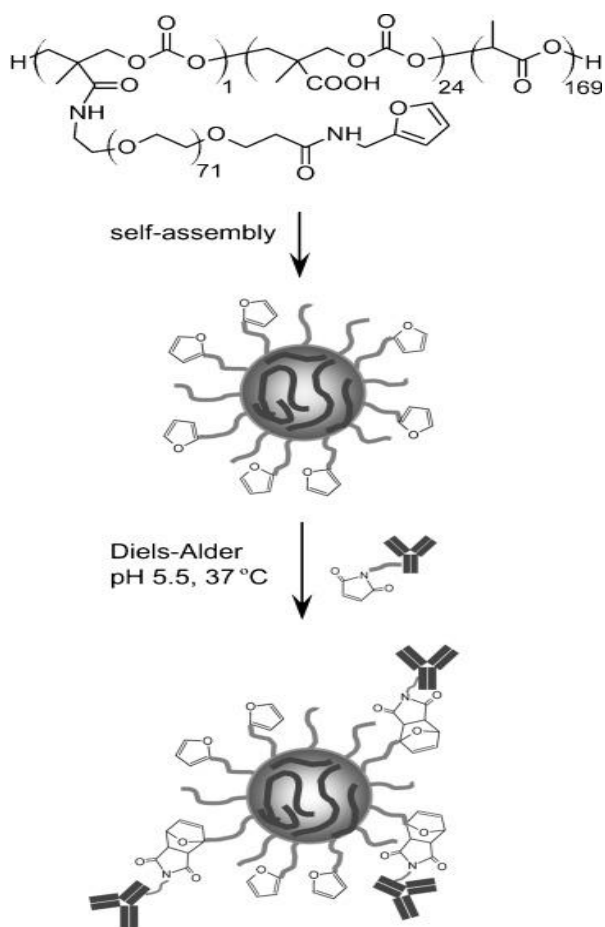


Figure 14 Self-assembly and functionalization of poly(TMCC-co-LA)-g-PEG-furan (28)

## 1.8 SMART TEXTILES

Generally, when we talk about a smart structure, we refer to something that, once subjected to a stimulus, can identify and interpret it, responding in a well-established and predetermined manner. A plant or a cell, for example, are able to detect what is happening in the surrounding environment, to process the information received by the receptors and to elaborate a response, with the aim of adapt itself to different situations.

It is not a novelty that material scientists try to create new materials imitating nature. The same has occurred with smart materials which can react to stimuli or changes in the surrounding environment. Based on the type of response we can subdivide smart materials in three different classes: passive, active and very active materials. Passive smart materials can only sense the environmental conditions or stimuli; active smart materials will sense and react to stimuli; very active smart materials can sense, react, and adapt themselves accordingly. (29)

Such materials have been applied in textile engineering to produce the so-called smart textiles. The way the fibers elaborates a stimulus and a response can be mediated by electronic devices (electronic textiles) or be an inherent property of the material used. An essential requirement, however, is that the resulting garment maintains the wearability, washability and mechanical resistance proper of a normal textile cloth.

Uncountable studies have been published about different solutions for smart textiles: nanoparticles used as filler, functionalization of surfaces by coating deposition or immersion in solutions and some examples of functionalization of fibers by the mean of click chemistry. This last method is the most related to the present work and some examples will be illustrated.

Shuoao et al.(30) success to functionalize cotton fabric grafting a N-isopropylacrylamide (NIPAAm) by UV-induced thiol-ene click reaction. NIPAAm is a temperature responsive smart material showing a transition temperature of 32 °C. Below this temperature, it undergoes a reversible lower critical solution temperature (LCST) phase transition, assuming a stretched molecular configuration which makes it hydrophilic. Above LCST the molecular configuration is shrunk, conferring it a hydrophobic behaviour.

The use of UV-induced thiol-ene reaction has a double advantage : it does not affect too much the hand feeling and is it possible to functionalize just one side of the final piece (illuminating it by UV light), avoiding possible unwanted consequence of direct skin contact.

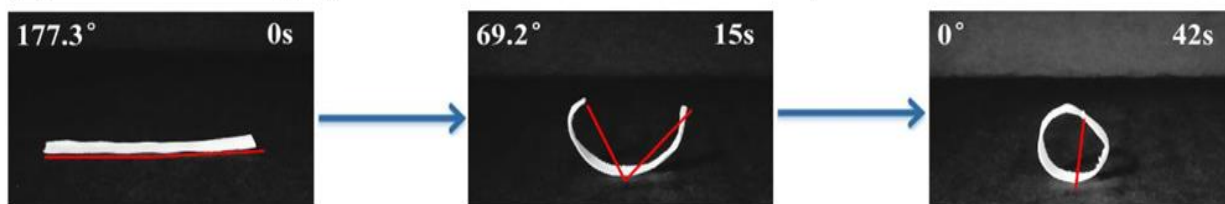
The so-created textile has been found to be responsive also to environmental humidity. Functionalization happens in two steps: initially, 3-mercaptopropyltriethoxysilane (MPTES)

is dissolved in a solution of ethanol and water and the cotton is immersed in it to obtain the thiol-based cotton fabric. Then click reaction to graft NIPAAm using UV radiation is performed.

The resulting surface bends when humidity decreases and temperature increases and vice versa, with a shape recovery of 82%, as shown in Figure 15.

A less grafting amount of the surface is reached with respect to traditional coating methods and this could influence the shape recovery ratio, although it assures a higher softness of the fabric.

(b) DRCF bending by thermal actuation in 50 °C dry air



(c) DRCF unfolding upon cooling down in moist

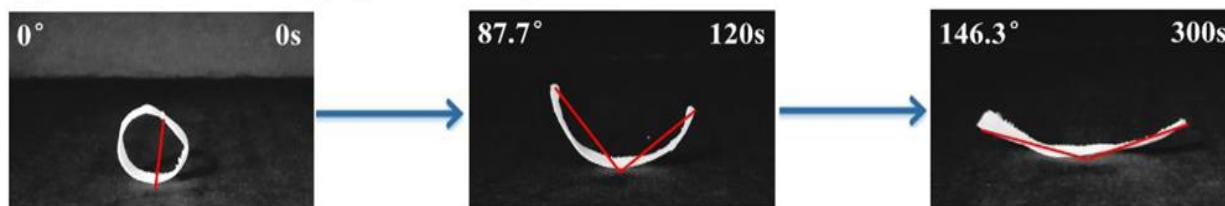


Figure 15 Shape memory behaviour of functionalized cotton (30)

Zhenjun et al. (31) perform the functionalization of azide-decorated polyimide nanofibers using alkyne terminated poly(methyl methacrylate) (PMMA). The process consists in the electrospinning of polyamic acid (PAA) followed by thermal imidization to obtain polyimide nanofibers (PI). Then is carried out a complicated process of functionalization involving the chloromethylation and azidization of PI nanofibers, the preparation of alkyne-terminated PMMA by ATRP of methyl methacrylate and click coupling between the azidized PI nanofibers and the alkyne-terminated PMMA using catalysts. Resulting fibers show a better interface compatibility with host matrix of PMMA.

In biomedical application, polymers nanofiber matrices are widely use thanks to their similarities with natural extracellular matrix, so, there are lot examples of conjugation of specific proteins or antibiofouling and antibacterial compounds.

The study that most resemble the idea of the present study is the one of Becker et al.(32). To an amino acid-based poly(ester urea)s (PEU) are incorporated pendant species via interfacial copolymerization. The pendent species include alkyne, azide, alkene, tyrosine–phenol, and ketone groups, in order to try different type of click reaction. The effective incorporation of clickable groups was confirmed by H NMR. The resulting polymer is dissolved in hexafluoroisopropanol (10 wt%) to operate electrospinning.

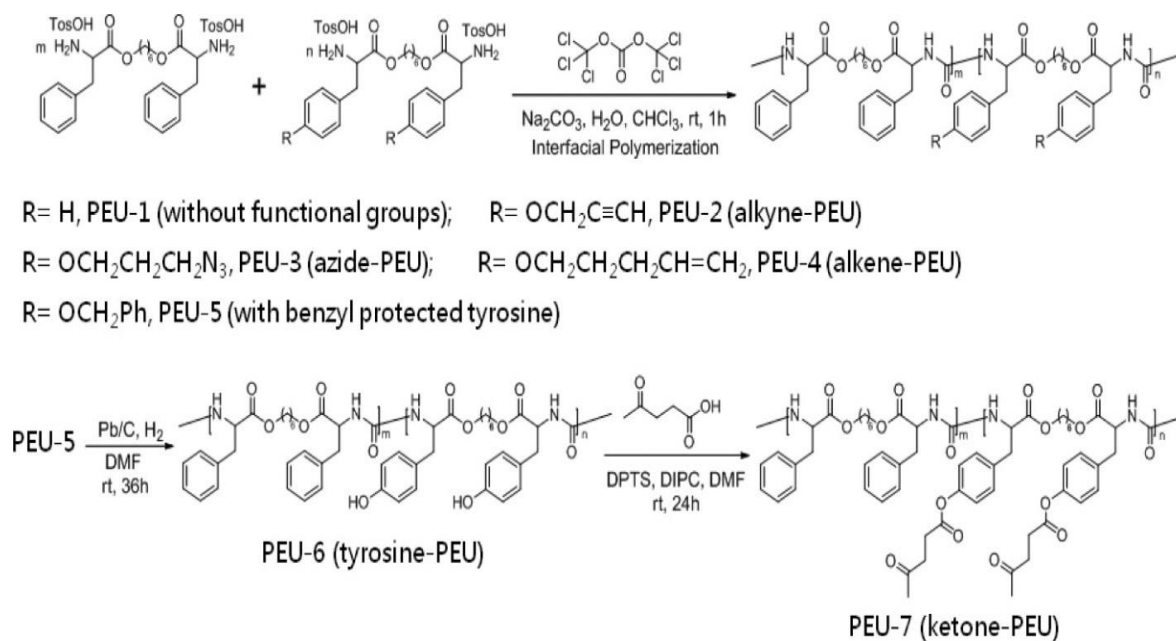


Figure 16 Different type of PEU produced by Becker et al. (31)

Seven different fibers were produced (Figure 16).

No differences were encountered during electrospinning between the PEU homopolymer and the functionalized ones.

All the different groups are incorporated and available for functionalization: CuAAC was used in PEU-2(alkyne-PEU) and PEU-3 (azide-PEU), thiol-ene addition was performed with PEU-4 (alkene-PEU) and oxime ligation occurred on PEU-7 (ketone-PEU). The “ene”-type addition was tried on PEU-6(tyrosine-PEU) but with no results because the reaction needs a strong basis which is incompatible with PEU.

Some methods involve the use of toxic catalyst, others need a complicated three-step functionalization and the majority utilizes polymers difficult to synthesize.

The idea of exploiting the DA reaction, instead, allows to functionalize polymer in a relatively easy way. In fact, producing a fiber which already contains the diene, will speed up the process, avoiding the tedious and not easy step of grafting diene to electrospun polymer and allowing a better distribution of diene along the fiber.

## 1.9 ELECTROSPINNING

The electrospinning is a technique employed to produce continuous and defect-free fibers of very small diameters, ranging from 2 nm up to micrometers, using electrostatic forces. The typical apparatus used in polymer fibers production is shown in Figure 17 and comprises: a spinneret, from which the polymer solution is extruded, a high voltage power supply and a plate, grounded, where the material is collected. There are two different assets, vertical and horizontal, the latter configuration is the one represented here.

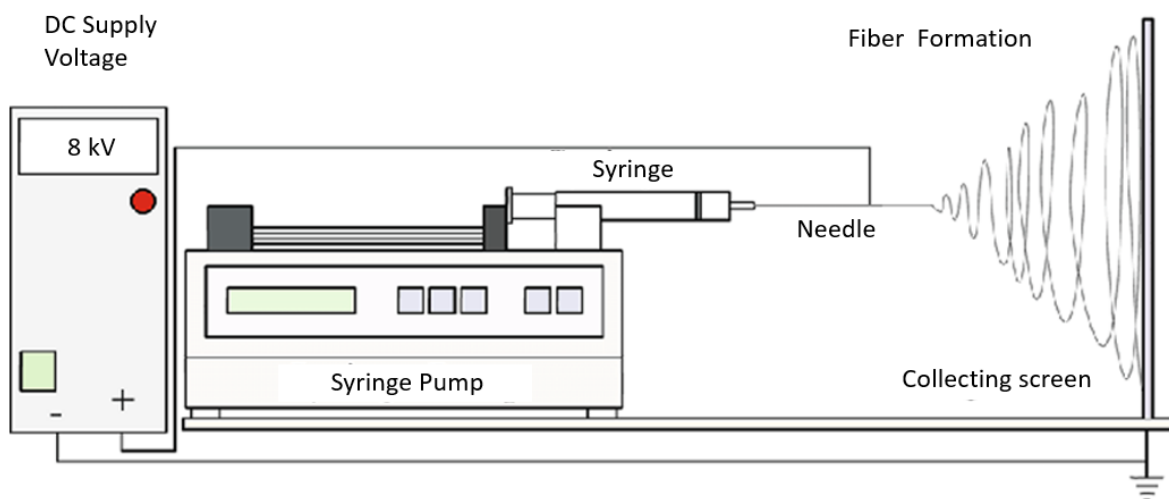


*Figure 17 Horizontal electrospinning setup (32)*

Polymers can be dissolved in solvent or present as melt. Once the electric field is applied on the spinneret's tip, where a drop of the polymer solution is held, an electric charge is induced on the surface of the drop. The electric field is adjusted in order to reach a critical value that allows the electric repulsive force to overcome the superficial tension of the liquid, destabilizing and stretching the drop in a shape called Taylor cone from which, finally, a filament of the solution starts to stream towards the grounded metal plate. In the space between the spinneret and the collecting plate, solvent evaporates, thus the collected material results in a polymer fiber.

Different parameters influence the process: solution properties (viscosity, conductivity, surface tension), distance between tip and collector, humidity, applied voltage, temperature.



## 1.10 CHARACTERISTICS OF THE POLYMERIC SOLUTION INFLUENCING THE ELECTROSPINNING PROCESS

### 1.10.1 Viscosity

Viscosity is considered a parameter playing a fundamental role in determination of final fiber's diameters and in the possibility or not to electrospinning the solution. Indeed, a critical amount of chain entanglements are needed to obtain a fiber. A too low viscosity results in interruption of filament, with creations of droplets (converting electrospinning in electrospray) in the worst case or with formation of beaded fibers due to a capillary wave breakup (Rayleigh instability).(33) The reason is that the coiled macromolecules of the dissolved polymer are transformed by the elongational flow of the jet into oriented, entangled networks that persist as the fiber solidifies. The contraction of the radius of the jet, which is driven by surface tension, causes the remaining solution to form beads. (34)

Increasing the viscosity of the solution, beads become bigger and the distance between subsequent beads lower, till they start to coalesce passing from spherical to spindle-like beads. During this process, the diameter of the fiber increases. Higher the viscosity, less defective the resulting fiber as can be seen from Figure 18. However, after a certain limit which differs for each solution, flow instability occurs due to high cohesiveness.

In general, a spinning solution with a viscosity of 1-20 poise values and surface tension of 35-55 dyn cm<sup>-2</sup> is considered a solution suitable for electrospinning. At viscosities of more than 20 poise, electrospinning is prevented. (35)

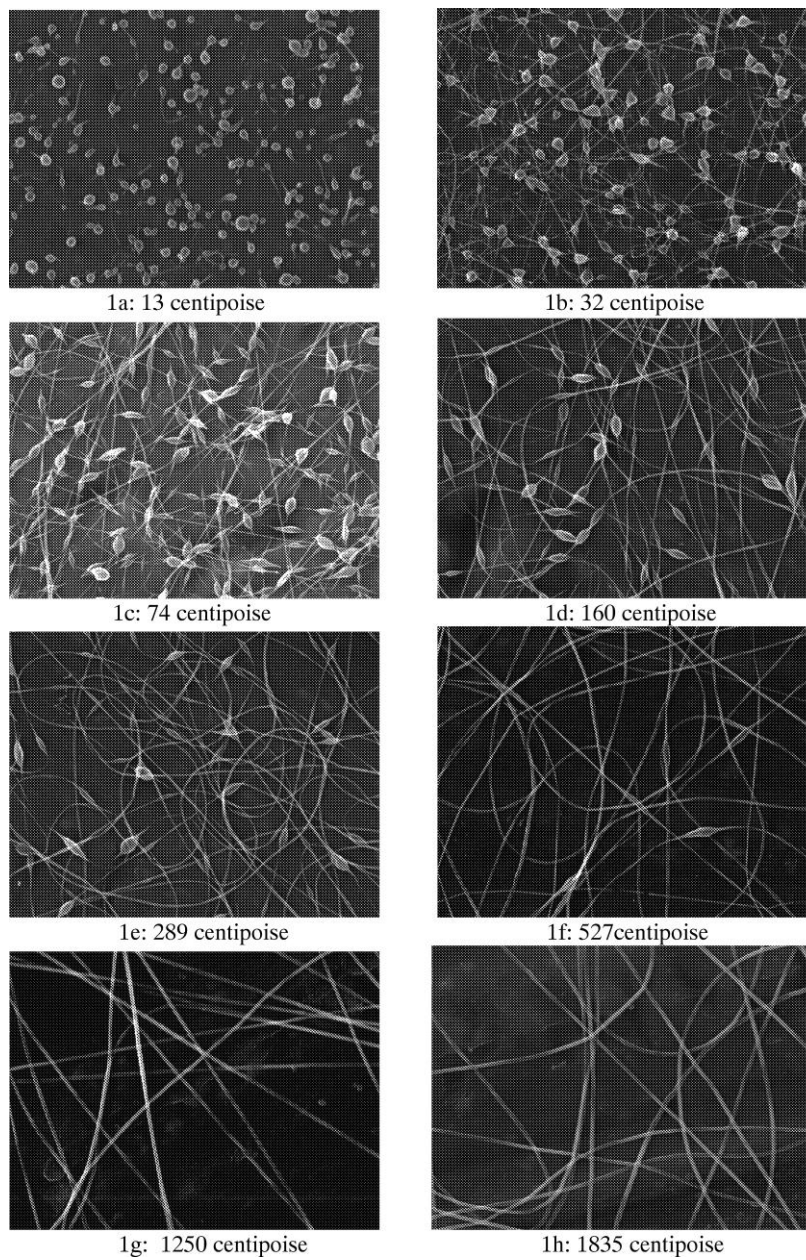


*Figure 18 Fibers resulting from electrospinning process at increasing viscosity of solution (34)*

### 1.10.2 Electric field and distance

Increasing the voltage and so the electric field strength (always remaining between the workability range) results in higher quantity of deposited fiber: a higher electrical field means a bigger amount of material that can be carried by the jet. Fiber diameter, however, decrease with the increase of electric field because of the more accentuated stretching provoked by a higher electrostatic force ( $f_e$ ) acting on the jet.

The formula regulating the electrostatic force acting on the jet is:

$$f_e = \frac{e(t)V}{h(t)}$$

Where  $e$  is the charge on the jet,  $V$  is the applied voltage, and  $h$  is the distance from the tip of the jet to collector.

From the previous formula can be seen that increasing the distance, the electrostatic force decreases, and with it decreases also the stretching, giving fibers with bigger diameter.

However, this is true only for the polymer melt because such behaviour is not encountered in solution electrospinning. (36)

It is reported in literature the possibility of a multiple jets formation, given by the high voltage applied. This has to be ascribed to the increase in the charge per unit area, which creates instability in the initial jet resulting in a split, necessary to reduce the charge per unit area.

### 1.10.3 Surface tension

Surface tension influences electrospinning and can be regulated working on the polymer solution. The solvent in this case plays a fundamental role and during its choosing must be taken into account its influence in determining surface tension, viscosity and solubility of the polymer.

For example, using solvent that easily evaporates during the process, like ethanol, assures an increase of viscosity, thus slowing the beads formation rate.

As explained before the ideal surface tension depend on the electric field applied.

#### 1.10.4 Temperature

Further variable in the machine setup is the temperature. In fact, it determines the viscosity of the solution in the spinneret and the solidification of the fiber once it reaches the collector. A too high temperature favours a low viscosity but not allow the fiber to solidify enough, while a too low temperature imply a low viscosity, not suitable for electrospinning.

#### 1.10.5 Molecular weight

Molecular weight affects rheology properties and electrical conductivity of the solution. As written by Koski et al. (37) at lower molecular weights ( $9.000-13.000 \text{ g mol}^{-1}$ ) correspond a non-completely stabilized and a bead-on-string structure. The diameter is between 250 nm and  $1 \mu\text{m}$ , with circular cross-section. Using higher molecular weight ( $13.000-23.000 \text{ g mol}^{-1}$ ) results in a stabilization of fiber structure with circular cross section and increased diameter ( $500 \text{ nm}- 1.25 \mu\text{m}$ ). Increasing the molecular weight ( $31.000-50.000 \text{ g mol}^{-1}$ ) the fibers produced are flat with an average size of  $1-2 \mu\text{m}$

## 1.11 ELECTROSPINNING OF THERMOPLASTIC POLYURETHANE

The necessity to electrospinning thermoplastic urethane born of the need, especially in medicine and in textile fields, to create fibers with high surface area to volume ratio and small pore size.

That of Pedicini and Farri (38) is one of the first study about the mechanical property of TPU fiber produced by electrospinning. In this work, a solution of dimethyl-formamide was electrospun and the stress-strain characteristic investigated. It was found that a higher tensile stress with respect to bulk TPU characterizes the fibers. It can be attributed both to the strain-induced orientation and to the molecular orientation occurring during the process.

Till now, we have referred to electrospinning of polymer solution but there is also the possibility to perform electrospinning of polymer melt. This technique implies a cheaper and solvent-free process. The parameters influencing the process are the same for polymer solution and for polymer melt. However, Lions et al. show the influence of tacticity in polymer melt: isotactic polymer result in a smaller and more oriented fiber.

Dasdemir et al. (36) compare the properties of electrospun TPU from solution and melt polymer. For the electrospinning of the solution, a 5kV voltage, a 6 cm distance and a concentration of 5 wt% were found to be optimal parameters. For the polymer melt the temperature range was assessed between 205-208 °C, the voltage incremented till 30 kV and the distance left equal, 6 cm.

Electrospinning of solution results in an homogenous dispersion on the collector while the fibers form the polymer melt are collected in a hill-like structure. These behaviours can be ascribed to the different viscosity, solidification speed and mass of the resulting fiber. The solution has a low viscosity, small diameter and proper time of solidification, which allow the jet to move towards most conductive zones (the ones less covered by fibers), while the polymer melt has opposite characteristics that make it stack in the same area.

In terms of productivity, the melt electrospinning is more efficient, with a quantity of deposited material four times higher than the solution electrospinning. As it is evident, the evaporation of solvent affects the weight of deposited fibers.

## 1.12 ELECTROSPINNING OF CLICKABLE FIBERS

The vast possibilities of click reactions and the ease and relatively easy scale-up capability of electrospinning make the production of electrospun clickable fibers an interesting technique to investigate. The attachment of ligand, biomolecules and small molecule to polymer allows the obtention of the so-called active platforms. Talking about nanofiber, the activation can occur in two different moment: before the electrospinning (direct spinning of clickable polymer) or once the fiber has been electrospun (post-spinning activation). The second method is the most used one thanks to the wide knowledge about surface activation (plasma, chemical vapour deposition, etc...) and it shows less problem in spin non-functionalized polymers. On the other hand, the post-spinning process presents problem of homogeneity of surface activation, so the direct spinning of clickable polymer is investigated to obtain an optimal surface distribution of reactive groups.

Huisgen-type copper-catalyzed azide–alkyne cycloaddition (CuAAC) was widely use in the post-spinning activation of fibers: for example, Fu et al. (39) successfully attached a thermal-responsive alkyne-terminated polymers of N-isopropylacrylamide (NIPAM) to block copolymers of 4-vinylbenzyl chloride (VBC) and glycidyl methacrylate (GMA) (PVBC-b-PGMA). The so-created polymer shows a temperature dependence wettability: at 25 °C it is hydrophobic (water contact angle 30 °), at 40 °C it is hydrophilic (water contact angle 140°C). Lot of studies are present in literature, using different types of click reactions but just few works talk about DA functionalization of fibers. One of these was carry out by Ozlem et al. (40), who synthetized a polylactide based copolymers containing furan groups and triethylene glycol (TEG) units as side chains to create biodegradable scaffolds with biomolecular immobilization and cell proliferation properties.

## 1.13 ELECTROSPINNING OF FUNCTIONALIZED TPU

Even scarcer are the references in literature regarding the electrospinning of clickable TPU, one of these is the work of Choi et al. (41), where an azido-diol was used in the synthesis of TPU. Two syringes were charged with two different solution: the first containing 25 wt% of “Normal-TPU” and the second containing 20 wt% of “Azido-TPU”. The difference between these two compounds are the composition of the polyol: poly(tetramethylene ether) glycol (PTMEG) for the “Normal-TPU” and poly(GAP-co-THF) for the “Azido-TPU” (Figure 19).



Figure 19 a) Poly(tetramethylene ether)glycol

b) Poly(GAP-co-THF)

The good processability proper of polyurethane, allows its production by electrospinning. Possibility of electrospinning for functionalized polymer enhances the exposition of the functional group thanks to the higher specific surface area and energy. Fibers with diameters between 1.3 and 2  $\mu\text{m}$  were collected on a rotating collector. A comparison between mechanical properties of “Normal-TPU” and “Azido-TPU” was performed. Stress-strain behaviour of the “Azido-TPU” shows a decline of 38,6% of the ultimate stress and of 39,9% of the ultimate strain with respect to the “Normal-TPU”. Furthermore, it was produced a film by spin coating, showing a slightly better mechanical performance than the electrosopun fibers: the reduction of ultimate stress and strain are 26,9% and 25,1% respectively. It seems clear that the addition of functional groups in the polyurethane results in a decrease of mechanical properties, however, even if poorer than normal polyurethane, they possess sufficient mechanical resistance to be used as flexible or soft material in the preparation of active platforms.

## 1.14 TAILOR SURFACE ENERGY AND WETTABILITY USING FURAN-MALEIMIDE DA REACTION

Being able to easily tailor the wettability of polymer is one of the most challenging task in polymer technology because it is necessary to change superficial behaviour, without altering the bulk composition.

Hydrophobicity, oil-repellent behaviour, adhesion and printability are just some of the properties related to surface. Furthermore, in multiphase polymers and composites, interfacial properties regulate the dispersion and adhesion of filler, pigments and polymer blend. A good wettability of polymer matrix implies a more homogeneous, faster and less energy demanding mixing process.

Surface technology is, indeed, a fast-growing field and not only limited to polymer but to every kind of material. The technology used for a specific class of materials can be easily adapted to other ones, thus can be interesting the application of DA on glass surfaces with the aim to control surface energy and wettability studied by Costanzo et al. (42). In this work, reversibility of DA is exploited to create tailorable surfaces, where a transition between hydrophobic to hydrophilic behaviour can take place. The idea is to control the functional surface using temperature: changing temperature results in a change in surface energy.

Firstly, the glass slide was silanized with 3-aminopropyltrimethoxysilane which then react with 2-furfuryl chloride in order to bear pendant furans which, finally, are functionalized using fluorinated maleimide. To assess the wettability of the surface contact angle measurement was performed. The principle of this technique is, explained in a very simplistic way, the higher the measured contact angle, the worse the wettability of the surface. In the untreated substrate, measured contact angle was  $23 \pm 3^\circ$ . Adding the different components this angle increase, meaning a shift towards hydrophobic behaviour, passing from  $70 \pm 3^\circ$  of the furan functionalized surface to  $101 \pm 9^\circ$  reached after the dienophile fluorinated maleimide is attached. The fluorinated alkyl chain reduces the surface energy thus resulting in higher contact angle. To assess the effective transition hydrophobic-hydrophilic, the sample was refluxed in toluene to induce the retro-DA. The contact angle measured once the dienophile was removed ( $70 \pm 6^\circ$ ) is similar to the one of furan functionalized surface.



Other example of hydrophobic functionalization by DA reaction is the one presented by Singha et al.(43), this time applied on a polyurethane. Polycaprolactone diol, 4,4'-methylenebis(phenyl isocyanate) and a chain extender synthesized by furfuryl amine and furfuryl glycidyl ether and bearing 3 pendant furan moieties were reacted to obtain a furan functionalized polyurethane (FPU). Maleimide functionalized polyhedral oligomeric silsesquioxanes (POSS-M) was subsequently grafted to the polymer (FPU-POSS-M) by DA reaction. Water contact angle measurement was performed on the surfaces of both FPU and FPU-POSS-M resulting in an increase of contact angle from 84° to 141.3°. After the retro-DA and further DA the same angles were measured. The consistent increase of hydrophobicity is ascribed not only to the POSS-M itself but also to the increased roughness that grafting involves, creating micro and nanometric structure where air is trapped.

## 2. MATERIALS AND METHODS

In this chapter, the materials employed for the synthesis of biobased polyurethane are described, as well as the followed polyurethanes synthesis protocol and electrospinning process and the characterization techniques and conditions used for the analysis of physicochemical, thermal, mechanical, morphological and surface properties. In the same way, the testing procedure followed for functionalization of the prepared electrospun platforms by click reactions is also described.

### 2.1 MATERIALS

The materials employed for the synthesis of biobased polyurethane are:

#### 2.1.1 Polymerization precursors

##### 2.1.1.1 *Poly(butylene sebacate)diol*

Poly(butylene sebacate)diol is a macrodiol derived from castor oil. It is synthesized via copolymerization of the sebacic-acid with 1,4 butanediol. In this work, the used Poly(butylene sebacate)diol has a number average molecular weight of  $3505 \text{ g mol}^{-1}$ .

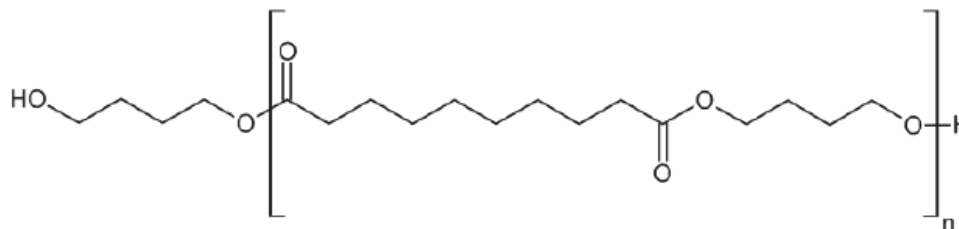


Figure 20 Poly(butylene sebacate)diol molecular structure

### 2.1.1.2 2,5-Bis(hydroxymethyl)furan

2,5-Bis(hydroxymethyl)furan (BHMF) is a heterocyclic organic compound, which is produced by the hydrogenation of 5-hydroxymethylfurfural (HMF), which is a biomass derived compound.

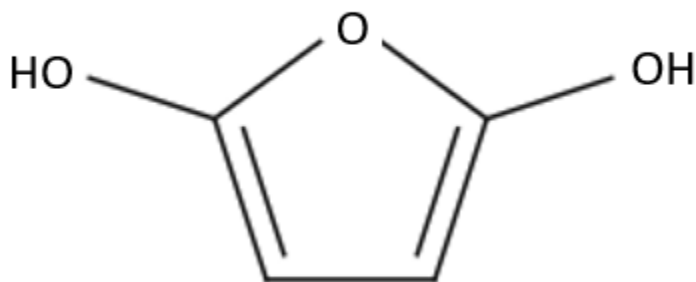


Figure 21 2,5-Bis(hydroxymethyl)furan molecular structure

BHMF has a density of  $1,28 \text{ g cm}^{-3}$ , a melting point of  $75 \text{ }^\circ\text{C}$  and a boiling point of  $275 \text{ }^\circ\text{C}$ . It is provided as a brownish to yellowish powder with molecular weight of  $128,1 \text{ g mol}^{-1}$ . In this work, BHMF has been used as chain extender, added to the prepolymer.

### 2.1.1.3 1,3-Propanediol

1-3 propanediol is a colorless liquid with boiling point of  $274 \text{ }^\circ\text{C}$ , molecular weight of  $76 \text{ g mol}^{-1}$  and density of  $1,06 \text{ g cm}^{-3}$ . It was used as chain extender in the synthesis of PD.

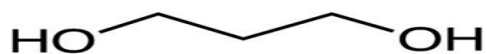


Figure 22 1,3-Propanediol molecular structure

#### 2.1.1.4 Hexamethylene diisocyanate

Hexamethylene diisocyanate (HDI) is an aliphatic, petroleum derived diisocyanate monomer with two isocyanate groups linked by a hexane-1,6-diyil group. It is colorless to yellowish liquid with a molecular weight of  $168,2 \text{ g mol}^{-1}$ , boiling point of  $255 \text{ }^\circ\text{C}$  and density of  $1,05 \text{ g cm}^{-3}$ .

It is not as used as aromatic isocyanates such as toluendiisocyanate (TDI) and 4,4-diphenylmethanediisocyanate (MDI) but the polyurethanes obtained by HDI show better light stability and enhanced crystallinity of the hard segment. Furthermore, the polyurethane obtained shows a better biocompatibility with respect the ones produced with MDI. (44)

It is used in the synthesis of the three polyurethanes, making it react with the macrodiol in the formation of the prepolymer and then reacting with the BHMf or PD once there are added in order to increase the molecular weight.

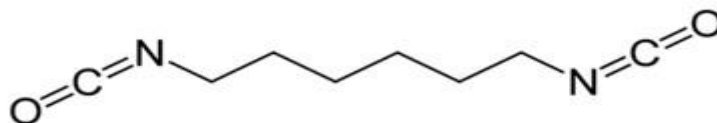


Figure 23 Hexamethylene diisocyanate molecular structure

## 2.1.2 Functionalizing compounds

### 2.1.2.1 Fluorescein-5-maleimide

Fluorescein-5-maleimide (5-MF), chemical name 1H-Pyrrole-2,5-dione, 1-(3',6'-dihydroxy-3-oxospiro (isobenzofuran-1(3H),9'-(9H)xanthen-5-yl)- is a derivative of fluorescein dye and has been used as labelling agent in order to assess the membrane functionalization via DA reaction. It was purchased by Tokyo Chemical Industry (TCI). It is a solid, red compound, light, temperature and air sensitive, featuring a molecular weight of 427,36 g mol<sup>-1</sup>. The high molar attenuation coefficient, > 80,000 M<sup>-1</sup>cm<sup>-1</sup>, makes it perfect to be used as labelling agent. The main excitation wavelength is 494 nm while the emission one is 518 nm (both in the range of visible light corresponding to green). It is mainly used in labelling proteins having free thiols, being 5-MF a sulfhydryl-reactive compound. However, the easy-accessible maleimide group makes its application suitable also in DA reactions with furan-containing compounds.

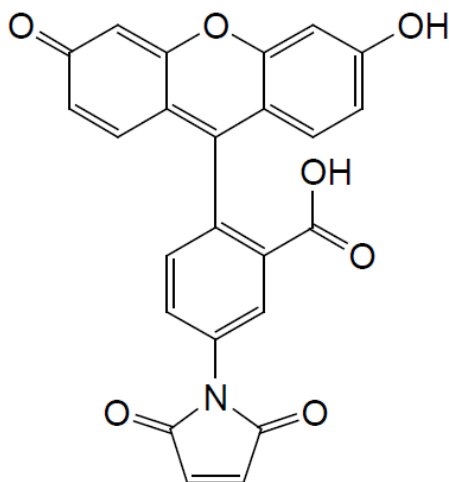


Figure 24 Fluorescein-5-maleimide molecular structure

### 2.1.2.2 Maleimide-end acid

3-(2,5-dioxo-2H-pyrrol-1(5H)-yl) propanoic acid (AMI) is a derivative of  $\beta$ -Alanine with a maleimide and carboxylic group. It is a white crystal to powder with molecular weight of 169,13 g mol<sup>-1</sup> and melting point of 104.5 °C.

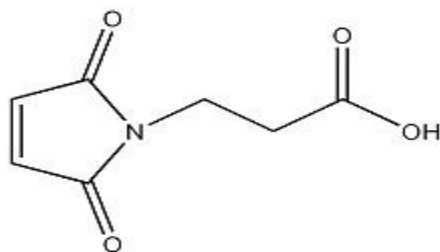


Figure 25 AMI molecular structure

## 2.1.3 Solvents

The solvents used for the electrospinning of synthesized polyurethanes and as medium of the functionalization of prepared platforms by means of click reactions are:

### 2.1.3.1 Chloroform

Chloroform,  $\text{CHCl}_3$  is a colorless, sweet-smelling, volatile halogenated solvent. It has a boiling temperature of 61 °C, a molecular weight of 119,4 g mol<sup>-1</sup> and a density of 1,49 g cm<sup>-3</sup>.

In this study it has been used, mixed with DMF, to dissolve the polymer and create the solution for the electrospinning process. In this sense, other two important characteristic of chloroform are the polarity index of 4,1 and the dielectric constant of 4,81.

Chloroform was provided by Sigma Aldrich.

### 2.1.3.2 Dimethylformamide

Dimethylformamide (DMF), chemical formula  $(\text{CH}_3)_2\text{NCHO}$  is a colorless liquid with a faint ammonia-like odor. It is an organic compound with density of 0,948 g cm<sup>-3</sup>, molecular weight of 73,1 g mol<sup>-1</sup> and boiling point of 153 °C. It is soluble in water and in most of the organic liquid.

In this work it was used with chloroform in the electrospinning solution. Its polarity index is 6,4 and its dielectric constant 36,71.

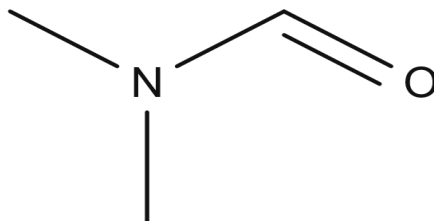


Figure 26 DMF molecular structure

### 2.1.3.3 Dimethyl sulfoxide (DMSO)

Dimethyl sulfoxide is an organic solvent with molecular formula  $(\text{CH}_3)_2\text{SO}$ . It is one of the strongest organic solvent, able to dissolve both polar and non-polar compounds.

It is a colorless liquid, with density of  $1,1 \text{ g cm}^{-3}$ , molecular weight of  $78,1 \text{ g mol}^{-1}$  and a boiling point of  $189 \text{ }^\circ\text{C}$ . It is soluble in waters and in a wide range of organic solvents.

It has been used as solvent to dissolve the Fluorescein-5-maleimide compound. to perform the functionalization of prepared electrospun platforms through click chemistry.

DMSO was purchased by Sigma Aldrich

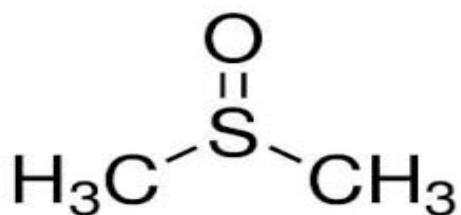


Figure 27 DMSO molecular structure.



## 2.2 SYNTHESIS

### 2.2.1 SYNTHESIS OF POLYURETHANES

The polyurethanes were synthesized using the prepolymer process.

The macrodiol was previously melted and dried using a rotovapor, at 90 °C, under vacuum for 2 hours.

Once the macrodiol was melted, it was transferred to the reactor which features a two neck round flask, a mechanical stirrer, a nitrogen line and a heating bath.

The heating bath was set at 90 °C and the mechanical stirrer at 80 rpm.

#### **Prepolymer reaction**

HDI was added to the macrodiol and the two necks were plugged with a mechanical stirrer and a silicon plug respectively. Nitrogen flux was insufflated using a needle inserted in the silicon plug. These conditions were maintained for 2.5 hours.

#### **Chain extender addition**

Once the prepolymer was formed, the chain extender was added and the mechanical stirrer's rotations increased up to 100 rpm, while bath temperature was left the same. Nitrogen flux was maintained constant and the reaction was carried on for 5 minutes, till a proper solution viscosity was reached. It has been decided to perform the second step of the reaction as fast as possible, in order to avoid the thermal degradation of BHMF.

Three different formulations were synthesized, using different chain extender types and changing the ratio macrodiol : diisocyanate : chain extender.

One formulation of 1,3-propanediol-containing polyurethane has been synthesized, using E82 as macrodiol, HDI as diisocyanate and 1,3-propanediol as chain extender in a ratio of 1:3:2. This polyurethane will be named from now on as PD.

Then, two different formulation of BHMF-containing polyurethane have been synthesized, using E82 as macrodiol, HDI as diisocyanate and BHMF as chain extender in a ratio of 1:3:2 and 1:4:3. From now on, these two polyurethanes will be referred as BHMF-2 and BHMF-3 respectively.

In the following tables are reported the quantities for the syntheses of studied polyurethanes.

## PD

Material	Equivalent	Weight (g)	Molecular weight (g mol <sup>-1</sup> )	Moles (mol)
Macrodiol	0.17	46,329	3505	0,0132
HDI	0.5	6,662	168	0.0396
PD	0.33	2,009	76	0,0264

*Table 2 Reactants and quantities for PD*

## BHMF-2

Material	Equivalent	Weight (g)	Molecular weight (g mol <sup>-1</sup> )	Moles (mol)
Macrodiol	0.17	45,199	3505	0,0128
HDI	0.5	6,499	168	0.0386
BHMF	0.33	3,301	128	0,0257

*Table 3 Reactants and quantities for BHMF-2*

## BHMF-3

Material	Equivalent	Weight (g)	Molecular weight (g mol <sup>-1</sup> )	Moles (mol)
Macrodiol	0.125	42,226	3505	0,0120
HDI	0.5	8,103	168	0.0480
BHMF	0.375	4,631	128	0,0360

*Table 4 Reactants and quantities for BHMF-3*

### Compression molding process

The so created polymer appears as a yellowish viscous liquid, which has undergone a compression molding process in order to obtain homogenous films, without trapped bubbles. So, it is spread on a Teflon sheet placed on a plane mold and pressed at 50 bar.



*Figure 28 Molding machine*

Then, a thermal cycle consisting of 10 hours at 100 °C and 3 hours at 20 °C (always maintaining the same pressure) is applied. The resulting films, weighting 55 g, are shown in Figure 29.



*Figure 29 Resulting films from molding process. From left to right PD, BHMf-2, BHMf-3.*

## 2.2.2 Synthesis of AMI

Maleimide-end acid was synthesized following the two-step reaction reported below. An acetic acid solution containing maleic anhydride at 10 % w/v (5 g in 50 mL) was added dropwise to an acetic acid solution with  $\beta$ -alanine at 9 % w/v (4.54 g in 50 mL). The mixture was stirred for 3 h at room temperature and a white suspension was obtained. After that period, 70 mL of HAc were added, while the temperature was raised until 115 °C and the mixture was stirred overnight. After one hour of reaction a limpid colorless solution was observed. At the end of the whole process, an orange oil was obtained. The solvent excess was removed under reduced pressure and the product was washed with 30 mL of toluene for three consecutive times, which was also removed under reduced pressure. The product was then purified by flash chromatography using a silica column (DCM/ethyl acetate 9:1). Finally, a white solid (AMI) was obtained (30 % w/w yield).

The FTIR spectrum of AMI is shown in Figure 30

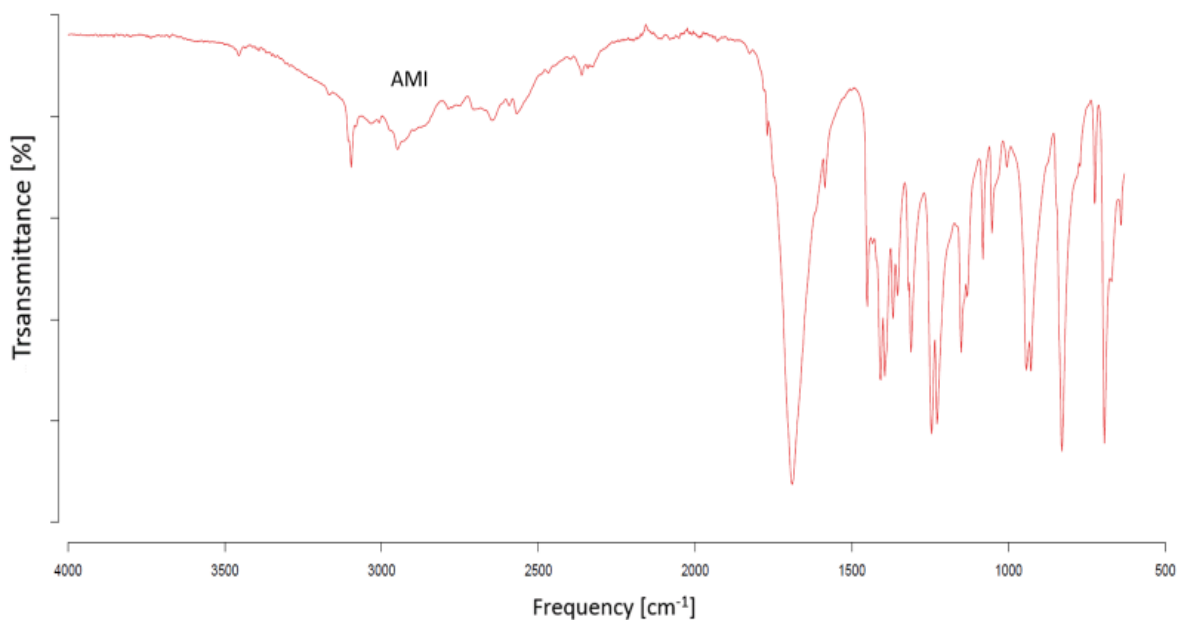


Figure 30 Spectrum of AMI

## 2.3 CHARACTERIZATION TECHNIQUES

### 2.3.1 Fourier transformed infrared spectroscopy (FTIR)

Fourier transformed infrared spectroscopy (FTIR) is a fast-responsive and nondestructive characterization technique used to identify the chemical structure and supramolecular arrangement of liquid, solid or gas samples, studying the absorption or transmission spectrum.

In this range of the IR spectra the photons' energy is not sufficient to promote an electron to a higher energy state but it can induce vibrations on the covalent bonds of the analyzed molecule. Each molecule, depending on the number of atoms  $n$ , has  $3n-6$  or  $(3n-5$  if it is linear) degree of vibrational freedom. The vibrational mode can be grouped in stretching and bending.

Stretching vibrations involve a change in the bond length of the atoms and can be symmetric or asymmetric.

Bending vibrations, instead, change the angle between two bonds. There are four different types of bending vibrations: scissoring, rocking, wagging, twisting. (Figure 31)

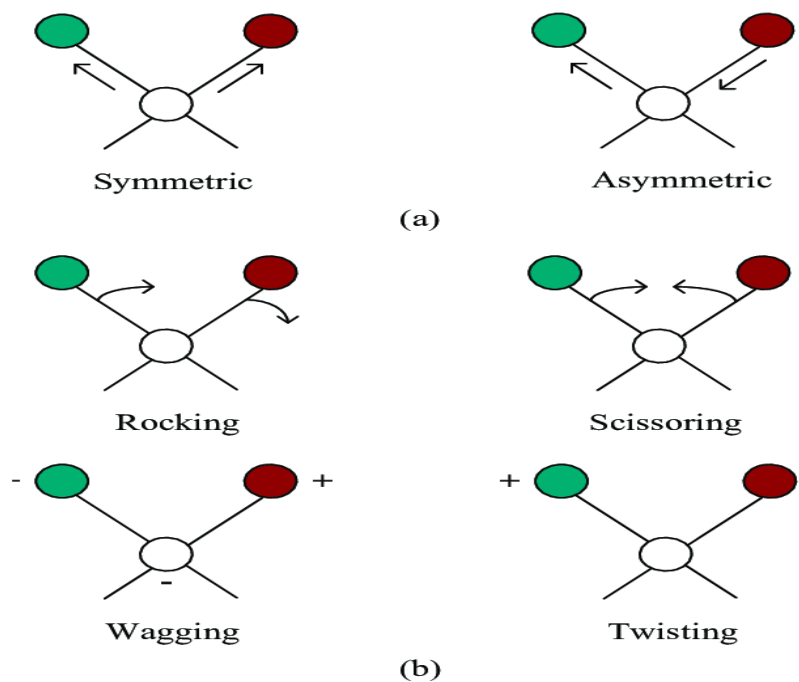
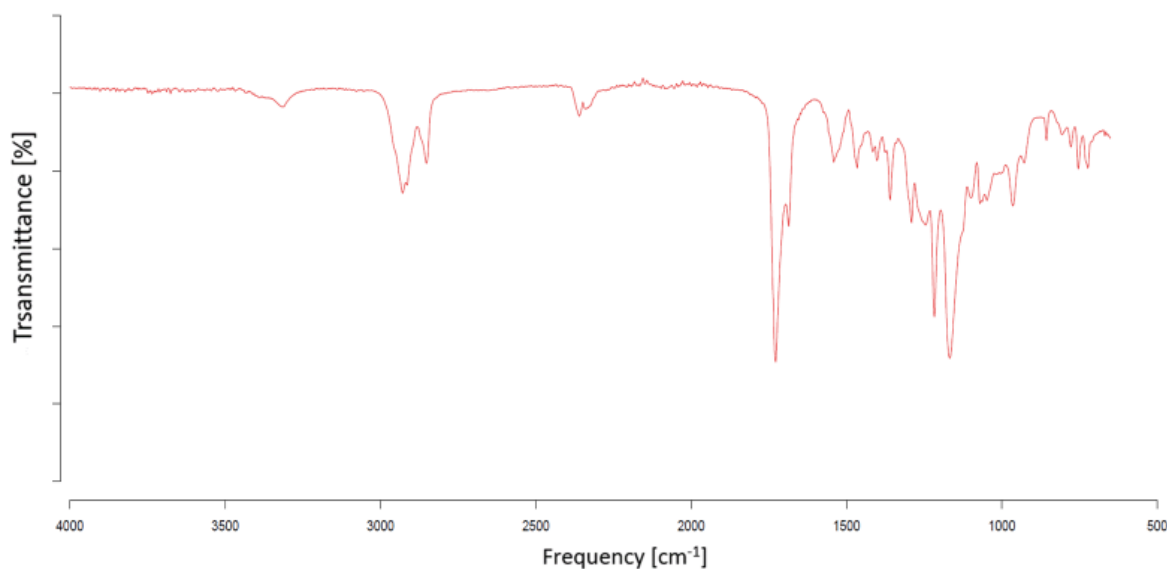


Figure 31 Molecular vibrations: a) Stretching vibrations, b) Bending vibration(45)

Energy required to produce different modes of vibration in different molecule is defined by a specific wavelength, which is absorbed, thus resulting in absorption peaks, composing the IR spectrum.

Infrared absorption of bonded atoms and groups are tabulated, allowing an easy indexing of the peaks.

The resulting graphs show on the x axis the wavenumber (1/frequency) and on the y axis the absorbance or transmittance (Figure 32).



*Figure 32 FTIR resulting graph*

Three different regions can be identified in an IR spectrum. In the range between 1450  $\text{cm}^{-1}$  and 600  $\text{cm}^{-1}$  there are lots of peaks, belonging to all possible manner of both bending and stretching vibrations between the molecules. It is difficult to assign each peak and the result is a complex spectrum which is unique: it is called the fingerprint region and it is used to assign the spectrum to a specific substance.

In the range 4000-1450  $\text{cm}^{-1}$  can be found the peaks corresponding to the stretching of diatomic units. In fact, the stretching vibrations occur at higher frequencies with respect the bending one: bending a bond is less energy demanding than stretch it. It is called the group frequency region.

Finally, the peaks present in the region 600-200  $\text{cm}^{-1}$  are attributed to the heavy atom vibrations with very low frequencies.

In this work, spectra were recorded at room temperature using a Nicolet Nexus spectrophotometer provided with a Specac MKII Golden Gate accessory equipped with a diamond crystal at a nominal incident angle of  $45^\circ$  and ZnSe lens. Measurements were run after averaging 32 scans with a resolution of  $4\text{ cm}^{-1}$  in the range from  $4000$  to  $600\text{ cm}^{-1}$ .



*Figure 33 Nicolet Nexus spectrophotometer*



### 2.3.2 Differential scanning calorimetry (DSC)

DSC is a characterization technique used in polymer technology to investigate the thermal transition of a polymer subjected to a thermal cycle. The main data which are usually collected are the glass transition temperature and the phase change temperatures.

The instrument is composed of two pans, a measurement chamber and a computer. In one pan is placed the sample to be investigated, the other one is usually empty and is used as reference. The probe is performed at constant heating rate.

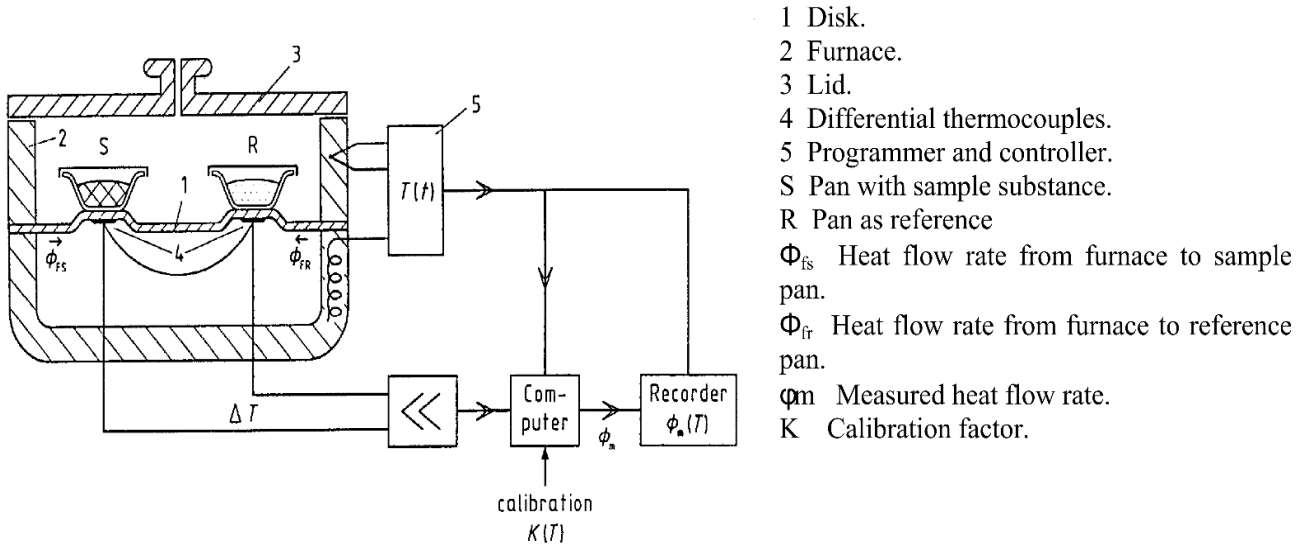


Figure 34 DSC instrument scheme(57)

The change in temperature of a giving sample is directly proportional to the enthalpy variation and inversely proportional to its specific heat capacity.

$$C_p = \frac{dH}{dT}$$

The machine records the heat flow provided to each pan in order to maintain the same temperature, plotting the results in a graph (thermograph) representing the temperature on the x-axis and the heat flow on the y-axis.

In the thermograph is possible to identify peaks which represent the transition of the sample

The instrument used in this work was a 3+ Mettler Toledo, shown in Figure 35



Figure 35 DSC 3+ Mettler Toledo machine

### 2.3.3 Dynamic molecular analysis (DMA)

DMA, sometimes called forced oscillatory measurement, is a characterization technique used to measure the viscoelastic properties of materials. It is widely used in polymer characterization and relies on the polymer's viscoelasticity: when a sample is subjected to a sinusoidal oscillating stress, it will respond with a sinusoidal oscillating strain and vice versa, until it remains within its elastic limit.

A perfect elastic material will respond to a sinusoidal input with an in-phase sinusoidal output (elastic or storage response) while a viscous material will respond with an out-of-phase sinusoidal output of  $\frac{\pi}{2}$  (viscous or loss response). A viscoelastic material will respond with a phase angle in between the two extremes mentioned before.

In a viscoelastic material when a sinusoidal stress is applied

$$\sigma = \sigma_0 \sin(\omega t)$$

the resulting deformation can be expressed as

$$\varepsilon = \varepsilon_0 \sin(\omega t + \delta)$$

Being  $\omega$  the frequency oscillation, at the time and  $\delta$  the phase difference between the applied stress and the resulting strain.

Knowing the input and the output it is possible to calculate the dynamic complex modulus  $E$ , which is the vector sum of the storage modulus  $E'$  and the loss modulus  $E''$ .

$$E' = \frac{\sigma_0}{\varepsilon_0} \cos \delta$$

$$E'' = \frac{\sigma_0}{\varepsilon_0} \sin \delta$$

$$E = E' + iE''$$

The ratio of the loss to the storage modulus is called the loss tangent ( $\tan \delta$ )

$$\tan \delta = \frac{E''}{E'}$$

It is an index of viscoelasticity of the material and it is represented in the resulting graph of DMA because it allows a fast and easy way to identify the glass transition temperature. Indeed, at  $T_g$  the loss modulus reaches its maximum while the storage modulus its minimum, resulting in a peak of the  $\tan \delta$ .

The equipment is basically composed of a motor and a driveshaft, which are responsible of the deformation of the sample and depending on the model, the applied force can be axial or torsional, a displacement sensor and a heater to increase the temperature of the sample. A schematic representation is provided by Figure 36

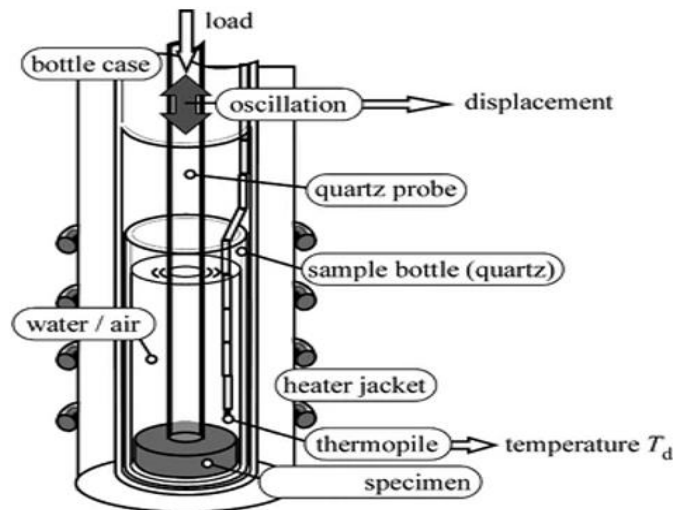


Figure 36 DMA instrument scheme (59)

The test can be either stress or strain controlled.

The samples were tested using an Eplexor 100 N analyser Gabo equipment, in a

temperature range between -100 °C and 200 °C at a scanning rate of 2 °C min<sup>-1</sup>. The resulting graphs are made plotting, E'-T, E''-T and tanδ -T curves.

### 2.3.4 Ultraviolet-visible spectroscopy (UV-vis)

Ultraviolet-visible spectroscopy (UV-vis) is a technique which relies on the light absorption at different wavelengths (part of the UV and visible spectra) of the analyzed sample. When irradiated with a light beam, a material absorbs different wavelengths, depending on electrons excited and thus on the presence of different functional groups. Wavelengths normally used range between 200 and 600 nm. The instrument can work in absorption or transmission mode, collecting the absorbed spectra and the transmitted, respectively.

The machine used is composed of two different cells of 0.1 mm. In one is present the reference solution in which the material is dissolved, (DMF : CHCl<sub>3</sub> 2:1) and in the other is placed the material dissolved in the solution.

Knowing the peak to consider, it can be monitored its increasing or decreasing and correlates it with a change in the system, typically a reaction occurring.

In this work an UV-3600 spectrophotometer from Shimadzu was used and a wavelength range between 280 and 600 was investigated.

### 2.3.5 Thermo-gravimetric analysis (TGA)

Thermo gravimetric analysis is a characterization technique which measures the change in weight of a sample when the material is heated and thus monitoring the exchange of material between it and the environment. It is used in order to study the temperatures for phase changes and the degradation behavior of materials. The instrument is composed of a pan located inside a furnace and monitored by a precision balance. The process can be conducted under different atmosphere, using air, inert or reactive gases, depending on the phenomena to be investigated.

Starting temperature is usually between 25 °C and 30 °C while the final temperature varies depending on the nature of analyzed sample: 600°C-800°C for organic materials and higher than 1000 °C for inorganic ones.

The results are plotted in a graph displaying weight losses and temperature. Aiding the interpretation of such a curve there are other curves that can be plotted: the first derivative, measuring the mass changing rate and the Evolved Gas Analysis (EGA) which analyzes the evolved gas by FTIR measurement.

The weight losses are caused mainly by chemical reactions (decomposition, combustion, reduction of chemical species present in the sample) or physical changes (vaporization, sublimation, desorption). For this work measurements were performed by using a TGA/DSC3+ Mettler Toledo analyzer. Samples in a weight range between 20 and 30 mg were submitted to a 10 °C min<sup>-1</sup> heating rate from 25 to 800 °C under nitrogen atmosphere in order to prevent the thermoxidative degradation.

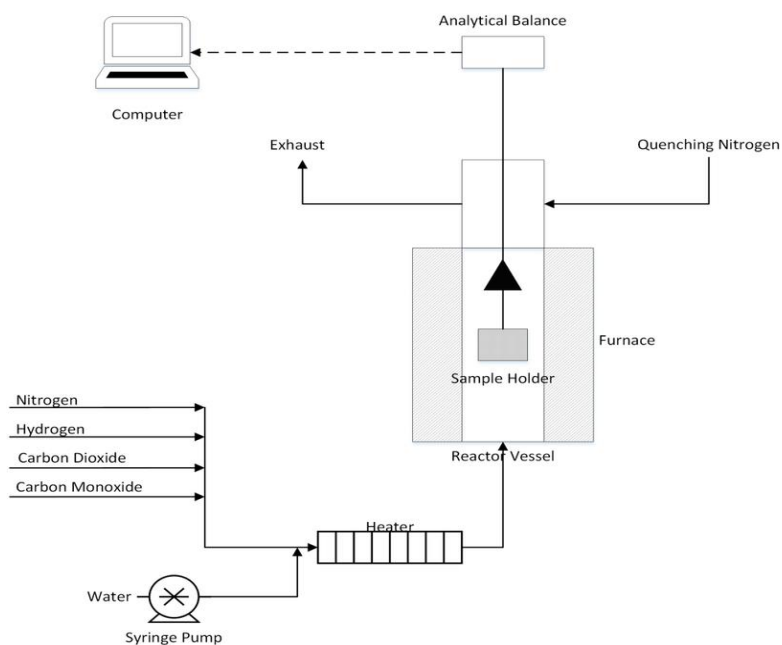


Figure 37 TGA instrument scheme(58)

### 2.3.6 Optical microscopy (OM)

Optical microscopy (OM) is a characterization technique that use a source of light (usually visible, UV, etc...) and a system of lenses to magnify images taken from samples. It is widely used to investigate surface morphologies.

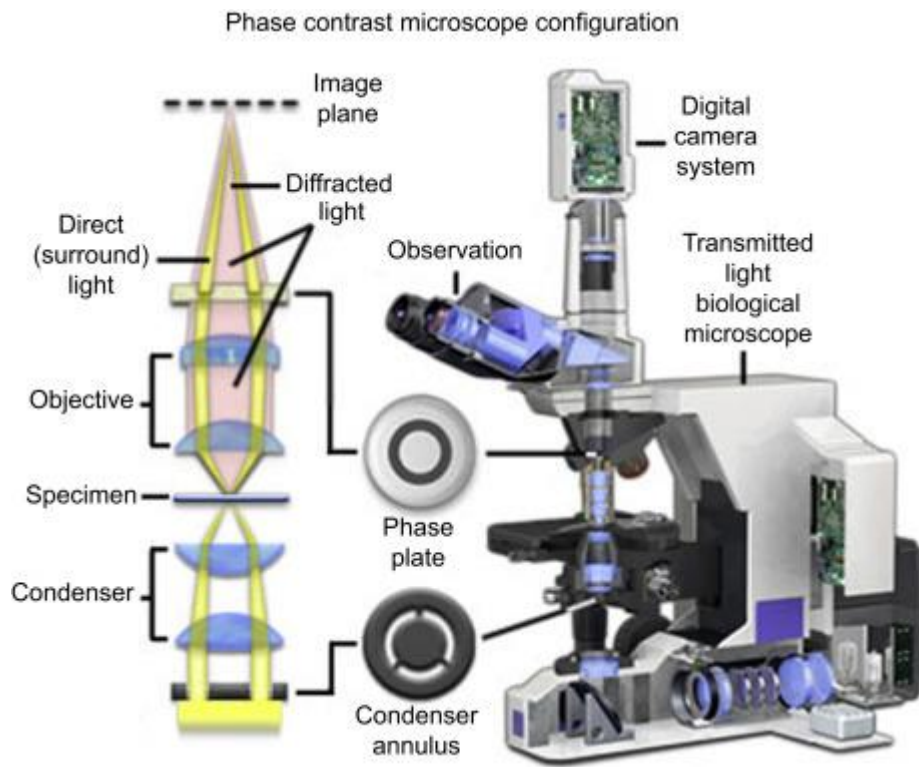


Figure 38 Representation of OM (46)

There are mainly three types of available optical microscopy, which differ for the type of light exposure:

- 1) Transmission: the beam is transmitted from a source on the opposite side of the specimen to the lenses, allowing light passes through the sample.
- 2) Reflection: used to examine opaque samples, it exploits the reflected light in order to visualize the sample's surface
- 3) Polarize: this configuration takes in advantage polarized light in order to analyze birefracting surfaces.

In this study, transmission visible light microscopy has been used in order to analyze the morphology of the electrospun fibers.

The OM model used in this work was a Nikon Eclipse 80i.



*Figure 39 Optical Microscopy*



### 2.3.7 Scanning electron microscopy (SEM)

Scanning electron microscopy (SEM) creates images by the mean of a focused electron beam scanned over a surface. It is used to collect information about surface topography and composition. The main difference with respect optical microscopy is that SEM relies on electrons instead of photons. This feature it allows to overcome the problem of limited resolution of the light used for illumination, which is that of the white light (200-250 nm). Indeed, electrons have a much shorter wavelength, thus allowing to reach better resolutions.

The finely focalized electron beam, while scanning the surface, collects a great number of signal emitted by secondary electrons, backscattered electrons, X-rays, absorbed and Auger electrons in order to detect the surface topography.

The great variety of manner by which the beam interact with the atoms makes the presence of alien particles a great problem. So, the analysis is performed under high vacuum.

As stated before using SEM it is possible to know the surface composition of the sample. This is thanks to the elastic backscattering phenomena which occur when the electron beam impact on high electronic density part of the surface, thus giving information about its composition.

The anelastic interactions are the responsible for the topographic information. In fact, such interaction permits the absorption of the incoming electrons and the emission of electrons from the conductive or valence band of the atoms of sample's firsts layers.

The electron beam is free to move along the surface and the emitted electrons are collected and processed by a compute. Another advantage of the SEM is to be totally unaffected by the color, opacity and transparency of the samples.

In this study SEM was used to investigate the fiber morphology and fiber diameters.

The equipment employed was a Hitachi S-4800 model.

### 2.3.8 Contact Angle

Contact angle measurement is the way to assess the wettability and surface tension of a material. These properties are fundamental characteristics referring to a surface because determine its suitability to be wetted by a liquid and so the adhesion between the two interfaces.

When a liquid is deposited on a solid surface, three interfaces are created: the one between the solid and the liquid, the one between the solid and the vapor and the one between the vapor and the liquid. The angle between the liquid vapor and the solid interface is called the contact angle.

In mathematical terms, the contact angle is defined by the Young equation:

$$\cos \theta_{Young} = \frac{\gamma_{sv} - \gamma_{sl}}{\gamma_{lv}}$$

being  $\theta_{Young}$  the contact angle,  $\gamma_{sv}$  the solid-vapor interface,  $\gamma_{sl}$  the solid-liquid interface and  $\gamma_{lv}$  the liquid-vapor interface interfacial tensions.

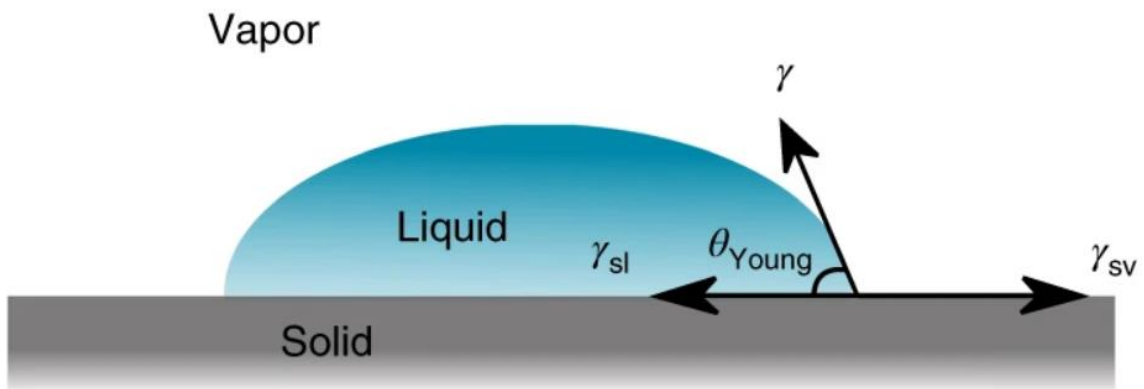


Figure 40 Representation of the three interfaces (47)

The material should be clean and as flat as possible. Inhomogeneity of the sample not properly cleaned surfaces and roughness strongly influence the contact angles measurement.

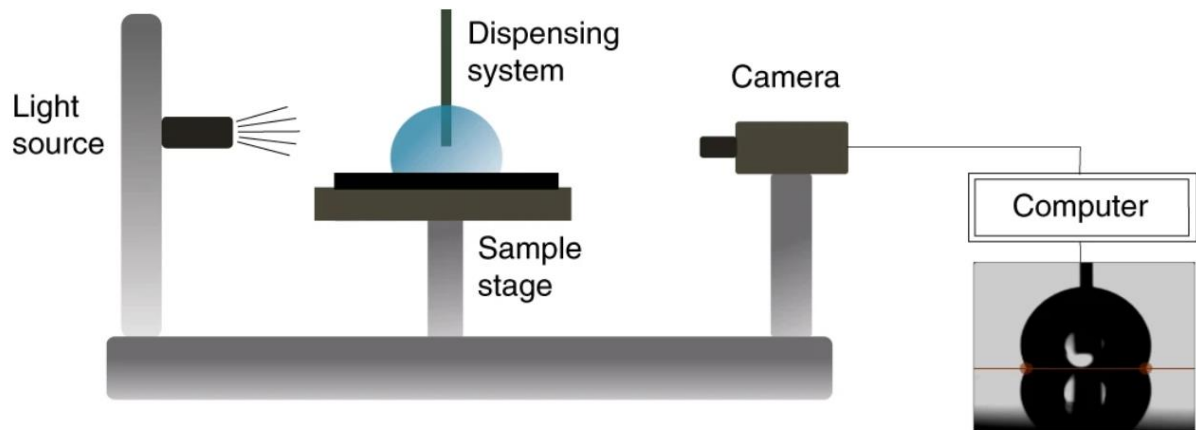


Figure 41 Contact angle's instrument scheme (47)

The probe can be performed in static or dynamic way. In static probe a drop of water is deposited from a syringe on the surface and not modified from the outside during the measurement, so the three-phase boundary are not moving. The contact angle is automatically calculated by the computer from a photo of the deposited drop.

In dynamic contact angle the drop is not deposited but is moving, moving also the three-phases boundary. The angles measured are referred as advancing and receding contact angles. This kind of measurement is used when the effect of the inhomogeneity and vaporization of water want to be minimized. The advancing and receding contact angles are not the same. This difference, called hysteresis, can also be used to assess the surface roughness of the sample.

The instrument used in this work was a SEO-Phoenix-300-Touch.

### 2.3.9 Electrospinning

Electrospinning process has been performed using Fluidnatek LE-10, Bioinicia (Spain) machine. The diameter of the spinneret was 0.8 mm. Electric field in the range of 6-15 kV has been utilized and flowing rate between 0.2 and 1 ml h<sup>-1</sup>. In order to collect the sample, an aluminum foil was placed on the collector. After 12 hours, the membrane stacked on foil was detached.



*Figure 42 Fluidnatek LE-10 electrospinning machine*

### 2.3.10 Tensile test

Tensile test is used to assess the mechanical properties of materials.

Two screw clamps hold the material, which is shaped in order to have two shoulder where the specimen can be gripped and a gauge with a smaller cross section where the deformation and failure occur.

Two extensometers measure the deformation along the axis the force is applied. Data are collected and processed in order to give a real time stress-strain ratio.

The gauge section of the film specimens was 20 mm long 4,9 mm wide and 1,3 thick mm, a load cell of 1 kN was mounted to perform the test, while for the membrane specimens was 40 mm long, 10 mm wide and between 0.1 and 0.2 mm thick and was used a load cell of 500 N .

An INSTRON 5967 was used to perform mechanical test.

### 3 RESULTS AND DISCUSSION

#### 3.1 DSC

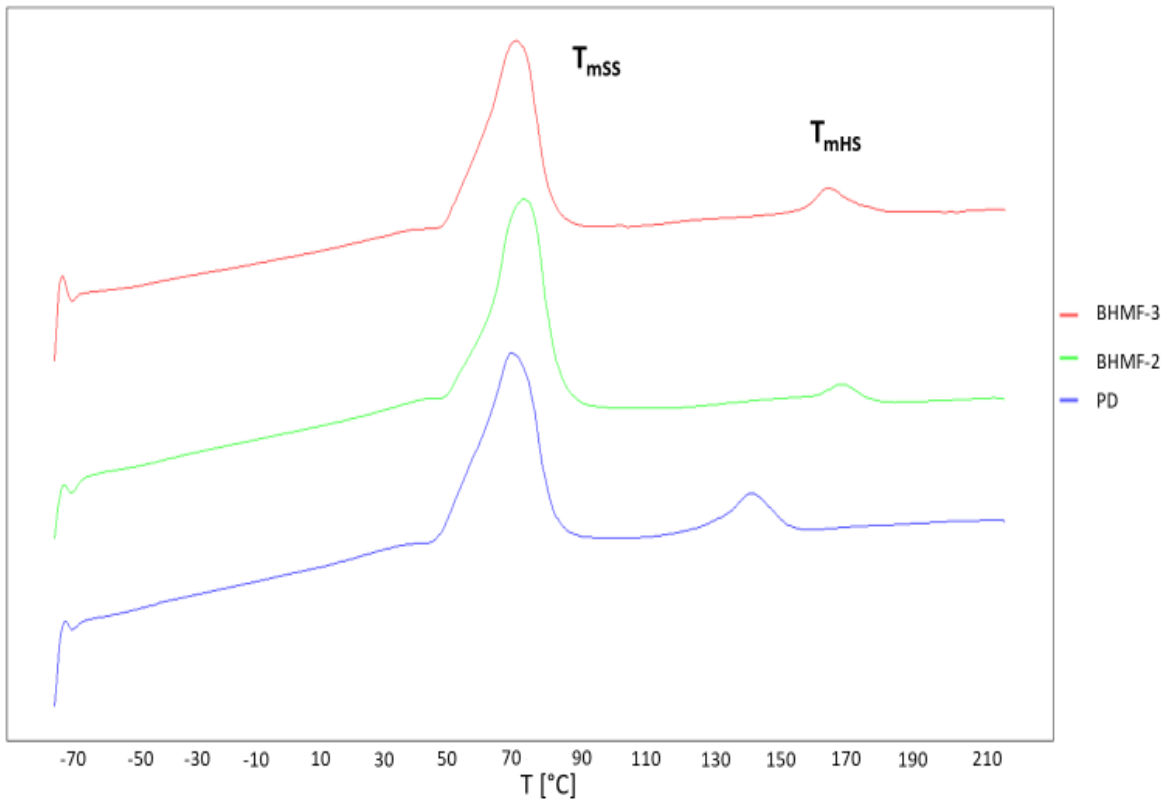


Figure 43 DSC thermograph of PD, BHMf-2 and BHMf-3 samples

Figure 43 shows the DSC thermograph of the synthesized polyurethanes. As can be seen the synthesized segmented polyurethanes display several thermal transitions.

Table 5 summarizes the glass transition temperature values obtained for the soft phase and the melting temperature and enthalpy values obtained for both soft and hard phases.

<b>Material</b>	<b>T<sub>gSS</sub></b> <b>(°C)</b>	<b>T<sub>mSS</sub></b> <b>(°C)</b>	<b>ΔH<sub>SS</sub></b> <b>(J g<sup>-1</sup>)</b>	<b>T<sub>mHS</sub></b> <b>(°C)</b>	<b>ΔH<sub>HS</sub></b> <b>(J g<sup>-1</sup>)</b>
PD	-47	66,3	43,6	140,4	8
BHMF-2	-40,44	70,3	43,8	168,5	1,82
BHMF-3	/	68	39	164	3,57

*Table 5 Thermal transition of the synthesized polyurethanes*

Soft phase shows a glass transition at low temperatures (T<sub>gSS</sub>), between -40 °C and -47 °C, and a melting transition (T<sub>mSS</sub>) around 66-70 °C. The glass transition temperature of hard segment (T<sub>gHS</sub>) has not been observed in the synthesized polyurethanes, probably because of the overlapping of T<sub>gHS</sub> and T<sub>mSS</sub>. A glass transition temperature around 60 °C has been reported for a polyurethane formed by PD and HDI (48). The endotherms observed around 140 °C for PD and around 165 °C for BHMF-2 and BHMF-3 polyurethanes can be assigned to the melting of hard segment crystallites (T<sub>mHS</sub>).

In order to be able to assess the exact transition temperature and the enthalpy, METTLER TOLEDO STAR<sup>e</sup> software has been used.

The melting enthalpy of the soft segment varies with the hard segment content. It can be noticed its decrease when the hard segment content increases. Indeed, a higher content of hard segment means a less significant soft segment organization in the structure. From the DSC results it can be assessed that the hard phase crystallinity of the PD sample is higher than the crystallinity of the BHMF- containing polyurethanes. This is supposed from the fact that the heat necessary to melt the microcrystalline hard segment is between 2 and 4 times higher than that needed for the BHMF-containing polyurethanes. This could be justified by the more ordered structure resulting from the use of propanediol as chain extender, which favors the formation of microcrystalline domain. (49)

What have to be taken into account in the overall comparison is also the difference in the chain extender. PD possess an aliphatic diol as chain extender while BHMF-2 and BHMF-3 possess a heterocyclic compound (BHMF) as chain extender. A polymer synthesized using an aliphatic diol as chain extender should give a softer material than the one synthesized using a heterocyclic one. Furthermore, the longer the chain extender, the longer the hard segment, which favors the hard segment segregation, thus influencing the crystallinity.

The difference in chain extender can be seen comparing the melting temperature. BHMF-containing polyurethanes has a melting temperature which is around 20 °C higher than PD's one.

A further confirmation of the high crystallinity of the PD and BHMF-2 can be noticed in the process of dissolution for the preparation of the electrospinning solution. Indeed, while BHMF-3 is readily dissolved by the mean of just stirring for 24h, BHMF-2 needs between 2 and 3 days under energetic stirring and PD need 1 day under energetic stirring and heating at 80 °C. This is supposed to be related at a higher cohesiveness of these two samples, which require a far much higher amount of energy to disrupt the crystalline domain.



### 3.2 DMA

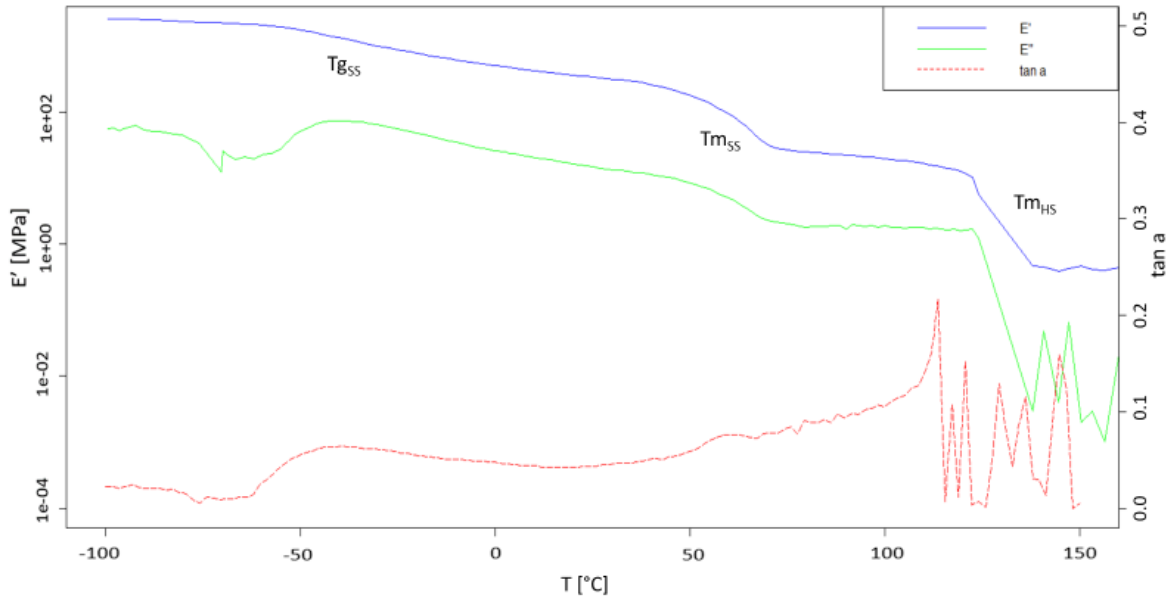


Figure 44 Storage and loss moduli and  $\tan \delta$  vs  $T$  of PD

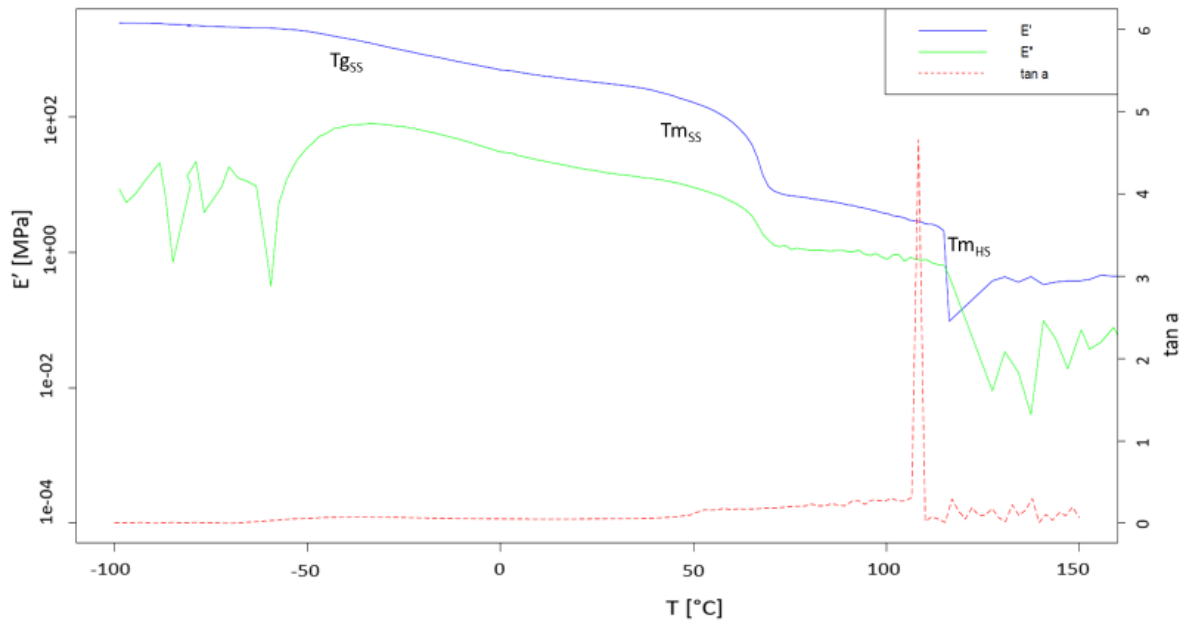


Figure 45 Storage and loss moduli and  $\tan \delta$  vs  $T$  of BHMf-2

Figure 44 and 45 show the storage and loss moduli ( $E'$  and  $E''$ ) and  $\tan \delta$  of the PD and BHMF-2 polyurethanes. BHMF-2 was taken as representative among of furan containing polyurethanes. Below soft phase glass transition temperature, which appears around  $-45$  °C, all materials display  $E'$  values of 2000-2800 MPa. Around soft phase glass transition temperature (around  $-45$  °C), a decrease in  $E'$  values and a maximum, even if very small, in  $\tan \delta$  can be observed. Regarding the position of the  $\tan \delta$  peak, a slight shift to higher temperature can be observed in BHMF-2 polyurethane.

The low temperature behavior of the polymer can explain both the content and the interaction between the hard segment and the soft segment. Indeed, the peak in the  $\tan \delta$  at low temperature is associated to the glass transition temperature of the soft segment ( $T_{gSS}$ ) and so considered as an indicator of phase separation. An increasing in  $T_{gSS}$  has to be ascribed to an interaction between a low amount HS and SS, which promote a mixing between the two segments. Instead, a decrease in  $T_{gSS}$  can be related to a higher amount of HS which results no more in a phase mixing but in a phase separation, creating well defined hard segment domains, thus not influencing the glass transition temperature of the SS.

Another characteristic feature indicating the increasing in phase separation is the broadening of the  $\tan \delta$  peak. In fact, narrower peaks are correlated to a more homogenous structure.

It can be seen here that increasing crystallinity in the hard segment, as observed in the DSC thermogram of PD polyurethane, favors phase separation and leads to slightly lower the  $T_{gSS}$  value.

### 3.3 TGA

The results of thermal gravimetric analysis performed on the samples were analyzed. None of the sample show a consistent weight loss before the 260 °C and the maximum degradation speed are all around 412 °C.

#### BHMF-3

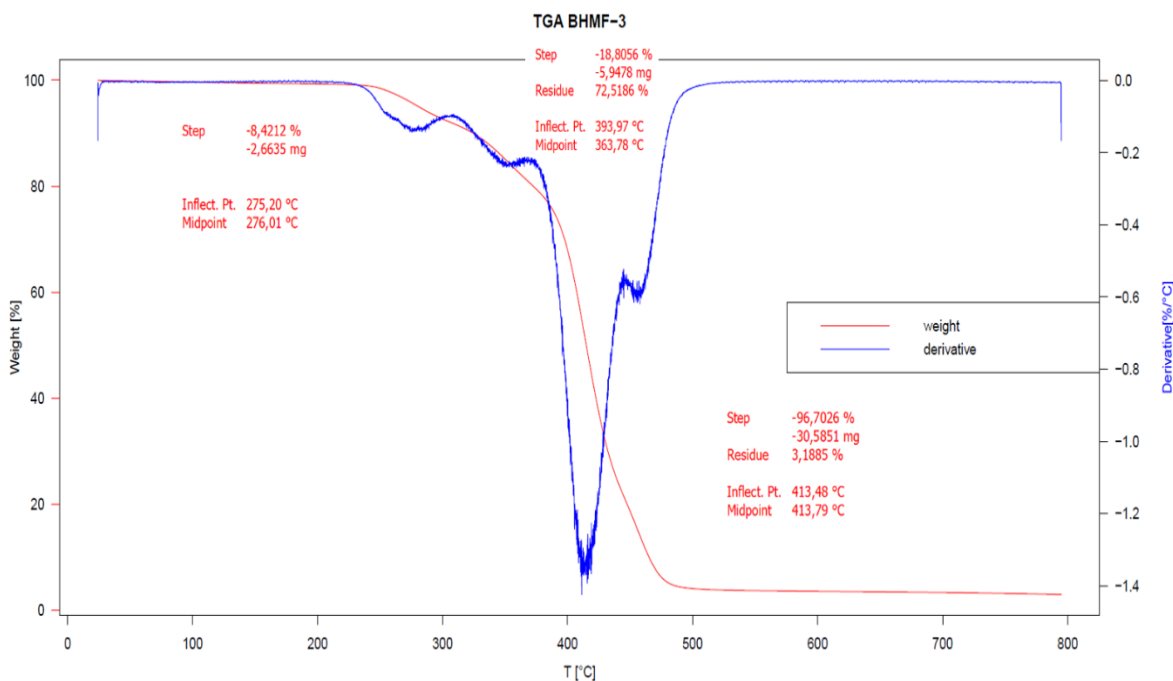


Figure 46 TGA and DTG curves of BHMF-3

The sample shows the initial peak starting around 250 °C, compatible with the urethane bond degradation temperature (250-330 °C). Once the urethane bond is broken, BHMF degrades and volatilize when the temperature reaches the second peak at 363 °C. As can be seen the percentage weight loss associated with both peaks is very similar to the percentage weight of BHMF and HDI contained in BHMF-3 initial formulation.

This is a further probe that the BHMF is present in polymer chain.

Another two peak appears at 413 °C which results from the degradation of polyol and

carbonaceous residues produced by the first degradation, respectively.

## BHMF-2

BHMF-2 shows similar features of BHMF-3 regarding the first peak but it occurs at a temperature a little bit higher denoting a higher thermal stability. The urethane bonds concentration is lower but the peak occurs at a higher temperature due to the higher crystallinity of BHMF-2. It is the only composition that does not show an intermediate peak around 360 °C, maybe due to the temperature shift of the urethane degradation peak and the lower amount of BHMF-2 and urethane that could result in an overlapping of the peaks. The degradation associated to polyol is observed at the same temperature.

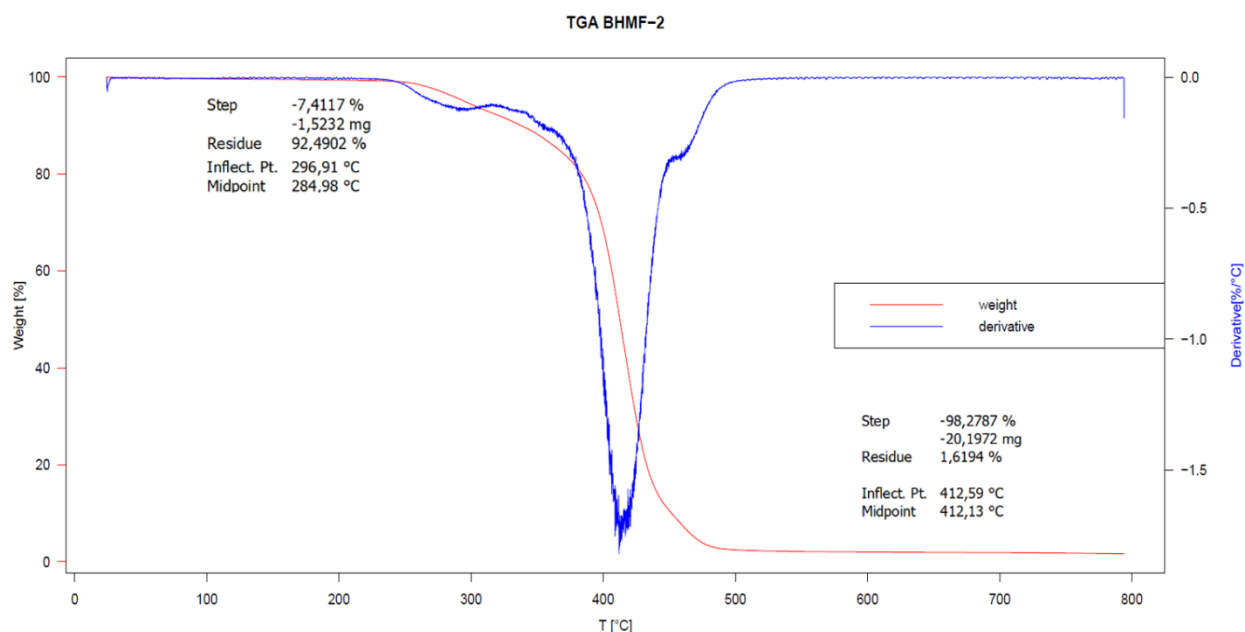


Figure 47 TGA and DTG curves of BHMF-2

## PD

PD is supposed to be the most crystalline between the three formulation and TGA analysis seems to confirm this. Indeed, the chain extender 1,3 propanediol has a boiling point of 213 °C but no degradation starts till 290-300 °C. This means that the urethane bond needs a big amount of energy to be broken, due to the high cohesiveness of the crystalline domains. As in polyurethanes containing furan groups, the polyol degradation temperature is not affected.

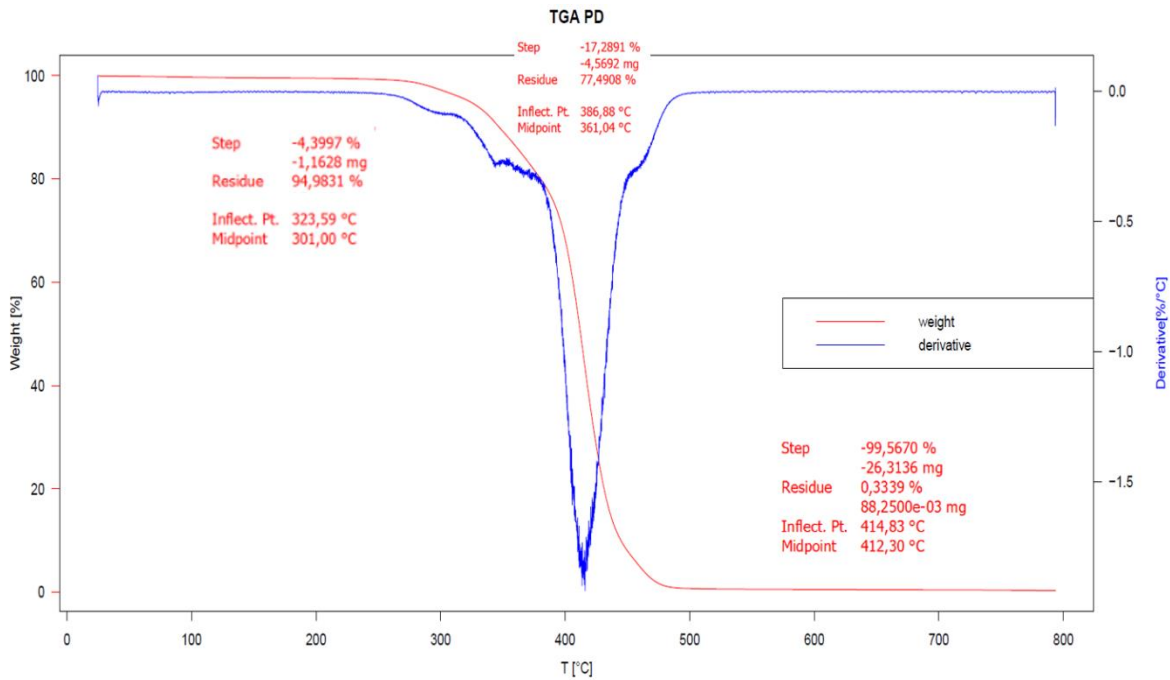


Figure 48 TGA and DTG curves of PD

## 3.4 FTIR

### 3.4.1 FTIR of films

Figure 49 shows the spectra of the synthesized polyurethanes, as well as the spectrum of HDI. They do not show the isocyanate group absorption band at  $2270\text{ cm}^{-1}$ , confirming that all isocyanate groups reacted during polymerization. Moreover, new bands appeared related to the urethane functional group, such as -NH stretching vibration ( $\nu_{\text{-NH}}$ ) in the range  $3200\text{-}3450\text{ cm}^{-1}$ , carbonyl stretching vibration ( $\nu_{\text{-C=O}}$ ) in the amide-I region in the range  $1630\text{-}1730\text{ cm}^{-1}$ , amide-II band at  $1535\text{ cm}^{-1}$  and the band at  $1260\text{ cm}^{-1}$ , assigned to amide-III in aliphatic urethanes.(50)

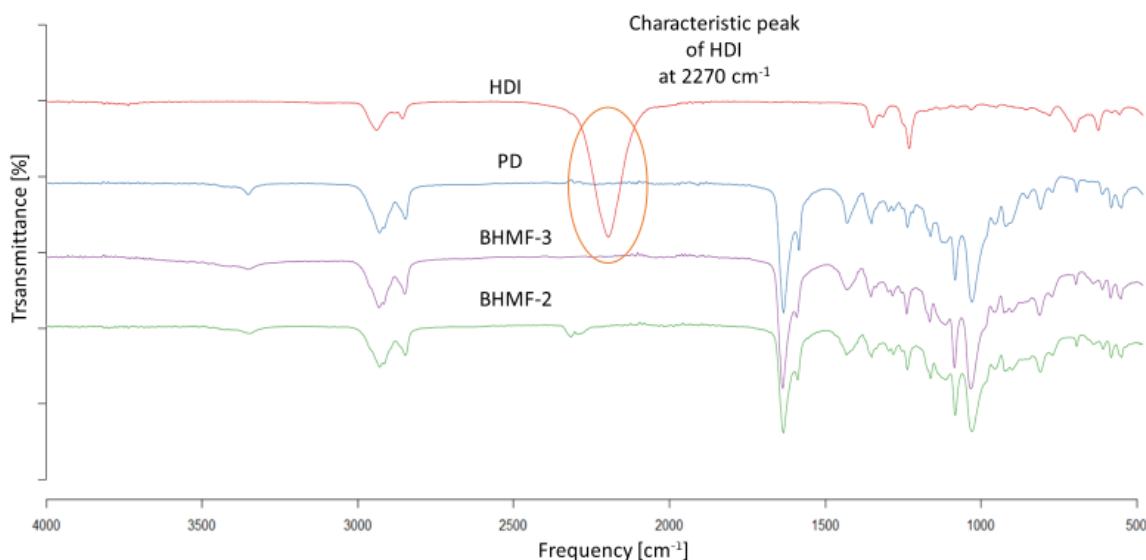


Figure 49 FTIR spectra of synthesized polyurethane and HDI

Observing the fingerprint region, the three samples seem to be very similar even if the chain extender is different. It could be justified by the low molar concentration or the low molar absorptivity of the chain extenders.

In fact, the absorbance in FTIR follows the Lambert-Beer law and can be expressed by the formula

$$A = \epsilon bc$$

Where  $A$  is the relative amount of light absorbed,  $c$  is the molar concentration of the chemical species,  $b$  the path length and  $\epsilon$  the molar absorptivity, quantifying how strongly a chemical species absorb light at a given wavelength.

Characteristic peaks which distinguish BHMF and can be also found in the furan-containing polyurethanes are the followings:

- 1)  $808\text{ cm}^{-1}$ , which corresponds to the bending of a three-substituted alkene created when the furan reacts
- 2)  $1450\text{ cm}^{-1}$ , which correspond to the C=C stretching of an aromatic compound

There are peaks which could corresponds to the ones listed before, but these peaks are present in all the samples, even in the PD, where no BHMF is present. Could happen that shifting and overlapping of the other groups' peaks masks the ones of BHMF, thus making difficult to recognize the effectiveness of the BHMF incorporation in the polymer chain.

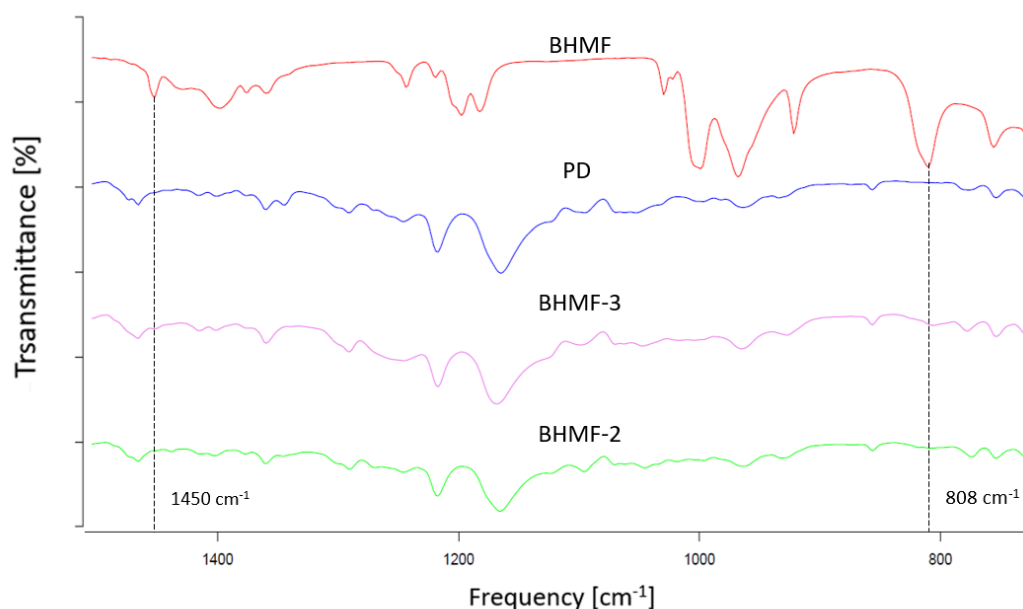


Figure 50 FTIR spectra of synthesized polyurethane and BHMF

However, peaks corresponding to hydroxyl stretching vibrations of BHMf, at frequency around  $3200\text{ cm}^{-1}$ , disappear in both the final polymers BHMf-2 and BHMf-3, thus becoming another probe of the possible furan incorporation in polymer backbone.

### 3.4.2 FTIR of membranes

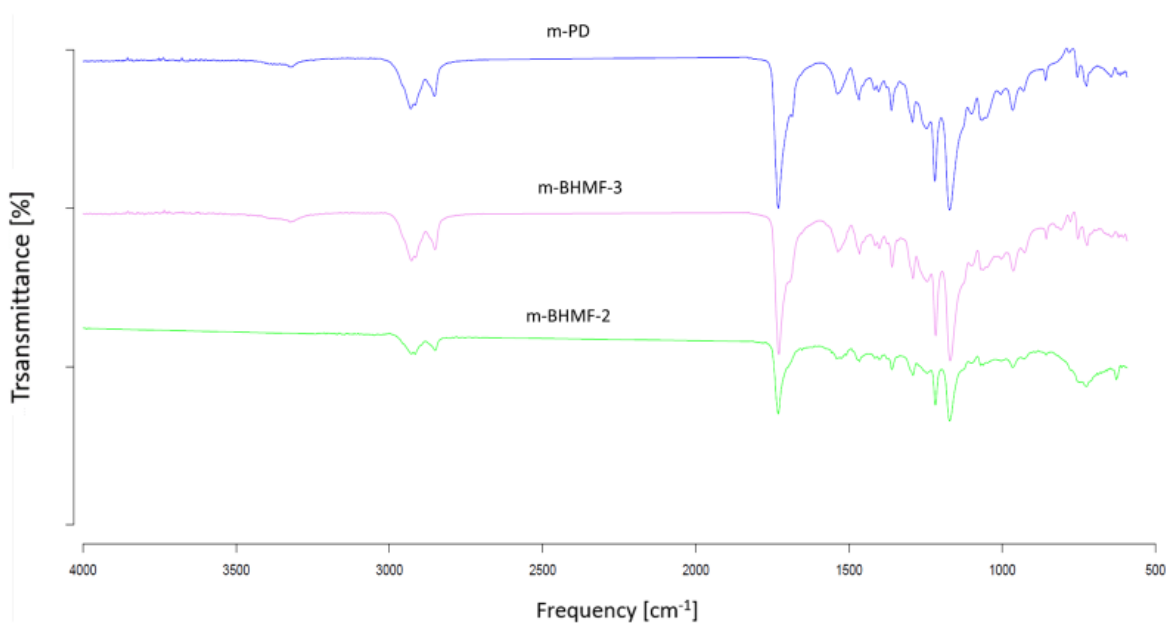


Figure 51 FTIR spectra of the membranes prepared from PD, BHMf-2 and BHMf-3

The spectra of the three membrane were collected. As for the spectra of the films, the same peaks are shown for the three polyurethane-based membraned.

Finally, the spectra of DMF, PD, BHMf-2 and BHMf-3 membrane have been collected, in order to assess the presence of DMF in the membrane. From the following spectra, it seems that no DMF is present in the membrane.



Assessing the presence of DMF or other solvent in the membrane is an important task because they can influence the contact angle measurement, introducing a polar or nonpolar component which is not present in the polymer formulation, which alter the angle measurement.

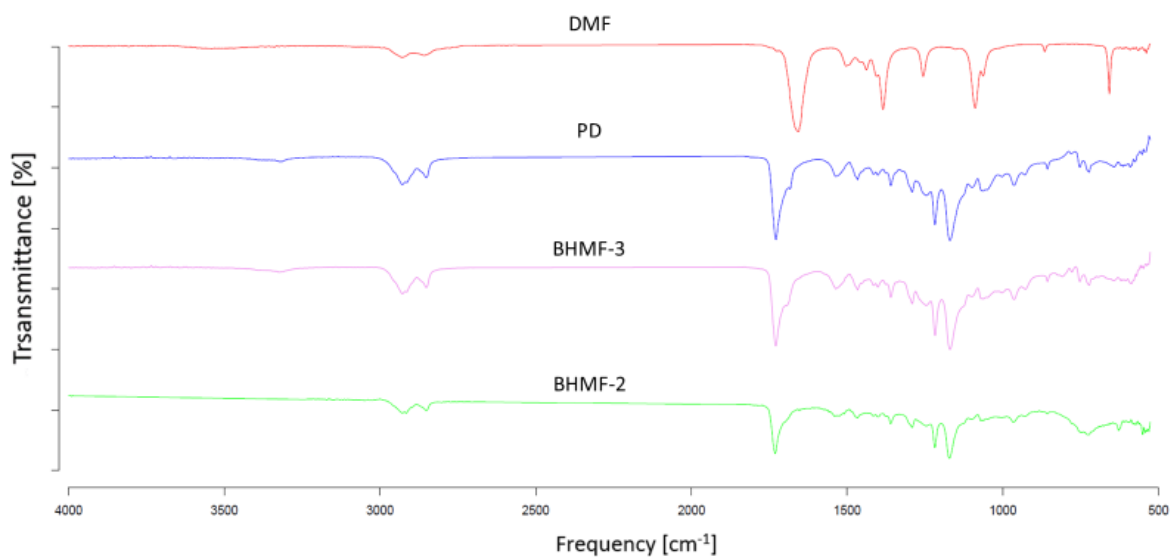


Figure 52 FTIR spectra of the membranes prepared from PD, BHMF-2, BHMF-3 and DMF

### 3.5 SOLVENT MIXTURE FOR ELECTROSPINNING

In order to being able to spin the polymer, it has to be dissolved in a suitable solution.

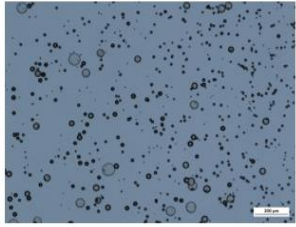
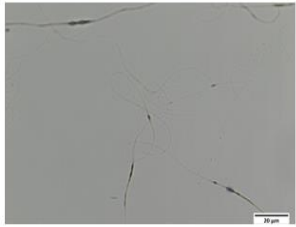
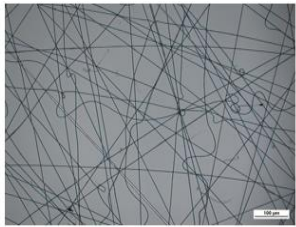
It was not an easy task.

Taking into account the literature, commonly used solvents are chloroform, dimethylformamide (DMF), tetrahydrofuran (THF), acetone, dimethyl sulfoxide (DMSO) and mixture of them.

Between the aforementioned solvents just the chloroform shows an efficient dissolution of the three different compound, while all the other are not able to dissolve the compound at weight concentration which can be used to produce the membrane.

Chloroform ( $\text{CHCl}_3$ ) is a high volatile solvent, having boiling point around 60 °C. This imply the fast vaporization of the solvent while the jet is reaching the collector, which should give a better fiber deposition and a smaller fiber diameter. A great issue of such a volatile solvent is the solidification of the material on the spinneret tip, which must be removed frequently. Such a problem avoids a continuous electrospinning and the jet interruption negatively affect the final membrane homogeneity, so, even if fibers can be produced, the quality is too poor, thus the possibility of using pure chloroform as solvent has been discarded.

In order to overcome this problem, different mixture have been tried, adding to chloroform different solvents in different amounts. Between the commonly used solvent has been selected the one with highest boiling point in order to equilibrate the chloroform volatility. Another variable playing a fundamental role in the searching of the perfect electrospinning solution is the polymer weight percentage in solution. Although easy to dissolve, a too low percentage of polymer gives not a continuous fiber, while a too high percentage was impossible to dissolve. The different attempts made, with the correspondent results, are shown in table 6.

Solution	Weight percentage	Result
CHCl <sub>3</sub>	7 %	
CHCl <sub>3</sub>	10%	
DMF:CHCl <sub>3</sub> 2:1	13%	

*Table 6 Solvent and solvent mixture, weight percentage and resulting fiber of different electrospinning attempts*

As can be seen from different attempts made, a too small amount of polymer produces particles instead of fiber, resulting in electro-spray instead of electrospinning. Such behavior can be explained considering the importance of the polymer solution's viscosity. Indeed, increasing the polymer content bigger fibers are produced with a more uniform diameter. Furthermore, the addition of DMF (boiling point at 150 °C) allows to maintain a continuous jet which can last for hours giving the possibility to produce homogeneous and large membranes with good mechanical properties.

PD was found to be the most difficult to dissolve in DMF: CHCl<sub>3</sub> in 2:1 ratio solvent mixture. The solubility of PD in the selected solvent is around 12 wt% which is the optimum concentration suitable to be electrospun. It was observed that at higher concentration the polymer solution is not perfectly homogenous, thus preventing the possibility of continuous electrospinning, while at lower concentration the fibers are not obtained, resulting in electro-spray.

Regarding the polymers containing furan, both BHMF-2 and BHMF-3 can be electrospun in a bigger concentration range: 12-15 wt% for the BHMF-2 and 16-20 wt% for the BHMF-3.

<b>Material</b>	<b>Weight percentage (wt%)</b>
PD	12
BHMF-2	13
BHMF-3	16

*Table 7 Weight percentage at which the best fibers are obtained for each polymer*

From the analysis of BHMF-2 and BHMF-3 can be seen a correlation between the furan content in polyurethane and its solubility in the solution of DMF and  $\text{CHCl}_3$ . More furan a compound possesses, easier it is to dissolve. It can find a relation with what has been supposed from the DSC results. A higher hard segment content results in a less ordered structure, taking into account both soft and hard domains, which is easier to dissolve. But this can not only be ascribed to the hard segment content, because the difference between PD and BHM-2 is just 1 wt%, but the first one is much more difficult to dissolve. So, it is probably the type of chain extender which influence the general properties of the polyurethane. PD possesses 1,3 propanediol as chain extender which is able to interact via hydrogen bond with hard segment of adjacent polymer chains, resulting in a more cohesive compound. BHMF, on the contrary, is not so favored to create hydrogen bonds, due to its higher steric hindrance, thus giving a less ordered and weaker polyurethane, easier to dissolve.

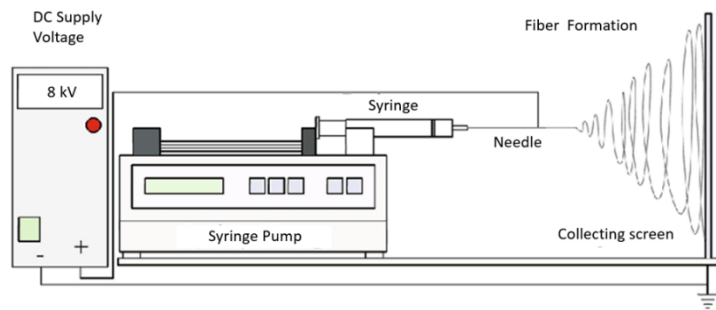
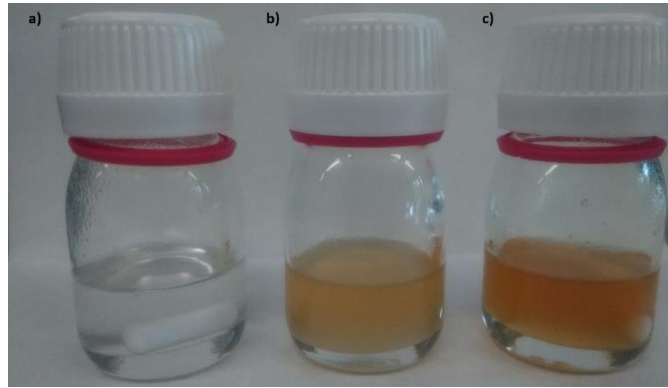
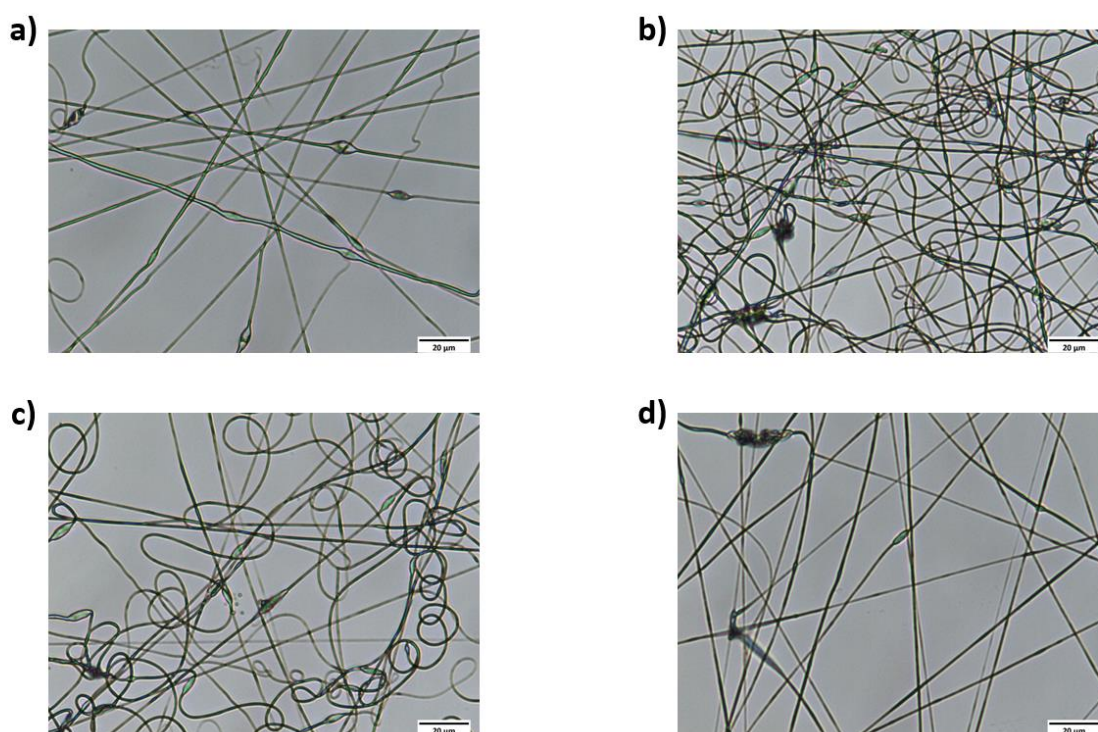


Figure 53 polymers before electrospinning: a) PD b)BHMF-2 c) BHMF-3, electrospinning equipment and one of the resulting membranes

### 3.6 ELECTROSPINNING RESULTS

Once assessed the right solvents ratio and the right weight percentage for each polymer, the others electrospinning variables have been investigated in order to obtain the best electrospinning setup in terms of quality of the fibers, quality of the membrane and spinnability ease .

As can be seen in Figure 54, increasing the distance of the collector and the voltage while decreasing the injection rate the fiber became thinner and with less beads and defects.



*Figure 54 Optical microscopy images of different electrospinning operation conditions using the polymer solution of PD 12%wt in DMF:CHCl<sub>3</sub> 2:1 a) 5kV, 7cm, 1ml h<sup>-1</sup> b) 6.7kV, 12cm, 1ml h<sup>-1</sup> c) 7.5kV, 15 cm, 0.2 ml h<sup>-1</sup> and d) 8 kV, 15 cm, 0.5 ml h<sup>-1</sup>*

The limited range of voltage applicable and the bad results obtained with PD has avoided a further investigation about the influencing operations conditions.

In fact PD is the most difficult compound to spin between the three. Not only it is very difficult to dissolve even at lower concentration but also the solution on the spinneret's tip tend to solidify, making very difficult to produce good quality membrane

## BHMF-2

The ease of spinnability of this solution allow to deposit fibers at very different range of voltage, distance and injection rate. Having encountered the perfect voltage and distance in 8kV and 15cm, it has been decided to investigate the effect of the different injection rate and distances have been evaluated. The goal was to investigate how can be increased the injection rate, meaning how much quantity of material can be deposited still having acceptable fibers and how a longer time of flight influences the fiber morphology.

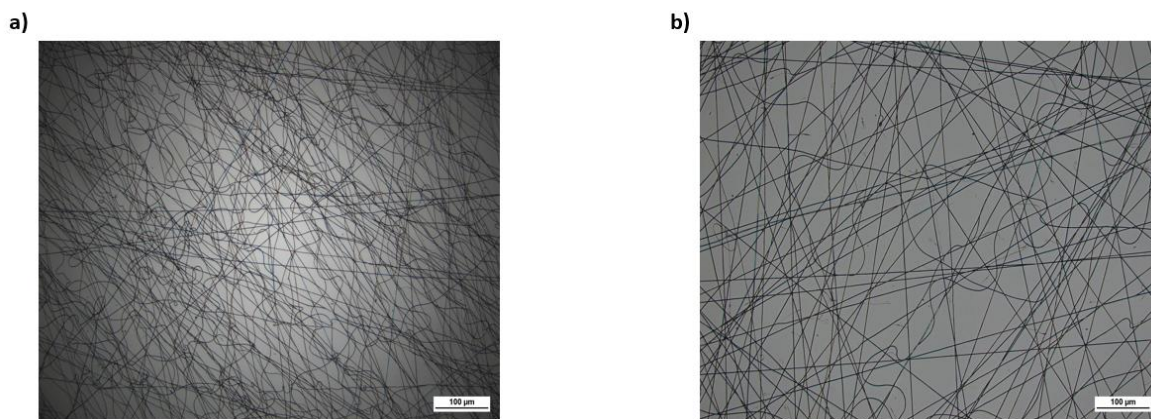


Figure 55 Optical microscopy images of electrospun mats obtained using polymer solution of BHMF-2 13 wt% at: a) 0.2 ml h<sup>-1</sup> 15 cm b) 0.2 ml h<sup>-1</sup> 20 cm

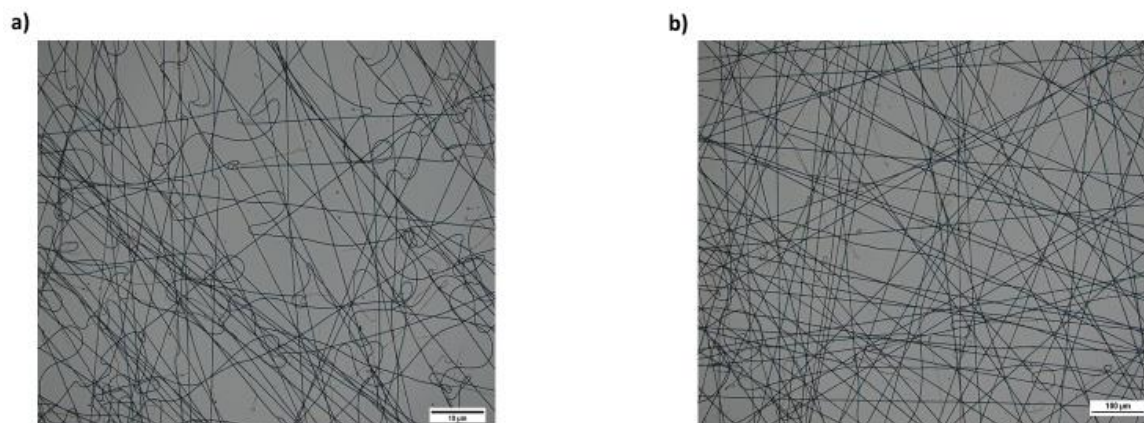


Figure 56 Optical microscopy images of electrospun mats obtained using polymer solution of BHMF-2 13 wt% at: a) 0.5 ml h<sup>-1</sup> 15 cm b) 0.5 ml h<sup>-1</sup> 20 cm

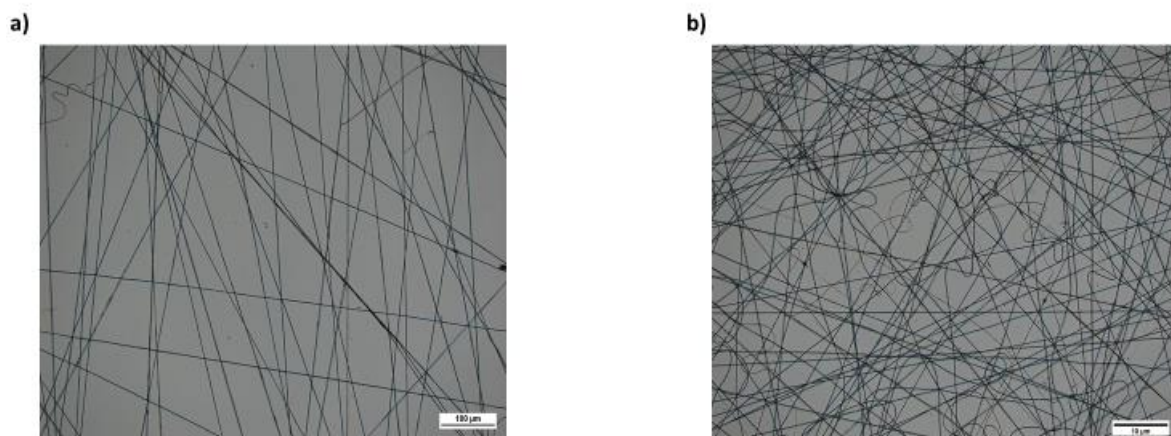


Figure 57 Optical microscopy images of electrospun mats obtained using polymer solution of BHMF-2 13 wt% at: a)  $1 \text{ ml h}^{-1}$  15 cm b)  $1 \text{ ml h}^{-1}$  20 cm

Injection rate does not affect particularly the diameters neither in thickness nor in diameters' distribution. What can be seen from the images is just a straighter fiber produced when increasing the injection rate.

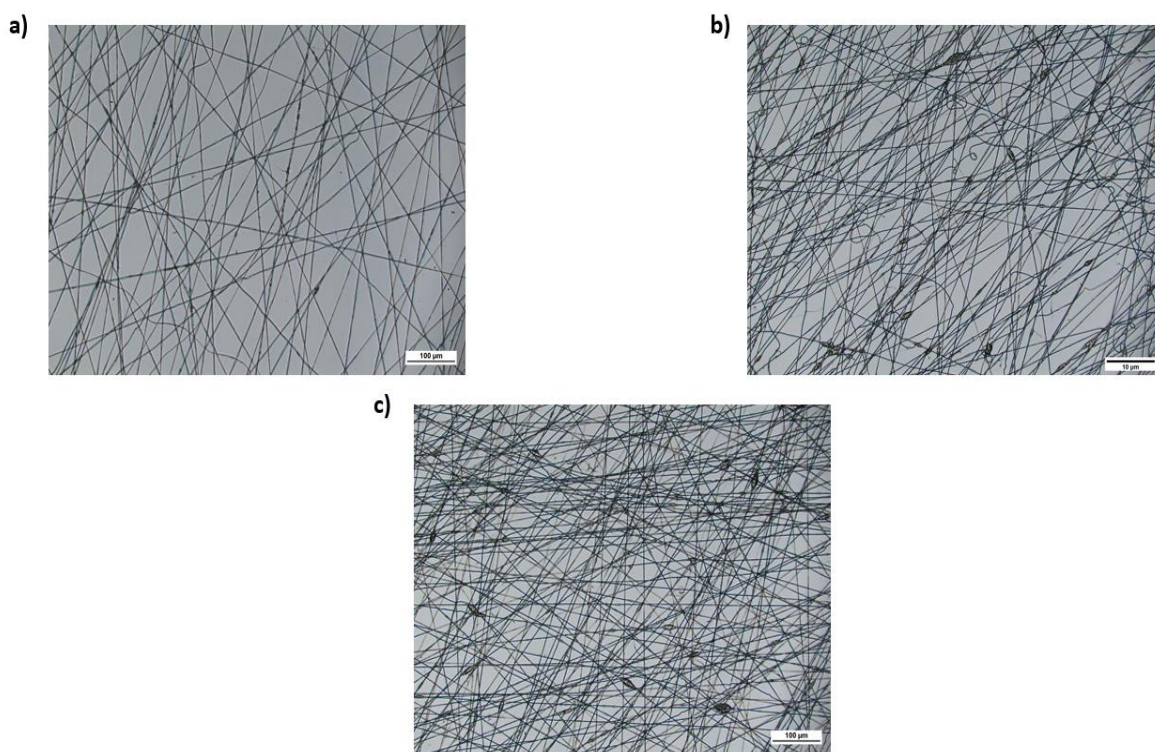


Figure 58 Optical microscopy images of different electrospinning operation conditions using the polymer solution of BHMF-2 14 wt% in DMF:CHCl<sub>3</sub> 2:1 : a) 6 kV, 15 cm,  $0,2 \text{ ml h}^{-1}$  b) 6 kV, 15 cm,  $0,4 \text{ ml h}^{-1}$  c) 6 kV, 15 cm,  $0,5 \text{ ml h}^{-1}$



Increasing the distance thinner and straighter fibers are produced.

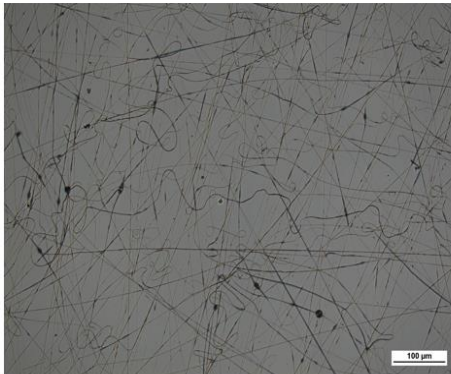
The high spinnability had encouraged a further investigation about the variation in morphology, thickness and homogeneity of the fiber when the weight concentration is increased from 13 to 14 wt%.

Increasing the quantity of polymeric material in the solution means increase its cohesiveness, resulting in flow instability. This instability lead to a worse quality of the fiber as can be seen from Figure 58, where lots of beads and inhomogeneous diameters are present.

### **BHMF-3.**

BHMF-3 needs a higher solid content in the electrospinning solution. In the following images are shown fibers electrospun from a solution containing 16 wt% of solid, dissolved in the same solvent mixture of DMF:CHCl<sub>3</sub> 2:1 . The best results in terms of fiber morphology and spinnability are reached with the 16 wt% solution.

a)



b)

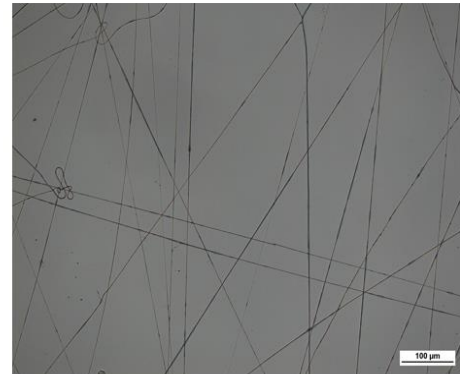


*Figure 59 Optical microscopy images of electrospun mats obtained using polymer solution of BHMF-3 16 wt% at: a) 0.2 ml h<sup>-1</sup> 15 cm b) 0.2 ml h<sup>-1</sup> 20 cm*

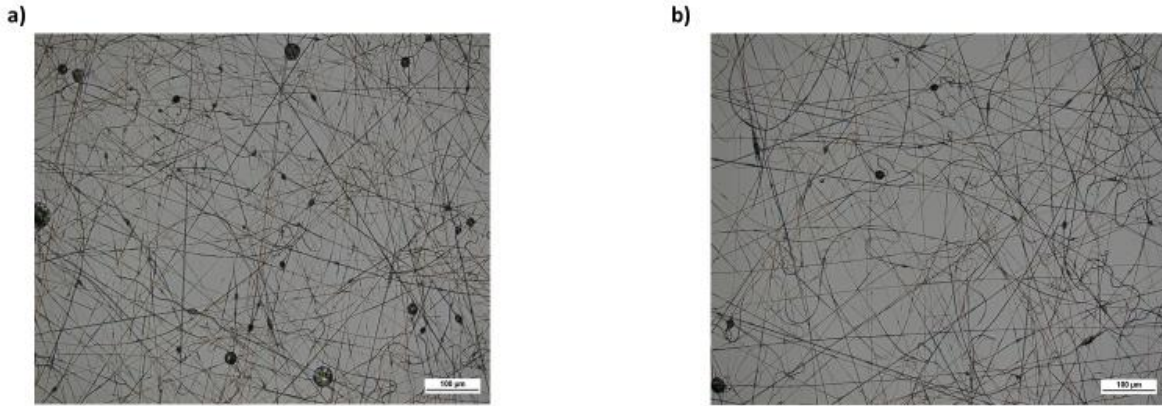


Figure 60 Optical microscopy images of electrospun mats obtained at using polymer solution of BHMf-3 16 wt% a)  $0.5 \text{ ml h}^{-1}$  15cm b)  $0.5 \text{ ml h}^{-1}$  20 cm

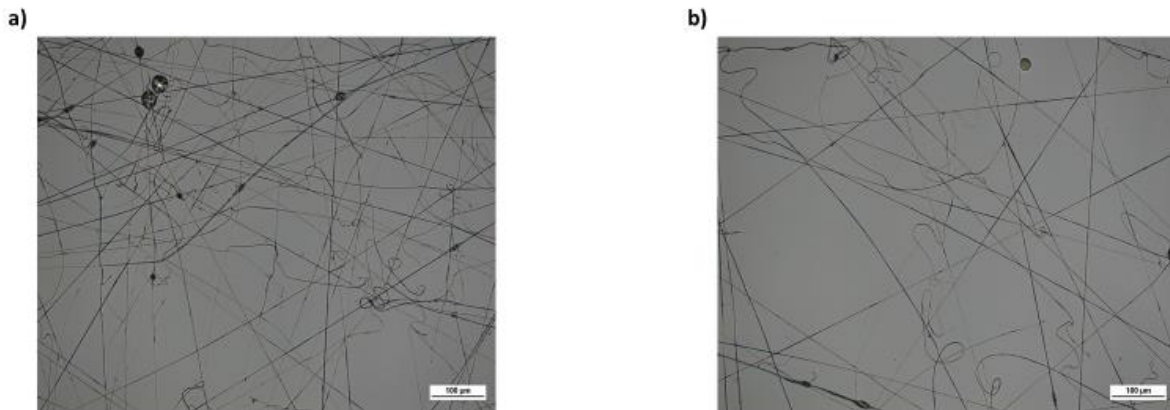


Figure 61 Optical microscopy images of electrospun mats obtained a using polymer solution of BHMf-3 16 wt% t: a)  $1 \text{ ml h}^{-1}$  15 cm b)  $1 \text{ ml h}^{-1}$  20 cm

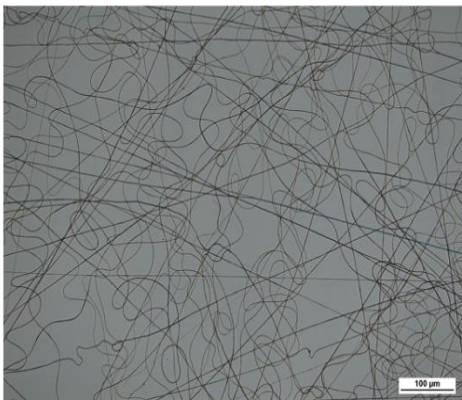
As shown in the Figures 59-61, generally the fiber quality of BHMf-3 is much worse than the BHMf-2's ones. Between the two different configurations tried, the one with the collector at 20 cm seems giving the best results. A longer time of flight of the fiber, means more time for the solvent to evaporate, due to the BHMf-3 interact more strongly with solvent. It can be seen also during the electrospinning process that this solution has no problem of solidification on the spinneret.

However, the diameter distribution is wide, meaning not uniform fibers at all.

## PD

PD shows the best fiber in terms of surface morphology and presence of defects. It also shows easy spinnability in a wide range of voltage, distances and injection rate. Only the solutions spun at  $1 \text{ ml h}^{-1}$  shows the presence of few defects, given maybe by the low voltage use.

a)



b)

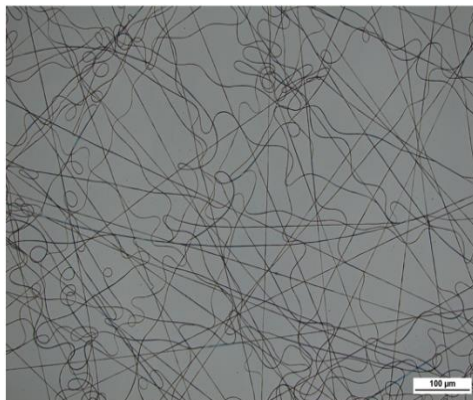
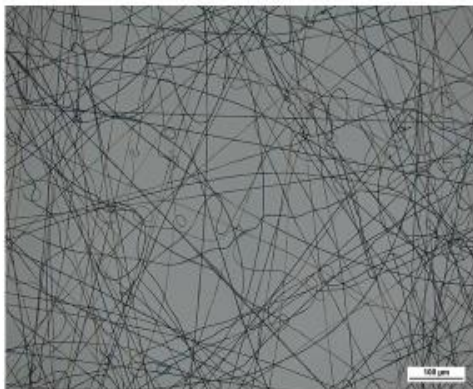


Figure 62 Optical microscopy images of electrospun mats obtained at using polymer solution of PD 12 wt% :  
a)  $0.2 \text{ ml h}^{-1}$  15 cm b)  $0.2 \text{ ml h}^{-1}$  20 cm

a)

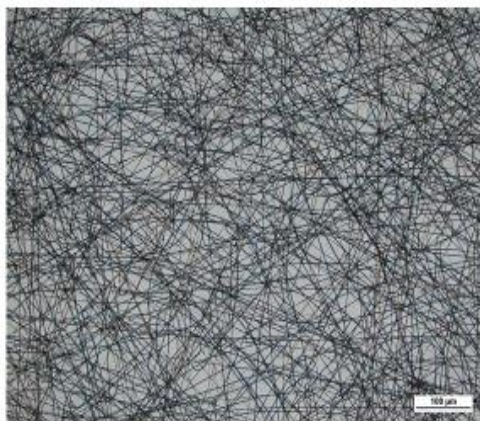


b)



Figure 63 Optical microscopy images of electrospun mats obtained at using polymer solution of PD 12 wt% :  
a)  $0.5 \text{ ml h}^{-1}$  15 cm b)  $0.5 \text{ ml h}^{-1}$  20 cm

a)



b)

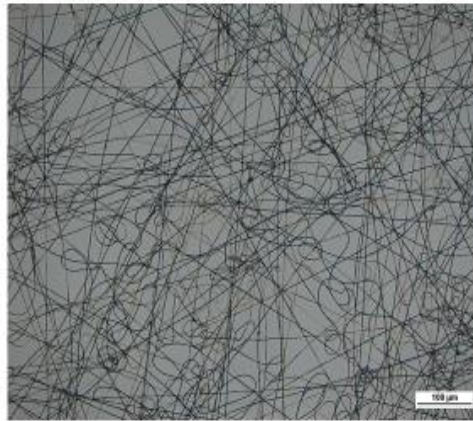


Figure 64 Optical microscopy images of electrospun mats obtained at using polymer solution of PD 12 wt% :  
a)  $1 \text{ ml h}^{-1}$  15 cm b)  $1 \text{ ml h}^{-1}$  20 cm

As can be seen a common feature of all the polymer solution is the helical shape assumed by the deposited fibers. It became more evident increasing the distance of the collector and the voltage applied and could be ascribed to the mechanical buckling instability when the jet impinges on the collector surface. (51)

If a high tensile strength is required, the problem of helical fiber can be overcome using a rotating collector, setting a proper speed which allows the deposition of perfectly aligned fibers.

Finally, different configuration of distance, voltage, injection rate and solid concentration have been demonstrated to be used in electrospinning of all compounds, confirming the high versatility of the polymer and its suitability to be produced in continuous way. Such characteristics are promising for a scaling up of the process.

## 3.7 PROOFS OF DA REACTION ON THE ELECTROSPUN MEMBRANE

### 3.7.1 Functionalization using 5-MF

In order to assess the possibility to perform a click-reaction on the electrospun membrane, a labelling agent has been utilized. The 5-MF is a fluorescent compound, mainly used in protein labelling thanks to the well-known reactivity between it and Sulphur, Sulphur through thiol-ene click reaction. It can be excited by wavelength in the range of 460-480 nm (even if the absorption spectrum presents some peaks at shorter wavelength).

It is a compound sensible to air and light, which has to be stored under Argon atmosphere in the dark.

This compound was selected due to its high fluorescence, the large spectra of absorption and, obviously, for the presence of maleimide in an easily accessible position which make the DA reaction easy to occur.

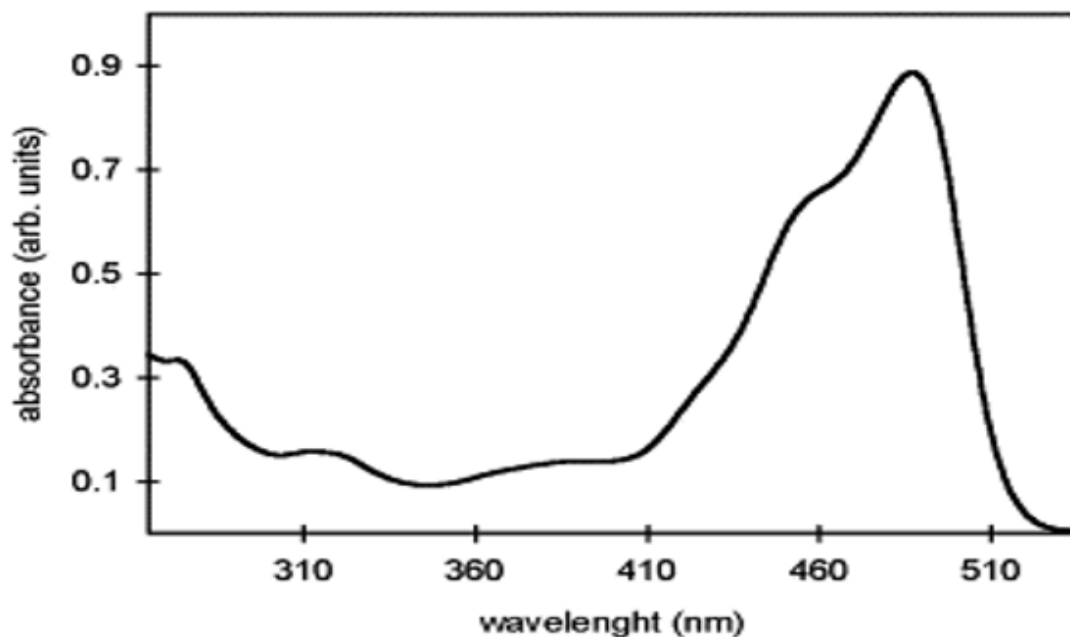


Figure 65 UV-vis Absorption spectrum of 5-MF

## **Dissolution**

There are no clear specifications on the solubility of the 5-MF on the producer website, even if other producers indicate it soluble in DMF, DMSO and even water. For this reason, has been tried different solvent mixtures.

First of all, the dissolution should not dissolve the membrane; pure DMF has been found to dissolve it, pure DMSO partly dissolve it while water doesn't affect it at all, being the polyurethane and consequently the membrane hydrophobic.

It has been opted for two different solvent mixture: the first one composed of 80% DMSO and 20% water in volume and the second one pure water.

## **Preparation of the sample**

In both the solution was added 5mg of 5-MF, then dissolved in 1ml of the two different solvent mixture.

Due to the high sensibility to light the weight of the compound was performed in a scarcely illuminated room and it was deposited in a vial covered by aluminum foil.

Once weighted the 5-MF the solvent was added and the solution has been exposed under a continuous flux of nitrogen for 10 minutes. Then a piece of membrane was deposited in a petri dish covered by aluminum sheet and the solution gently dropped on it. All the operation has been performed in a scarcely illuminated place in order to preventing light induced degradation of the fluorescent labelling compound. The same operational mode has been used for both the solutions.

The system (membrane + labelling agent) was then put in the oven at a temperature of 65 °C. The temperature was chosen as low as possible between the range of temperatures at which DA is supposed to occur. The reasons were mainly two. The first is the melting point of the soft segment (74-77 °C), which is the main component. The second was the not clear behavior of the 5-MF at high temperature. indeed, in literature it is applied in different ranges of temperature: when used in proteins labelling the reaction is performed in a range between 4 °C and 25 °, while in the labelling of nanoclays there are examples of application at temperature higher than 200 °C (52), even if a changing in emission relative intensity has been shown.

The normal time required to make DA reactions happens is few hours but has been decided to leave the sample in the oven for 24 hours in order to be sure the reaction occurs. A longer time at a temperature below the retro-DA temperature does not affect the adduct formed. The labelled membranes were then rinsed in water.

### Visual analysis of the sample and under UV light

At a first glance the solution of pure water has not dissolved the 5-MF. As can be seen in fig 67 the labelling agent is present in lumps with strong red color (the same of the 5-MF) indicating the failure in dissolve it. Instead, the solution of DMSO and water show a yellow color, confirming the effectively dissolution of the 5-MF and it seems well distributed all over the surface of the membrane.

The supposition made by the visual analysis were confirmed by the UV light analysis. It have been used two different wavelengths to excite the system: 254 nm and 365 nm. The results are represented in Figure 66.

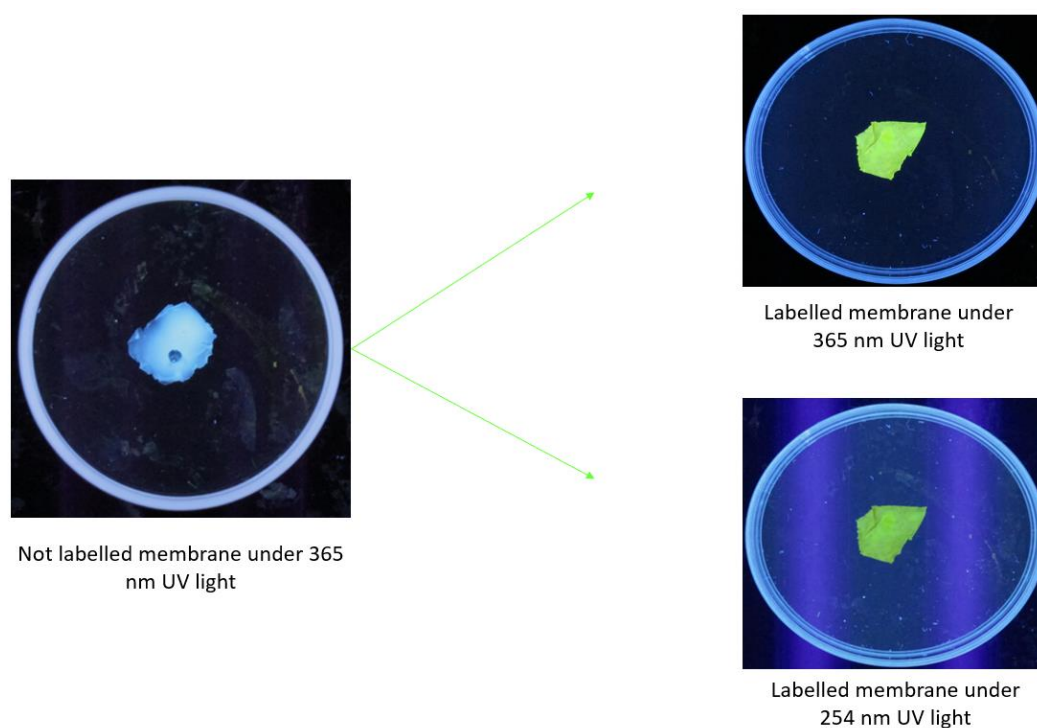
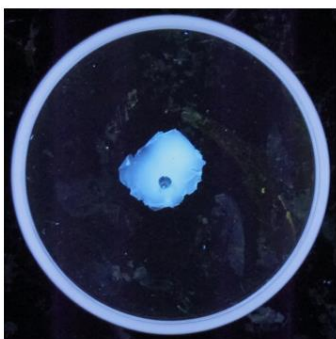
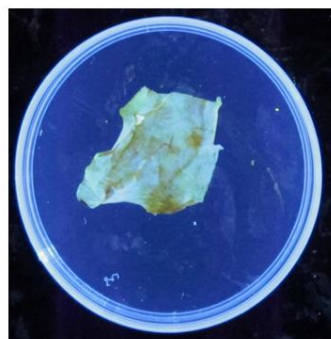


*Figure 66 Membrane in solution of 80% DMSO + 20% water: without labelling agent (left) and with labelling agent (right), exposed to two different wavelengths.*



Not labelled membrane under 365 nm UV light



Labelled membrane under 365 nm UV light

*Figure 67 Membrane in solution of water: without labelling agent (left) and with labelling agent (right)*

In the specification of the producer, the wavelength of excitation is 480 nm but, as can be seen from the absorption spectra, 5-MF presents absorption peaks also at lower wavelengths. The emitting wavelength is of 518 nm, corresponding to the green. From this probe it seems the reaction has occurred. However, the spectrofluorometer results are inconclusive, giving different emission and absorption peaks each probe. This can be due to the multiplicity of influencing factor and the not easy manipulation of the compound that could have been influenced the right development of the procedure.

A final verdict is given by FTIR analysis of the 5-MF functionalized membrane.

The characteristic peaks of DA adduct between furan and maleimide are two:

- 1) The stretching vibration band of  $-C=C-$  bond of DA adduct at  $1457\text{ cm}^{-1}$
- 2) The stretching vibration band of the carbonyl group of maleimide at  $1698\text{ cm}^{-1}$

Both the peaks can be appreciated in the FTIR analysis of the functionalized membrane while they are not present in the not functionalized membrane (Figure 68).



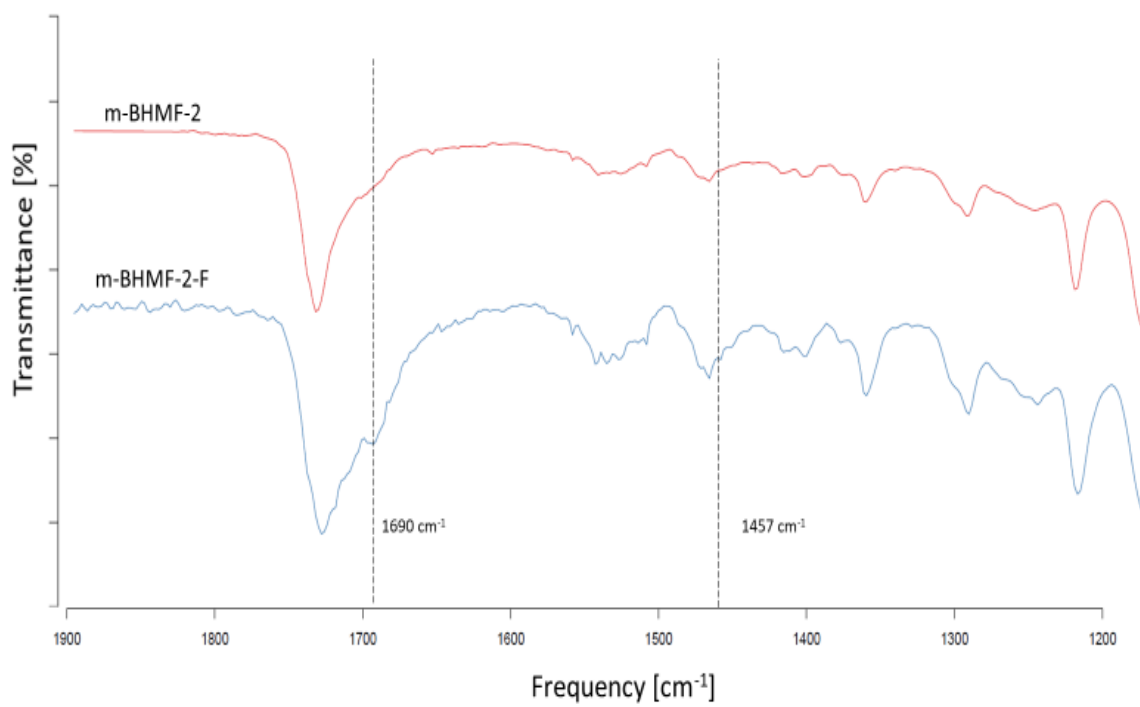


Figure 68 FTIR spectra of the same membrane before and after the functionalization

### 3.7.2 DA reaction between BHMF-2 membrane and AMI assessed by FTIR

A further probe of the DA reaction has been performed in order to surely assess the membrane's capability to undergo a click reaction.

AMI compound was chosen because it can be also dissolved in water. However, better results are reached when DMSO is used as solvent.

The reaction between maleimide and furan has been assessed by the means of FTIR.

An excess of maleimide, in a ratio 1:2 furan to maleimide has been used, to be sure to make react all the available furans. In each gram of BHMF-2 are present 0.46 mmol of furan, while in each gram of BHMF-3, 0.65 mmol.

One sample has been prepared, using BHMF-2

Material	Sample (g)	AMI (g)
BHMF-2	0,093	0,014

*Table 8 Quantities of BHMF-2 membrane and AMI present in solution*

AMI was dissolved in 2ml of water or DMSO for BHMF-2.

The sample has been maintained in oven at 65 °C for 20 h in order to promote DA reaction and then dried at room temperature for 6 hours.

Finally the FTIR spectra has been collected and compared with the not functionalized

sample.

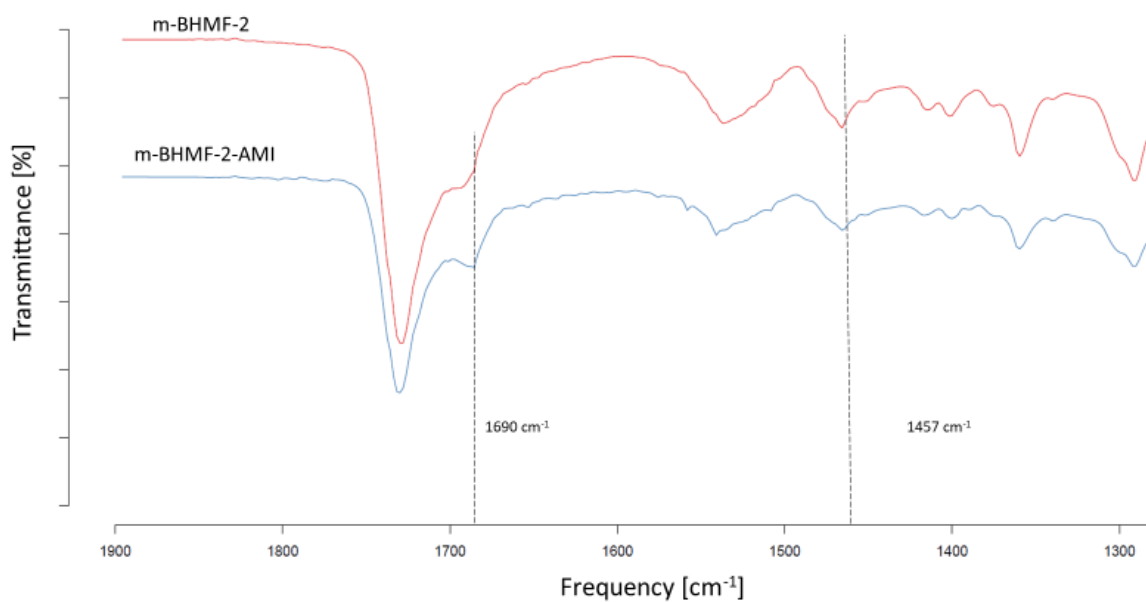


Figure 69 Spectra of BHMF-2 membrane not functionalized (m-BHMF-2) and functionalized with AMI (m-BHMF-2-AMI)

The peak at  $1690 \text{ cm}^{-1}$  is characteristic of a primary amide, which is exactly what we expect to find once the DA between furan and maleimide has occurred

### 3.8 UV-vis MONITORING OF DA REACTION

DA reaction was monitored via UV-vis spectroscopy in order to assess time and temperature necessary for the reaction to occur.

UV-vis is one of the most used technique to monitor the progress of a reaction because it allows to clearly follow the consumption of the reagents. Indeed, it rely on the Lambert-Beer law, thus decreasing the concentration of a given species, also its absorption peak will decrease confirming the reaction is occurring

Due to the complications of monitoring via UV-vis the functionalization of a membrane, it has been decided to control the reaction happening in the electrospinning solution.

Initially, a sample containing just AMI and DMF in a concentration of  $25 \text{ g l}^{-1}$  and a sample containing BHMF-2 dissolved in DMF and  $\text{CHCl}_3$  has been used to find the maleimide peak to monitor. It was found around 278 nm, which is in the range 270-300 nm taken as reference in most of the works regarding this argument.

Then, DA reaction has been performed taking a 0.5 ml of the electrospinning solution BHMF-2 dissolved in 5ml of DMF and  $\text{CHCl}_3$  2:1 and adding 2ml of the solution of AMI and DMF with concentration  $25 \text{ g l}^{-1}$ . The final system was continuously stirred and heated at  $70 \text{ }^\circ\text{C}$ .

At 20, 60, 100, 180 and 240 minutes the solution was analyzed. As can be seen from Figure 70, the peak referred to maleimide (278 nm) decreases, thus indicating the reaction is going on.

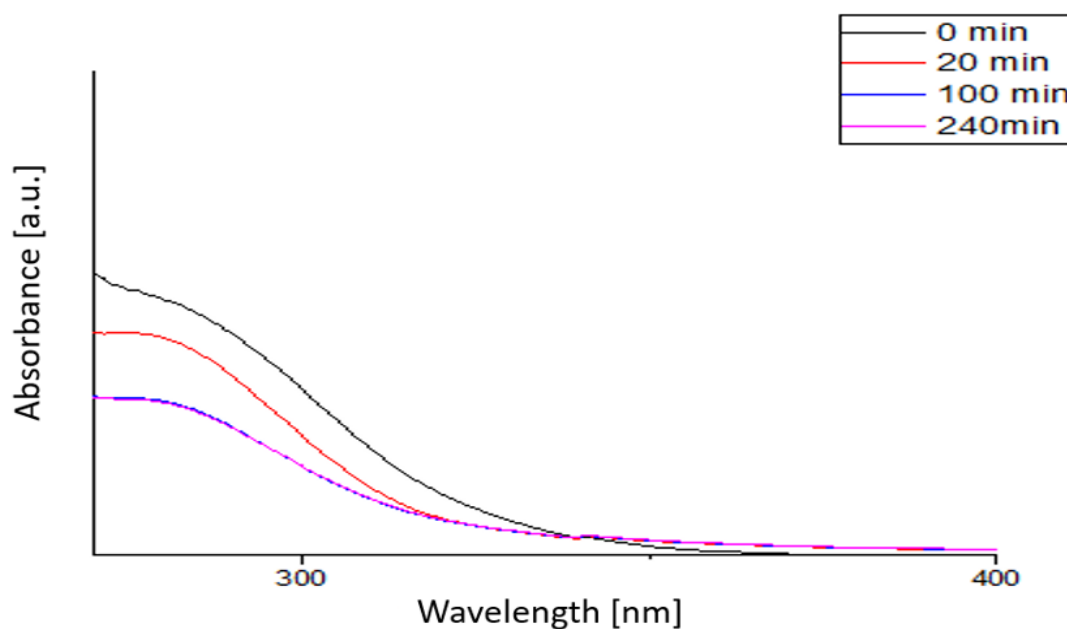


Figure 70 UV-vis monitoring of DA reaction between BHMF-2 and AMI

The quantity of maleimide in the system was quite low, in order to not saturate the spectra and thus allowing to follow the evolution of the peak. However, as can be seen from Figure 70, the peak decrease constantly during the first 100 minutes, indicating the consumption of maleimide. Between the sample analyzed at 100 minutes and the one analyzed at 240 minutes there is no difference at all, meaning that all the available furan groups have reacted.

With the previous results, the possibility of functionalizing the polymer before the electrospinning has been proved.

The following step was the electrospinning of the functionalized solution. In order to do so, 20 mg of maleimide were dissolved in the DMF used to dissolve BHMf-2 in the usual electrospinning solution (Table 3) The system was then left 14 h at 70 °C under constant stirring.

Unfortunately, the analysis of FTIR spectra and contact angle show no difference at all with respect the not functionalized membrane, thus indicating an unsuccessful functionalization.

Then the retro-DA has been investigated, increasing the temperature of the system to 120 °C. Only two sample has been taken because, as shown in Figure 71, after 40 minutes, all the maleimide was released.

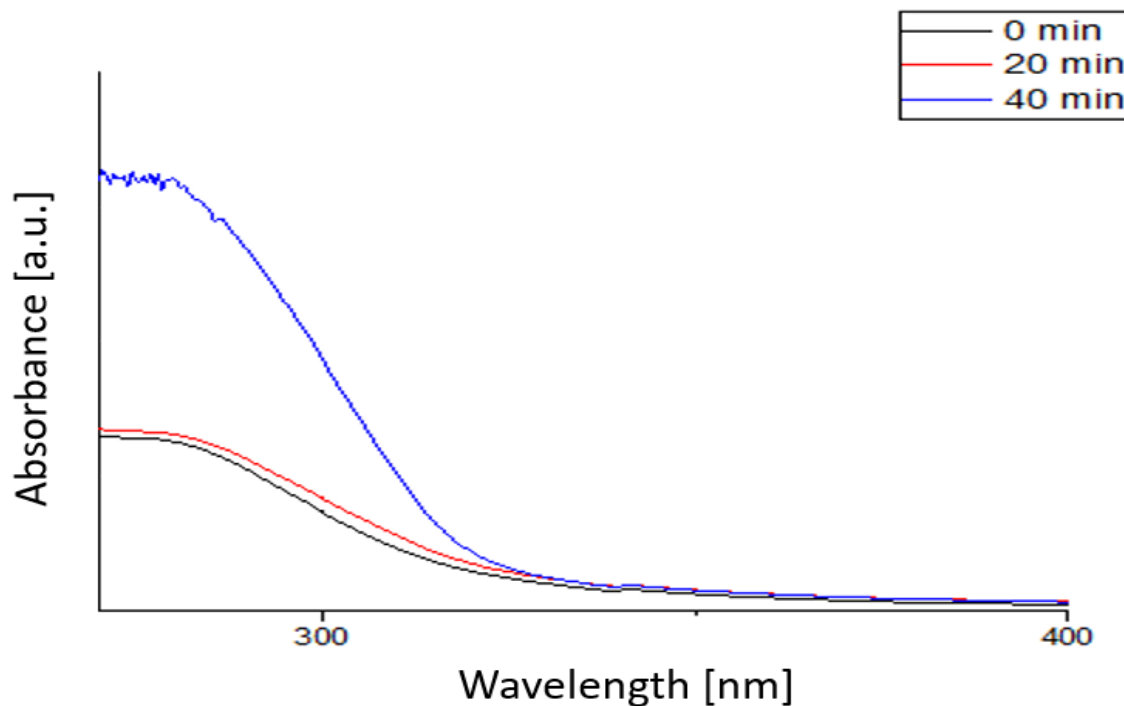
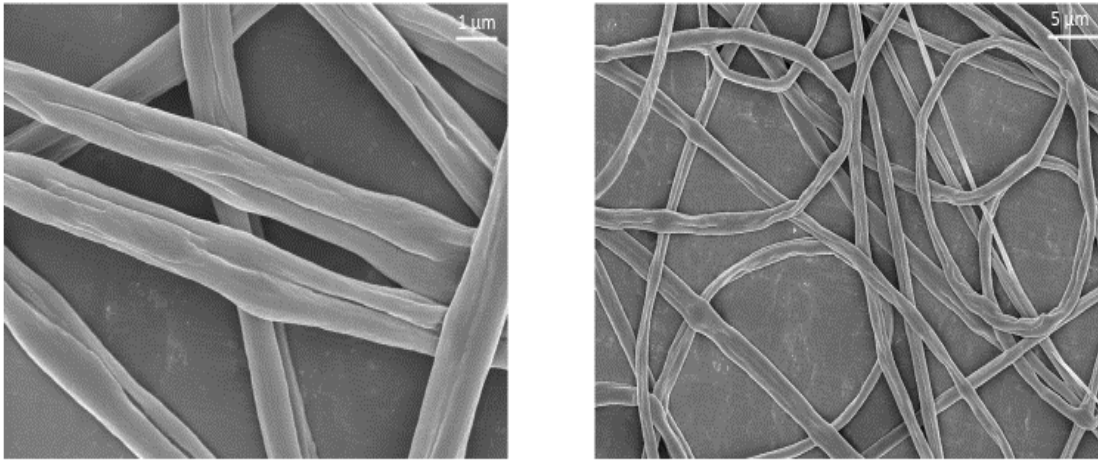


Figure 71 UV-vis monitoring of retro-DA reaction between BHMf-2 and AMI

### 3.9 SEM RESULTS

SEM analysis was performed initially on the three samples PD, BHMf-2 and BHMf-3. In order to have a reliable comparison the same conditions were used in the electrospinning setup: 9 kV of applied voltage, 0.5 ml h<sup>-1</sup> of injection rate and 15 cm the distance between the collector and the spinneret. The collection time was set to 30 seconds. The results are shown below.



*Figure 72 SEM images of BHMf-2 electrospun mats*

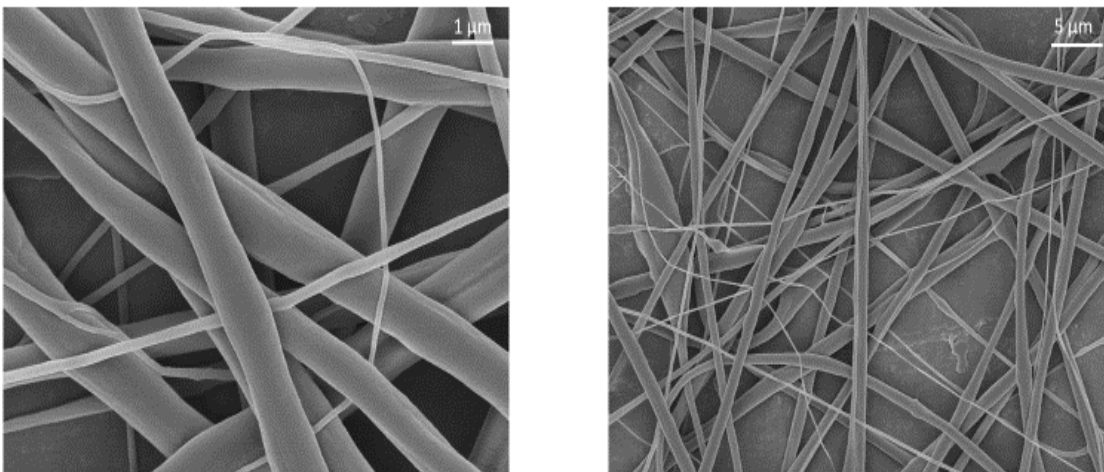


*Figure 73 SEM images of BHMf-3 electrospun mats*

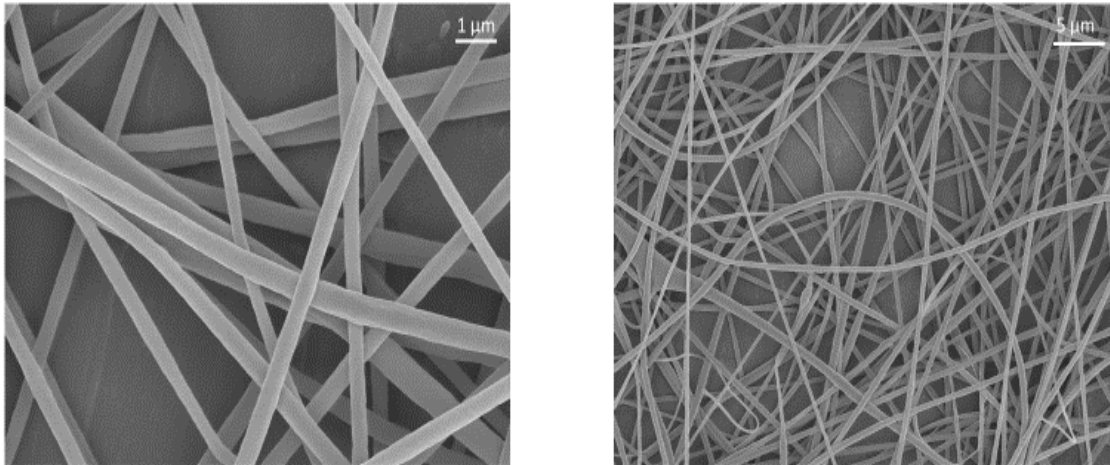


Figure 74 SEM images of PD electrospun mats

Once obtained the images of SEM, the diameters normal distribution has been calculated for every sample, using imageJ software. The results are shown below

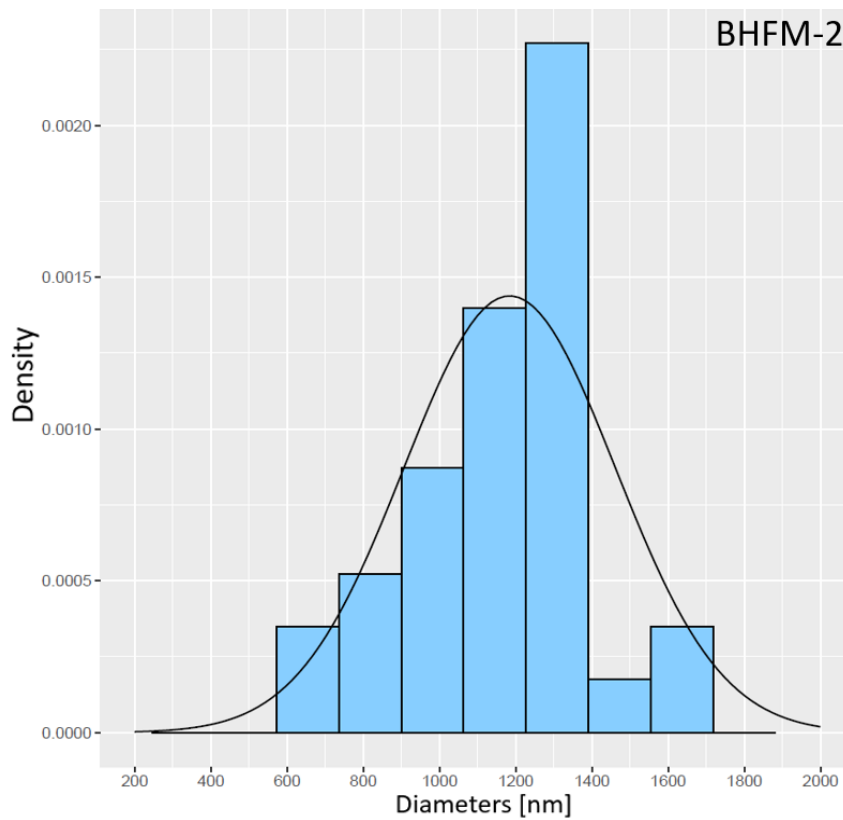


Figure 75 Diameters distribution of BHF-2

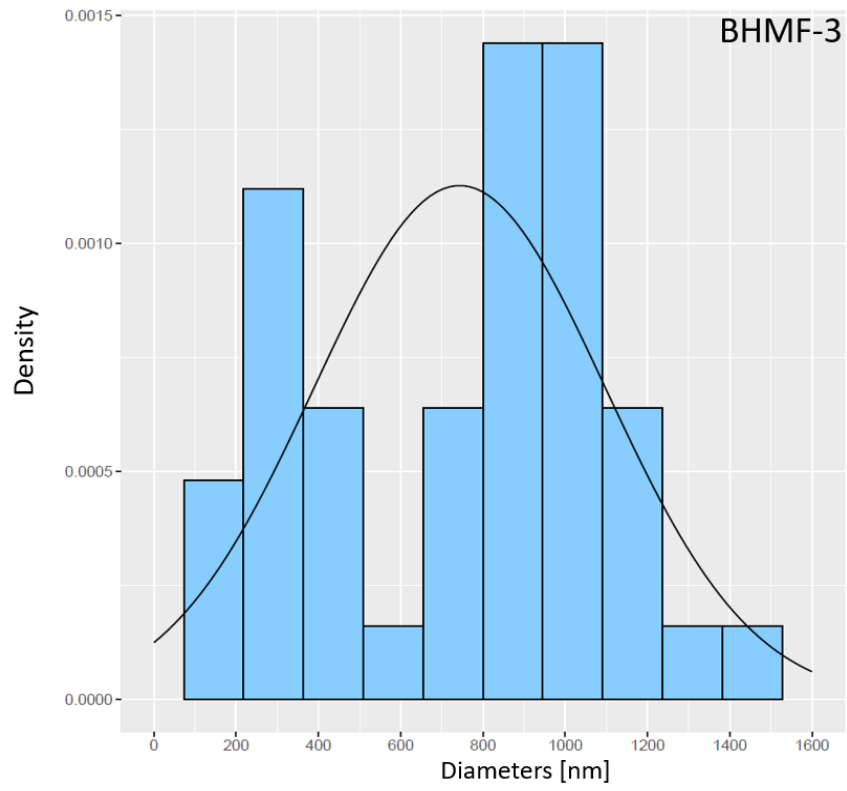


Figure 76 Diameter distribution of BHMf-3

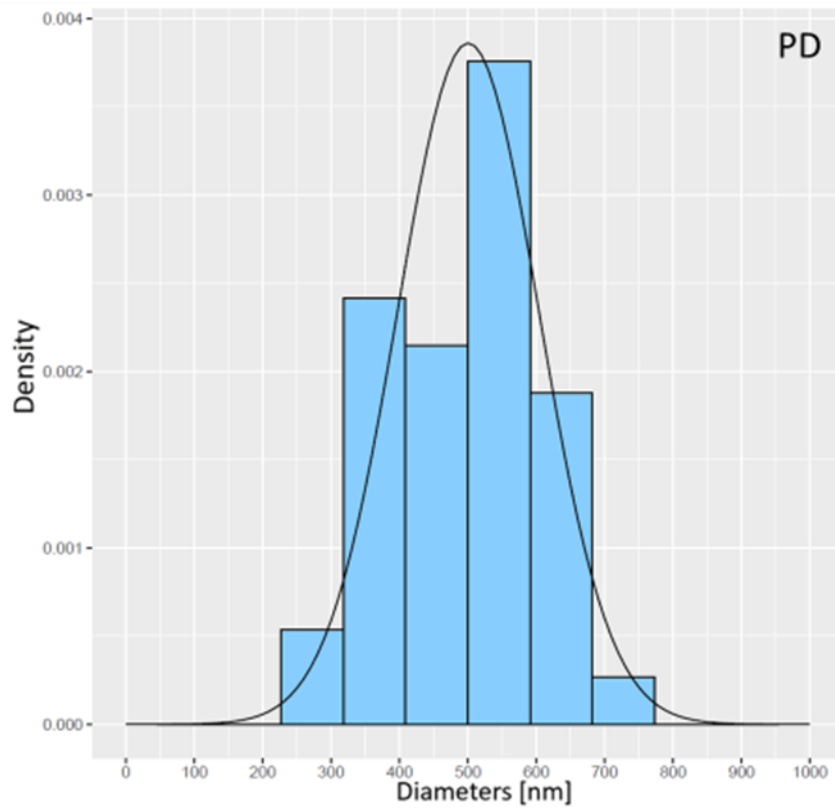


Figure 77 Diameter distribution of PD



<b>Material</b>	<b>Mean fibers diameter (nm)</b>	<b>Standard Deviation (nm)</b>
PD	500	102
BHMF-2	1184	273
BHMF-3	743	349

*Table 9 Mean fiber diameter and standard deviation of the three systems*

As can be seen there are important differences in the morphology and diameters of the fibers resulting from the three different solutions. First of all, the diameter of the fibers does not increase linearly with the increasing in weight content of the solution, which is instead a common feature of lots of studies regarding electrospun nanofibers.(53,54)

Another interesting result is the difference in the pores size.

Indeed, a smaller fiber usually results in smaller pore size (54). However, in the majority of the works, is considered just the mean diameter of the fiber but not the standard deviation. It is true that, at same standard deviation, at smaller fibers corresponds smaller pores but at different standard deviation this is not true.

Indeed, as can be seen from the Table 9 and Figure 76, BHMF-3 shows a bimodal distribution of the fibers, which affect the pores size.

Comparing the pores area of the BHMF-3 and PD, using imageJ software, can be seen that BHMF-3 possesses a lower void area, and so a lower pore size respect PD(31% against 50% of void area), even if the mean diameter of BHMF-3 is twice the mean diameter of PD.

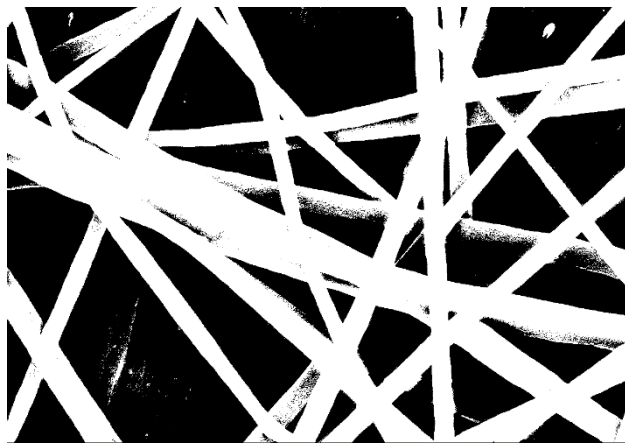


*Figure 78 PD void area (in black)*



*Figure 79 BHMf-3 void area (in black)*

Finally, the functionalization of a membrane using AMI was observed using SEM. As can be seen in the image of functionalized membrane, there are white small particles that are attached to the fibers, while in the not functionalized one, the presence of these particle is not detected.

However, this could not be taken as confirmation of the functionalization, because the particles seen in the images could be just deposited on the fibers, being trapped in the membrane.

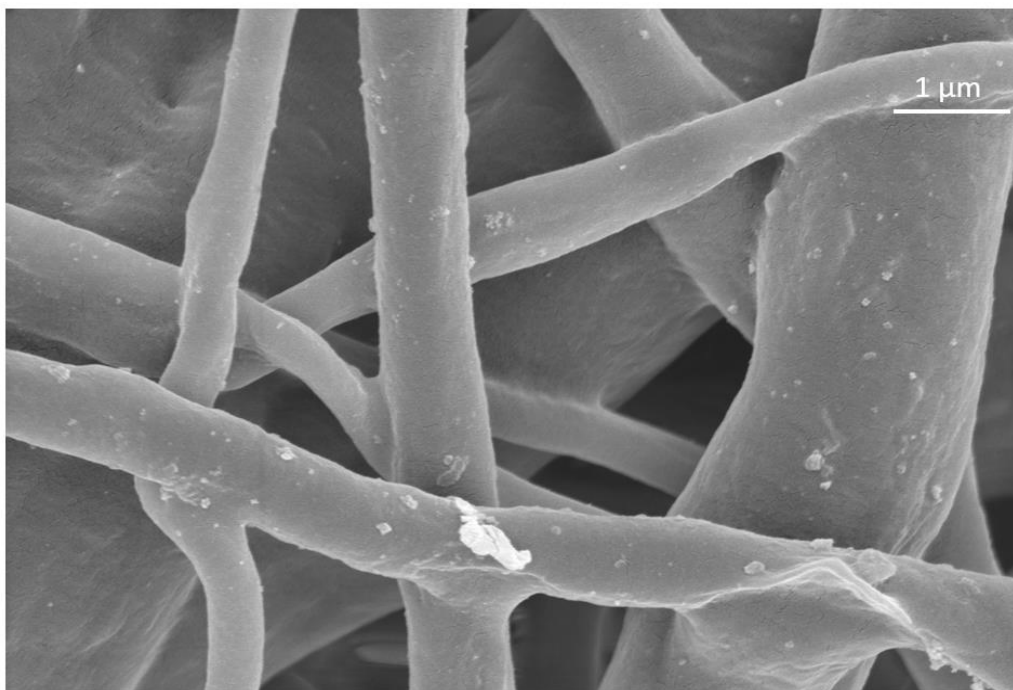


*Figure 80 Functionalized membrane*

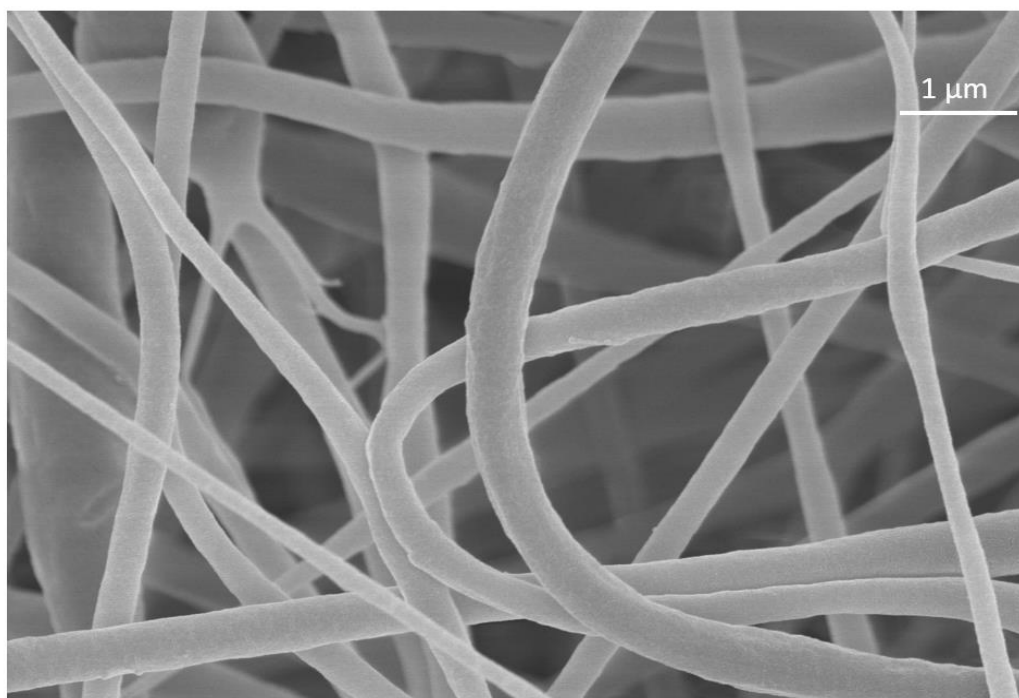


*Figure 81 Not functionalized membrane*

### 3.10 CONTACT ANGLE

The results of static contact angle measurements have proven a good hydrophobicity of the untreated polyurethane membrane with contact angle in the range of 125-130 °. A mean of 6 measurements has been performed in different parts of the sample in order to provide a statistically reliable result. In fact, the samples produced by electrospinning are not always perfectly homogenous, as also observed by SEM, due to a different amount of material deposited in different part of the collector and the presence of stream instability which could create artifact negatively affecting the surface roughness. The photos and tables of the different samples analyzed are provided below.

Polyurethanes usually show a quite low hydrophobicity, which is a favorable characteristic thinking about their use as coatings.

In this case, however, the hydrophobicity is quite high, and it varies proportionally with the BHMF content while the solid weight percentage in the electrospinning solutions seems to not affect its surface wettability.

A quite good hydrophobicity was predictable from the fact that the solid is easily dissolved, even if not completely, in chloroform, a solvent possessing a low relative polarity index of 0.259. It can be argued that the solvent mixture used in the electrospinning process is a mixture of chloroform and DMF, both considered a-polar or of low polarity if compared to water, thus probably influencing the resulting surface energy of the membrane. However, all the solvent should evaporate during the electrospinning and the following drying process. In this sense, a comparison between membrane and DMF spectra have allowed to be sure of the absence of DMF in the final composition. All the peaks of DMF (1663, 1385, 1089  $\text{cm}^{-1}$ ) are absent in the membrane's spectrum. Chloroform was assumed as not present and thus not investigated, due to the much lower boiling point with respect DMF.

### 3.10.1 Film contact angle

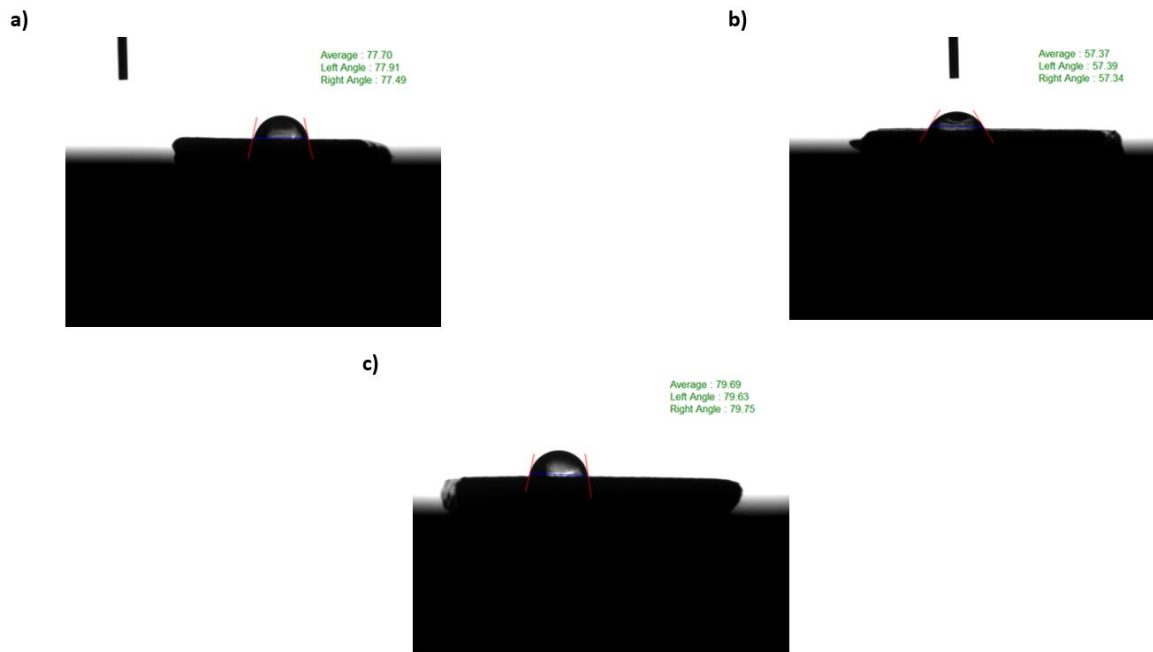


Figure 82 Photographs of the contact angle measurements on the films of:  
a) PD b) BHMF-2 c) BHMF-3

The films have been investigated, in order to see if the same trend of membranes is found. The contact angle measurements show a hydrophilic and BHMF-3 and PD samples seem to present same angle values. BHMF-2, instead, shows a very low contact angle.

### 3.10.2 Membranes contact angle

Regarding the furan-containing membranes, the higher content of hard segments, in BHMf-3, results in a higher polarity of the compound. Higher polarity of the surface means a lower contact angle, but this is not detected from contact angle measurements, on the contrary, higher the furan content, higher the hydrophobicity of the membrane.

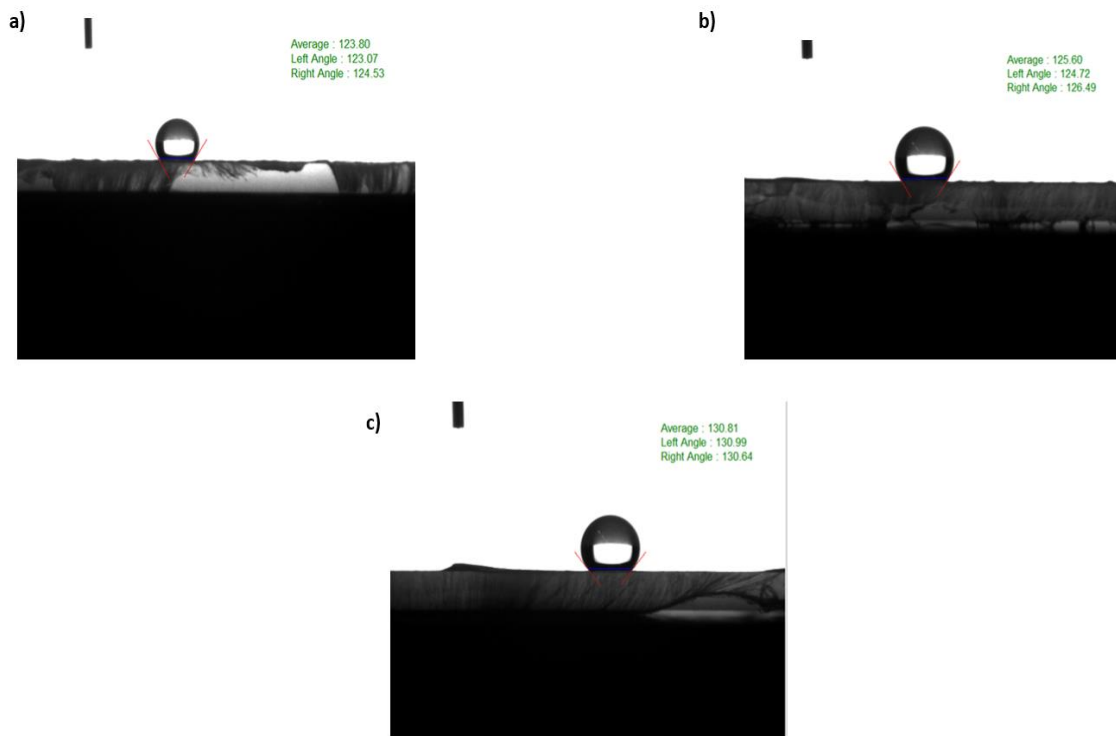


Figure 83 Photographs of the contact angle measurement of the membranes: a) PD b) BHMf-2 c) BHMf-3

A definitive explanation regards the fibers diameter of the membranes.

Has shown in the Table 9, BHMf3 is not the compound showing the lower diameters of the fibers but it shows the lowest void area between the three samples, resulting in the lowest pore size. Exactly the small pore size can be related to the very high hydrophobicity of BHMf-3. The same correlation between pore sizes and hydrophobicity was found by Dongjiang et al. (61). Generally, the contact angles of electrospun membranes are far lower than the contact angles of the films of the same material. Furthermore, as found by Huang et al. (55), at decreasing the fiber diameter increases the contact angle. It is justified by the specific surface area which, increasing when fiber diameters decrease, affect the surface

roughness of the membrane and thus his hydrophobic behavior, counterbalancing the increase of polar groups content. PD membrane, despite its lower nanofiber diameter, showed higher contact angle values. This could be related with the more homogeneous surface of nanofibers (see figure 74) in PD membranes.

<b>Material</b>	<b>Film contact angle (°)</b>	<b>Membrane contact angle (°)</b>
PD	76,5	119,7
BHMF-2	55,5	124,4
BHMF-3	79,7	126,9

*Table 10 Contact angles values of the film and the membrane*

Lots of modification has been proposed to Young equation in order to include surface roughness in the model. One of the most used is the Wenzel model, which includes a factor  $r$ , which is the ratio between the real surface area and the apparent one:

$$\cos \theta' = r \cos \theta = \frac{S_r}{S_a} \cos \theta$$

Where  $S_r$  is the real surface and  $S_a$  is the projected one.

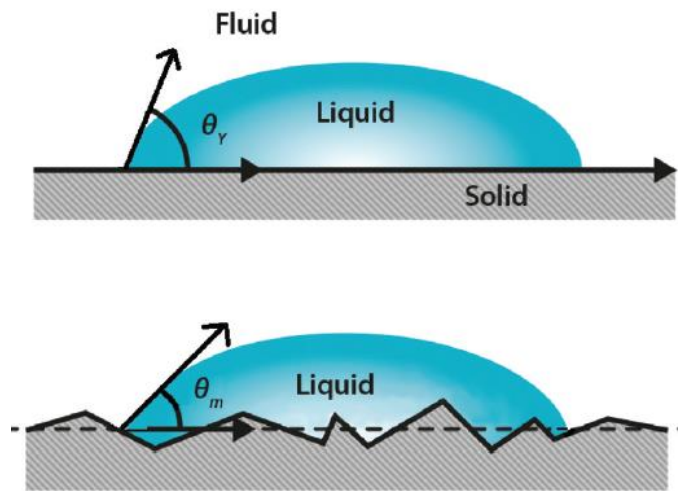


Figure 84 Effect of the surface roughness: Young model and Wenzel model (60)



## 3.11 MECHANICAL PROPERTIES

### 3.11.1 Mechanical properties of films

Uniaxial tensile test has been performed on the three samples. The graphic comparing them is shown in Figure 85.

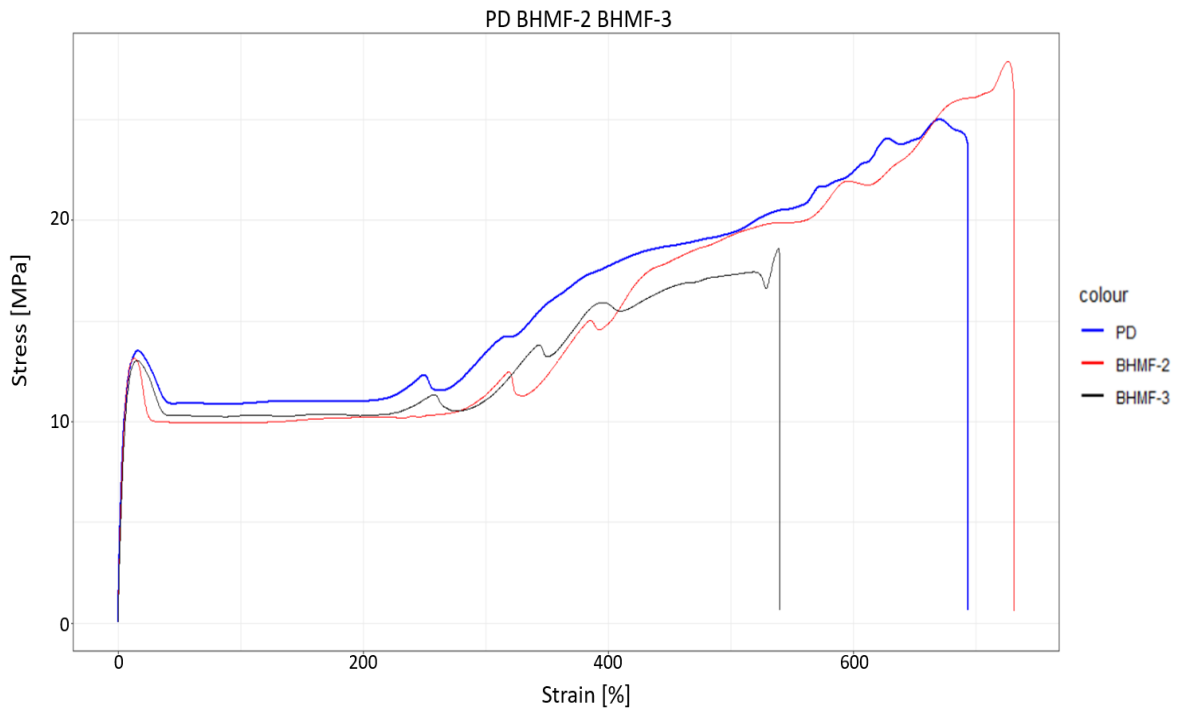


Figure 85 Stress-strain graphs comparison of the synthesized PD, BHMf-2 and BHMf-3 polyurethanes

The BHMf-2 and the PD samples show similar behavior, both possessing a higher deformation at break and a higher ultimate tensile strength with respect the BHMf-3 sample.

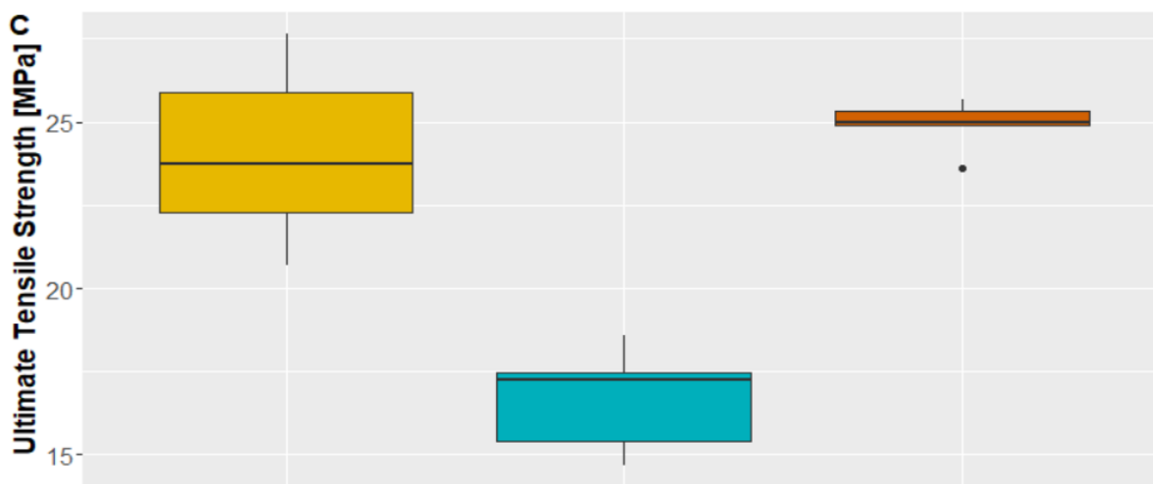
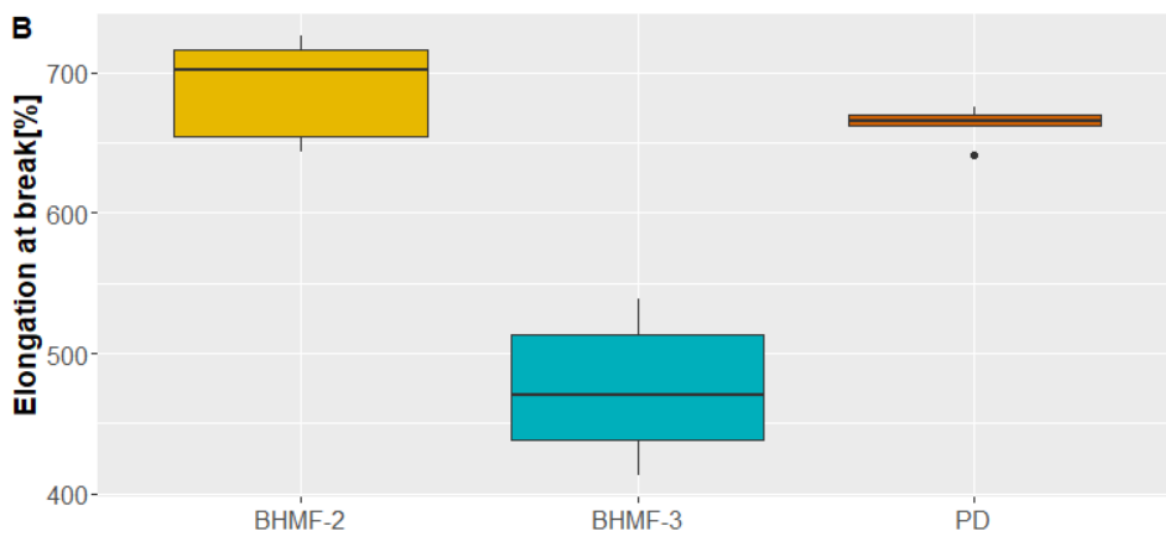
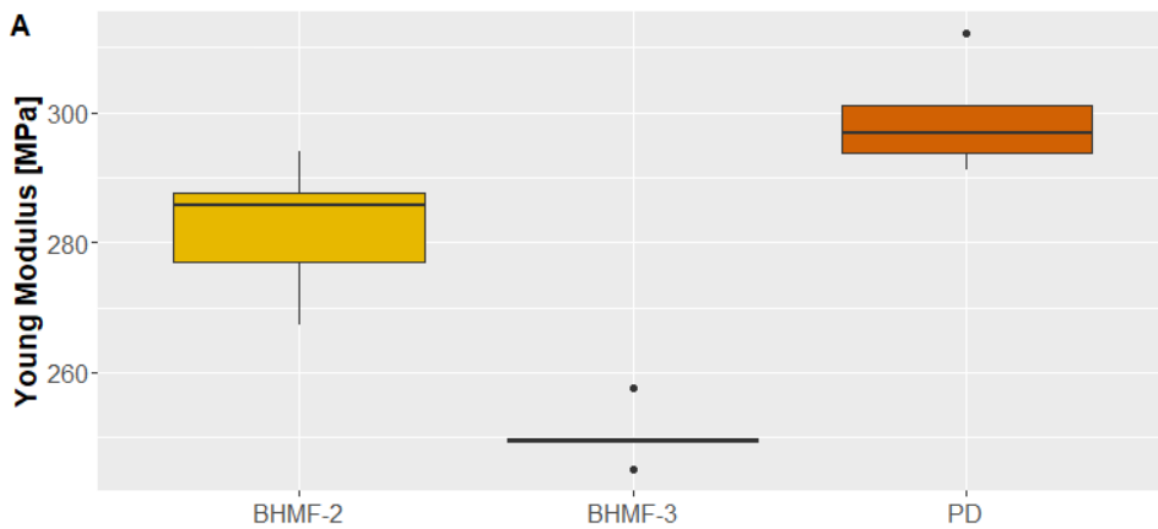


Figure 86 Boxplot of Young Modulus, Elongation at break and Ultimate tensile Strength of the three synthesized polyurethanes

The three analyzed samples seem to be only partially influenced by the type of chain extender, as can be deduced by the mechanical properties, even if in DSC analysis the difference seems quite evident. In fact, the two samples containing a ratio macrodiol: diisocyanate : chain extender of 1:3:2 show quite similar mechanical properties, even if the chain extender are aliphatic for the PD and heterocyclic for the BHMF-2. So, it has been hypothesized that the ratio of soft to hard segment, and so the chain extender content in the polyurethane and not the type, has a primary influence on the formation of crystalline domain. Indeed, crystallinity is directly proportional to the soft segment content. Hard segment are highly polar components which react quite fast and this does not allow the organization in crystalline structures. On the contrary, soft segment are constituted by an aliphatic high molecular weight polyol with an elevate tendency to crystalize and can reorganize themselves, resulting in more crystalline structures. The similar behavior of PD and BHMF-2 could be ascribed to a similar percentage of hard segment: 16 wt% for the PD and 18 wt% for the BHMF-2. The hard segment determines the mechanical properties of the polyurethane being the responsible of its rigidity. Generally, when deformation is applied to polyurethanes, the soft segment, which has a low modulus is extended in the first stage of deformation, and as the strain is increased, stress is transferred to the hard domain. There is a limit after which the percentage of hard segment could negatively affect the mechanical properties, affecting the formation of crystalline domains. This could be the reason of the quite lower mechanical properties of the BHMF-3 sample, which contains a 23 wt% of hard segment, implying the rupture of the samples at lower deformation.

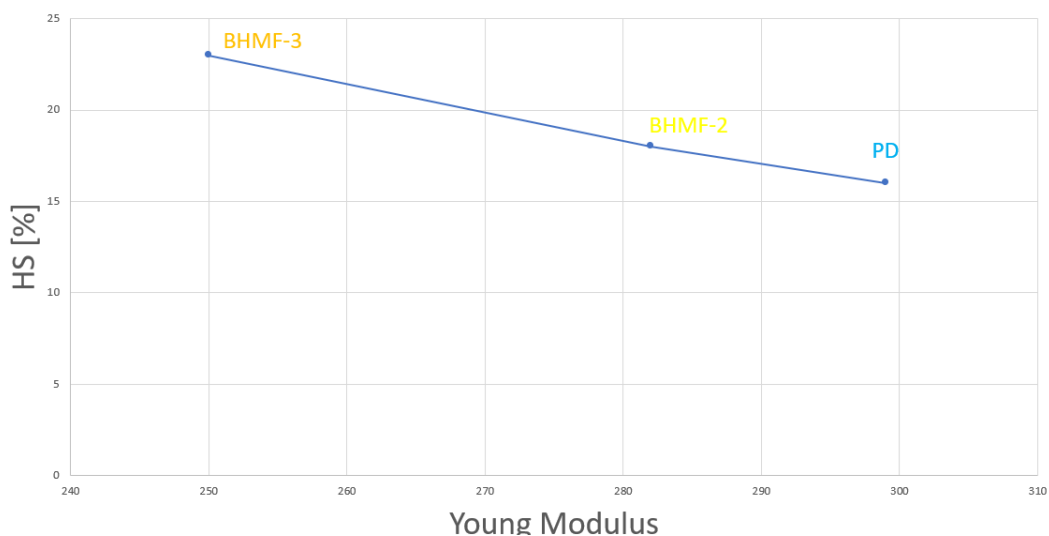


Figure 87 Relation between HS content and resulting Young modulus

Furthermore, difference in crystallinity, mainly in the soft segment, can easily explain the strange tendency of the three compounds, which show lower Young modulus at increasing content of hard segment.

### 3.11.2 Mechanical test of the membrane.

After the films, membranes were mechanically tested.

The specimen was prepared cutting rectangles measuring 60mm X 10mm and thicknesses ranges between 0.1 and 0.2 mm. The samples were then glued between two cardboard frames and clamped to the machine. Before starting the test, the lateral side of the cardboard were cut. The gauge length was set at 40 mm.

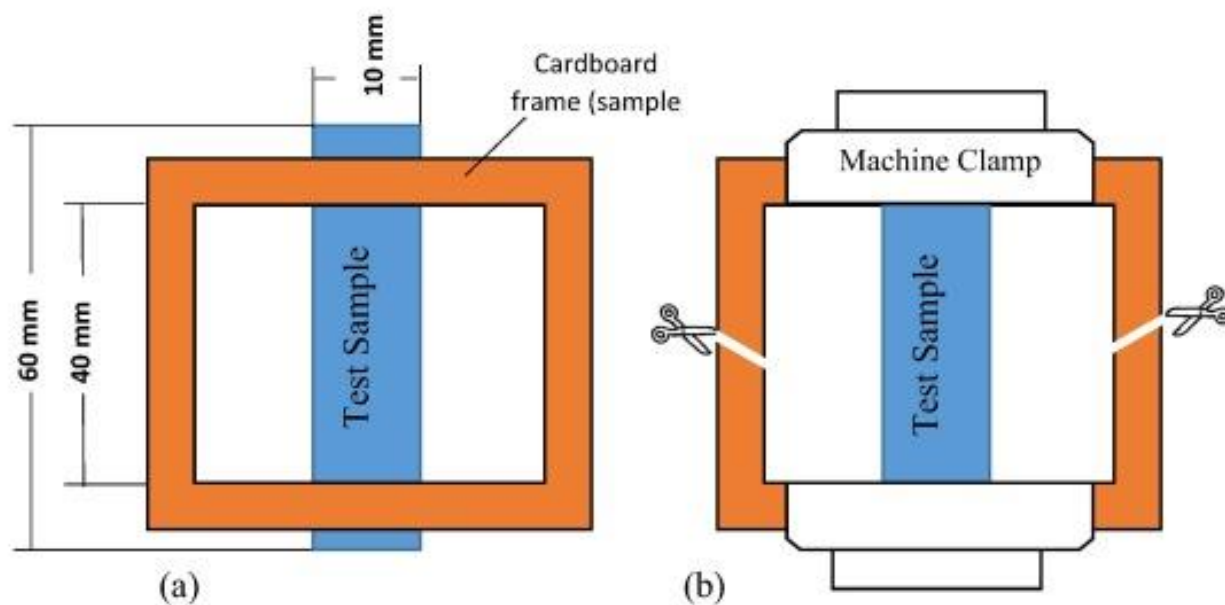


Figure 88 Configuration of the membranes mechanical test (53)

The samples were produced setting electrospinning trying to reach the same membranes' thickness and a continuous process. Conditions and thickness are reported on Table 11.

Material	Applied field (kV)	Injection rate (ml h <sup>-1</sup> )	Collector distance (cm)	Collection Time (min)	Mean thickness (mm)
PD	12	1	20	90	0.15
BHMF-2	10	0.75	20	90	0.14
BHMF-3	8.6	1	20	90	0.1

Table 11 Electrospinning conditions of each membrane tested

The results are shown in Figure 89.

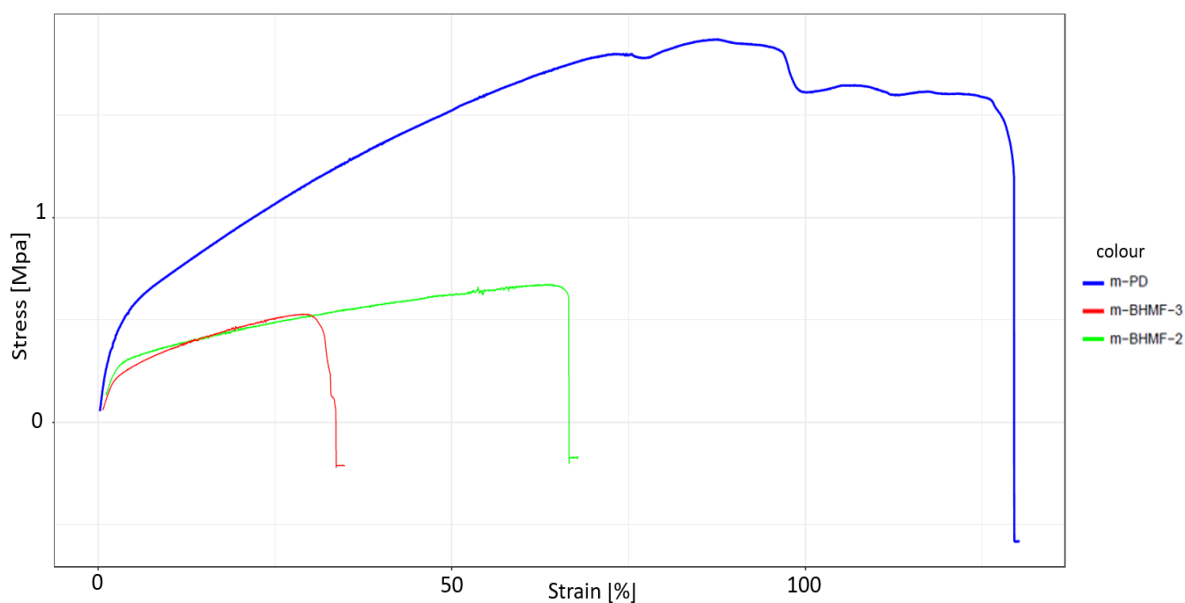


Figure 89 Stress-Strain graph of the membranes

The specimens are produced with different condition and this could have been influenced the resulting mechanical properties.

PD is the composition which shows, from the SEM and optical microscopy analysis, the best fiber morphology, the absence of defects and the small diameter distribution concur in create a very homogeneous material. Exactly the homogeneity is thought to be the reason of its good mechanical properties.

Furthermore, as in the study of Doustgani et al. (18), also here can be seen a relation between the applied electric field and the resulting mechanical properties, the latter increasing with applied voltage.

## 4 CONCLUSION AND FUTURE PROSPECTIVES

### 4.1 CONCLUSIONS

In this work, BHMf chain extender, HDI diisocyanate and E82 macrodiol have been reacted to produce a new polyurethane containing furan in the backbone chain. Two different formulations, containing different amount of BHMf have been produced. A reference polyurethane containing 1,3 propanediol as chain extender was also produced. Chemical compositions were characterized via FTIR, while mechanical and thermal properties was characterized by DSA, DSC and tensile test.

The results which has been presented show very good mechanical properties for the BHMf-2, very similar to the reference sample's ones, while lower mechanical properties of the BHMf-3.

The reduction of Young modulus with the increasing of hard segment content has been attributed to a lower crystallinity of BHMf-3 given by the lower soft segment content. However, the mechanical properties of BHMf-3 are still acceptable, considering that the higher furan content implies a higher possibility of functionalization.

Once these polymers were characterized, a further step has been undertaken, producing membrane by electrospinning. The decision to produce very thin fibers by electrospinning was dictated by the geometrical consideration that the volume to surface area ratio increase, decreasing the diameter of the fiber, thus exposing an higher number of furan which can be functionalized.

The results of electrospinning process were good. It has been proved that the electrospinning process is continuous and thus continuous fibers could be produced. Resulting fibers were homogenous, presenting very low presence of defects and narrow diameters distribution. The membranes produced show high hydrophobicity, good mechanical properties and the possibility to be easily functionalized.

This work was carried out considering the end of life of the final polymer trying to minimize its environmental footprint.

One of the big problems in polymer recycling is the presence of additives which, once reacted with the virgin polymer, strongly affect the recyclability of the compound.

Using DA to functionalize the polymer surface could be another way to improve its

recyclability.

Indeed, in this work, a polyurethane with a biobased content of between 85 and 88 wt % (which can be increased to 100 wt% changing the diisocyanate) it has been functionalized in a green, easy and reversible way. Creating a performing biodegradable polymer is quite difficult and only in the last years the industry has started a serious investigation about this topic. The clickable properties of the DA reaction allow to rethink the way a biodegradable polymer is thought. Many times, a small percentage in weight of a fundamental but non-biodegradable and non-recyclable additive precludes both recyclability and biodegradability. Usually, the solution is looking for a green alternative of such component, which implies spending money and time on research, with results that could be unsuccessful. The clickable reactions make a polymer seems like a puzzle, which can be easily dismantled in different parts, thus allowing a non-biodegradable part to be recycled and not precluding the overall biodegradability of the system. Such a property permits to use existing, cheaper and more effective molecules as functionalizing agent and still allowing a green end of life of the product. Furthermore, biodegradability is not always the better choice, the possibility of recovering parts of the polymer with an easy process impacts in a favorable way on the Life Cycle Assessment analysis of a product.

From another point of view, DA mechanism allows to re-functionalize surfaces in an easy way. Lots of polymeric product are thrown away because damage or wearing affects the surface properties of the manufacture and a re-functionalization is either too expensive or not possible to be performed on the product. Using DA as functionalization technique, lifetime of such products could be increased.



## 4.2 FUTURE DEVELOPMENT

The production method could be implemented using mechanochemical chemistry. A polymer similar to the one synthesized in this work, just with a different diisocyanate (MDI instead of HDI), has been produced by Oh et al. (56) using mechanochemical chemistry with optimal results. Such method allows for a faster and greener one-pot synthesis which could be scaled up to industrial production.

Regarding the polymer structure, in this work the renewable part of BHMF-2 is 88% while for BHMF-3 is 85 wt% due to the use of petroleum-based HDI as diisocyanate. Synthesizing a completely biobased polymer is absolutely an accessible challenge.

Another important step that will open new application horizons is the possibility of producing biocompatible membranes. Currently the biocompatibility of BHMF-2 and BHMF-3 membranes is currently being tested. The wide range of maleimide-containing molecules used in medicine combined with the possibility to produce it in very thin membrane, could make this compound a promising platform to be used in biomedical engineering.

## BIBLIOGRAPHY

- (1) Plastics Europe. Plastics – the Facts 2017. :24.
- (2) Akindoyo JO, Beg MDH, Ghazali S, Islam MR, Jeyaratnam N, Yuvaraj AR. Polyurethane types, synthesis and applications – a review. RSC Adv 2016;6(115):114453-114482.
- (3) Datta J, Kasprzyk P. Thermoplastic polyurethanes derived from petrochemical or renewable resources: A comprehensive review. Polym Eng Sci 2018;58:E14-E35.
- (4) Kolb HC, Finn MG, Sharpless KB. Click Chemistry: Diverse Chemical Function from a Few Good Reactions. Angew Chem Int Ed 2001;40(11):2004-2021.
- (5) Kolb HC, Finn MG, Sharpless KB. Click Chemistry: Diverse Chemical Function from a Few Good Reactions. Angew Chem Int Ed 2001;40(11):2004-2021.
- (6) Blasco E, Sims MB, Goldmann AS, Sumerlin BS, Barner-Kowollik C. 50th Anniversary Perspective: Polymer Functionalization. Macromolecules 2017;50(14):5215-5252.
- (7) Nair DP, Podgórski M, Chatani S, Gong T, Xi W, Fenoli CR, et al. The Thiol-Michael Addition Click Reaction: A Powerful and Widely Used Tool in Materials Chemistry. Chem Mater 2014;26(1):724-744.
- (8) Xu LQ, Pranantyo D, Neoh K, Kang E, Fu GD. Thiol Reactive Maleimido-Containing Tannic Acid for the Bioinspired Surface Anchoring and Post-Functionalization of Antifouling Coatings. ACS Sustainable Chem Eng 2016;4(8):4264-4272.
- (9) Meldal M. Polymer “Clicking” by CuAAC Reactions. Macromol Rapid Commun 2008;29(12):1016-1051.
- (10) Durmaz H, Dag A, Altintas O, Erdogan T, Hizal G, Tunca U. One-Pot Synthesis of ABC Type Triblock Copolymers via in situ Click [3 + 2] and Diels–Alder [4 + 2] Reactions. Macromolecules 2007;40(2):191-198.
- (11) Funel J, Abele S. Industrial Applications of the Diels–Alder Reaction. Angew Chem Int Ed 2013;52(14):3822-3863.
- (12) Chang C, Liu Y. Functionalization of multi-walled carbon nanotubes with furan and maleimide compounds through Diels–Alder cycloaddition. Carbon 2009;47(13):3041-3049.
- (13) Wool RP. Self-healing materials: a review. Soft Matter 2008;4(3):400-418.

- (14) Willocq B, Khelifa F, Brancart J, Van Assche G, Dubois P, Raquez J-. One-component Diels–Alder based polyurethanes: a unique way to self-heal. *RSC Adv* 2017;7(76):48047-48053.
- (15) Post W, Susa A, Blaauw R, Molenveld K, Knoop RJI. A Review on the Potential and Limitations of Recyclable Thermosets for Structural Applications. *Polymer Reviews* 2020;60(2):359-388.
- (16) Gu L, Wu Q. Recyclable bio-based crosslinked polyurethanes with self-healing ability. *J Appl Polym Sci* 2018;135(21):46272.
- (17) Xu J, Li Z, Wang B, Liu F, Liu Y, Liu F. Recyclable biobased materials based on Diels–Alder cycloaddition. *J Appl Polym Sci* 2019;136(18):47352.
- (18) Limpricht H. Ueber das Tetraphenol, C<sub>4</sub>H<sub>4</sub>O. *Ber Dtsch Chem Ges* 1870;3(1):90-91.
- (19) Batool Z, Xu D, Zhang X, Li X, Li Y, Chen Z, et al. A review on furan: Formation, analysis, occurrence, carcinogenicity, genotoxicity and reduction methods. *Crit Rev Food Sci Nutr* 2020:1-12.
- (20) Gandini A, Belgacem MN. Furans in polymer chemistry. *Progress in Polymer Science* 1997;22(6):1203-1379.
- (21) Hu F, La Scala JJ, Sadler JM, Palmese GR. Synthesis and Characterization of Thermosetting Furan-Based Epoxy Systems. *Macromolecules* 2014;47(10):3332-3342.
- (22) Meng J, Zeng Y, Chen P, Zhang J, Yao C, Fang Z, et al. Flame Retardancy and Mechanical Properties of Bio-Based Furan Epoxy Resins with High Crosslink Density. *Macromol Mater Eng* 2020;305(1):1900587.
- (23) Pfeifer S, Lutz J. Development of a Library of N-Substituted Maleimides for the Local Functionalization of Linear Polymer Chains. *Chemistry – A European Journal* 2008;14(35):10949-10957.
- (24) Yang S, Wang J, Huo S, Wang J, Tang Y. Synthesis of a phosphorus/nitrogen-containing compound based on maleimide and cyclotriphosphazene and its flame-retardant mechanism on epoxy resin. *Polym Degrad Stab* 2016;126:9-16.
- (25) Fang Y, Du X, Yang S, Wang H, Cheng X, Du Z. Sustainable and tough polyurethane films with self-healability and flame retardance enabled by reversible chemistry and cyclotriphosphazene. *Polym Chem* 2019;10(30):4142-4153.

- (26) Singh D, Chauhan NPS, Mozafari M, Hiran BL. High-Temperature Resistive Free Radically Synthesized Chloro-Substituted Phenyl Maleimide Antimicrobial Polymers. *Polym Plast Technol Eng* 2016;55(18):1916-1939.
- (27) Salewska N, Boros-Majewska J, Łącka I, Chylińska K, Sabisz M, Milewski S, et al. Chemical reactivity and antimicrobial activity of N-substituted maleimides. *Journal of Enzyme Inhibition and Medicinal Chemistry* 2012;27(1):117-124.
- (28) Shi M, Wosnick J, Ho K, Keating A, Shoichet M. Immuno-Polymeric Nanoparticles by Diels–Alder Chemistry. *Angewandte Chemie International Edition* 2007;46(32):6126-6131.
- (29) Ghahremani Honarvar M, Latifi M. Overview of wearable electronics and smart textiles. *The Journal of The Textile Institute* 2017;108(4):631-652.
- (30) Bai S, Xu R, Wang W, Yu D. Dual-response of temperature and humidity asymmetrical cotton fabric prepared based on thiol-ene click chemistry. *Colloids and Surfaces A: Physicochemical and Engineering Aspects* 2019;567:104-111.
- (31) Chang Z, Xu Y, Zhao X, Zhang Q, Chen D. Grafting Poly(methyl methacrylate) onto Polyimide Nanofibers via “Click” Reaction. *ACS Appl Mater Interfaces* 2009;1(12):2804-2811.
- (32) Lin F, Yu J, Tang W, Zheng J, Xie S, Becker ML. Postelectrospinning “Click” Modification of Degradable Amino Acid-Based Poly(ester urea) Nanofibers. *Macromolecules* 2013;46(24):9515-9525.
- (33) Luzio A, Canesi VE, Bertarelli C, Caironi M. Electrospun Polymer Fibers for Electronic Applications. *Materials* 2014;7(2).
- (34) Fong H, Chun I, Reneker DH. Beaded nanofibers formed during electrospinning. *Polymer* 1999;40(16):4585-4592.
- (35) Amariei N, Manea LR, Berteza AP, Berteza A, Popa A. The Influence of Polymer Solution on the Properties of Electrospun 3D Nanostructures. *IOP Conference Series: Materials Science and Engineering* 2017;209:012092.
- (36) Dasedemir M, Topalbekiroglu M, Demir A. Electrospinning of thermoplastic polyurethane microfibers and nanofibers from polymer solution and melt. *J Appl Polym Sci* 2013;127(3):1901-1908.
- (37) Koski A, Yim K, Shivkumar S. Effect of molecular weight on fibrous PVA produced by electrospinning. *Materials Letters* 2004;58(3):493-497.

- (38) Pedicini A, Farris RJ. Mechanical behavior of electrospun polyurethane. *Polymer* 2003;44(22):6857-6862.
- (39) Fu GD, Xu LQ, Yao F, Zhang K, Wang XF, Zhu MF, et al. Smart Nanofibers from Combined Living Radical Polymerization, "Click Chemistry", and Electrospinning. *ACS Appl Mater Interfaces* 2009;1(2):239-243.
- (40) Kalaoglu-Altan O, Kirac-Aydin A, Sumer Bolu B, Sanyal R, Sanyal A. Diels–Alder "Clickable" Biodegradable Nanofibers: Benign Tailoring of Scaffolds for Biomolecular Immobilization and Cell Growth. *Bioconjugate Chem* 2017;28(9):2420-2428.
- (41) Choi J, Moon DS, Jang JU, Yin WB, Lee B, Lee KJ. Synthesis of highly functionalized thermoplastic polyurethanes and their potential applications. *Polymer* 2017;116:287-294.
- (42) Dirlam PT, Strange GA, Orlicki JA, Wetzel ED, Costanzo PJ. Controlling Surface Energy and Wettability with Diels–Alder Chemistry. *Langmuir* 2010;26(6):3942-3948.
- (43) Behera PK, Mondal P, Singha NK. Self-Healable and Ultrahydrophobic Polyurethane-POSS Hybrids by Diels–Alder "Click" Reaction: A New Class of Coating Material. *Macromolecules* 2018;51(13):4770-4781.
- (44) Bidegain B, alonso-varona A, Teodoro P, Corcuera M, Eceiza A. Studies on the morphology, properties and biocompatibility of aliphatic diisocyanate-polycarbonate polyurethanes. *Polym Degrad Stab* 2015;122.
- (45) Yu H, Bai X, Qian G, Wei H, Gong X, Jin J, et al. Impact of Ultraviolet Radiation on the Aging Properties of SBS-Modified Asphalt Binders. *Polymers* 2019;11(7):1111.
- (46) Di Gianfrancesco A. 8 - Technologies for chemical analyses, microstructural and inspection investigations. In: Di Gianfrancesco A, editor. *Materials for Ultra-Supercritical and Advanced Ultra-Supercritical Power Plants*: Woodhead Publishing; 2017. p. 197-245.
- (47) Huhtamäki T, Tian X, Korhonen JT, Ras RHA. Surface-wetting characterization using contact-angle measurements. *Nature Protocols* 2018;13(7):1521-1538.
- (48) Saralegi A, Rueda L, Fernández-d'Arlas B, Mondragon I, Eceiza A, Corcuera MA. Thermoplastic polyurethanes from renewable resources: effect of soft segment chemical structure and molecular weight on morphology and final properties. *Polym Int* 2013;62(1):106-115.
- (49) Sánchez-Adsuar MS. Influence of the composition on the crystallinity and adhesion properties of thermoplastic polyurethane elastomers. *Int J Adhes Adhes* 2000;20(4):291-298.

- (50) Yilgor I, Yilgor E, Guler IG, Ward TC, Wilkes GL. FTIR investigation of the influence of diisocyanate symmetry on the morphology development in model segmented polyurethanes. *Polymer* 2006;47(11):4105-4114.
- (51) Yu J, Qiu Y, Zha X, Yu M, Yu J, Rafique J, et al. Production of aligned helical polymer nanofibers by electrospinning. *European Polymer Journal* 2008;44(9):2838-2844.
- (52) Diaz CA, Xia Y, Rubino M, Auras R, Jayaraman K, Hotchkiss J. Fluorescent labeling and tracking of nanoclay. *Nanoscale* 2013;5(1):164-168.
- (53) Tarus B, Fadel N, Al-Oufy A, El-Messiry M. Effect of polymer concentration on the morphology and mechanical characteristics of electrospun cellulose acetate and poly (vinyl chloride) nanofiber mats. *Alexandria Engineering Journal* 2016;55(3):2975-2984.
- (54) Hekmati AH, Khenoussi N, Nouali H, Patarin J, Drean J. Effect of nanofiber diameter on water absorption properties and pore size of polyamide-6 electrospun nanoweb. *Text Res J* 2014;84(19):2045-2055.
- (55) Huang F, Wei Q, Cai Y, Wu N. Surface Structures and Contact Angles of Electrospun Poly(vinylidene fluoride) Nanofiber Membranes. *ACS Nano* 2008;13(4):292-301.
- (56) Oh C, Choi EH, Choi EJ, Premkumar T, Song C. Facile Solid-State Mechanochemical Synthesis of Eco-Friendly Thermoplastic Polyurethanes and Copolymers Using a Biomass-Derived Furan Diol. *ACS Sustainable Chem Eng* 2020;8(11):4400-4406.
- (57) HUMBOLDT UNIVERSITÄT ZU BERLIN MATHEMATISCH-NATURWISSENSCHAFTLICHE FAKULTÄT I INSTITUT FÜR PHYSIK. Investigation of Polymers with Differential Scanning Calorimetry.
- (58) Tanksale A, Chan F. Biomass gasification using reactive flash volatilisation technology. ; 2014.
- (59) Miki T, Sugimoto H, Kanayama K. Thermoplastic behavior of wood powder compacted materials. *J Mater Sci* 2007;42:7913-7919.
- (60) Biolin scientific. Influence of surface roughness on contact angle and wettability.
- (61) Yang D, Xu Y, Xu W, Wu D, Sun Y, Zhu H. Tuning pore size and hydrophobicity of macroporous hybrid silica films with high optical transmittance by a non-template route. *J Mater Chem* 2008;18(45):5557-5562

